농학박사학위논문

삼지닥과 Edgeworoside A의 항골다공증 및 천남성의 미백 효과에 관한 연구

Investigation of the anti-osteoporotic activity of *Edgeworthia papyrifera* and Edgeworoside A and anti-melanogenic activity of *Rhizoma arisaematis*

2018 년 2 월

서울대학교 대학원

농생명공학부 농생명공학전공

김 판 수

A DISSERTATION FOR THE DEGREE OF DOCTOR OF PHILOSOPHY

Investigation of the anti-osteoporotic activity of *Edgeworthia papyrifera* and Edgeworoside A and anti-melanogenic activity of *Rhizoma arisaematis*

삼지닥과 Edgeworoside A의 항골다공증 및 천남성의 미백 효과에 관한 연구

February 2018

Pan-Soo Kim

MAJOR IN AGRICULTURAL BIOTECHNOLOGY

DEPARTMENT OF AGRICULTURAL BIOTECHNOLOGY

GRADUATE SCHOOL

SEOUL NATIONAL UNIVERSITY

Investigation of the anti-osteoporotic activity of *Edgeworthia papyrifera* and Edgeworoside A and anti-melanogenic activity of *Rhizoma arisaematis*

Advisor: Professor Jin-Ho Seo

A dissertation submitted in partial fulfillment of

The requirements for the degree of

DOCTOR OF PHILOSOPHY

to the Faculty of Department of Agricultural Biotechnology

at

SEOUL NATIONAL UNIVERSITY

by

Pan-Soo Kim

February 2018

농학박사학위논문

Investigation of the anti-osteoporotic activity of *Edgeworthia papyrifera* and Edgeworoside A and anti-melanogenic activity of *Rhizoma arisaematis*

삼지닥과 Edgeworoside A의 항골다공증 및 천남성의 미백 효과에 관한 연구

지도교수 서 진 호

이 논문을 농학박사학위논문으로 제출함

2018 년 2 월

서울대학교 농생명공학부 농생명공학전공

김 판 수

김판수의 농학박사학위논문을 인준함

2018 년 2 월

위 원 장 유 상 렬 (인/서명)

부위원장 서 진 호 (인/서명)

위 원 최 영 진 (인/서명)

위 원 권 대 혁 (인/서명)

위 원 조 동 형 (인/서명)

ABSTRACT

Natural products have been considered a rich source of new drugs, nutraceuticals and cosmeceuticals for decades. Efforts on discovering new bioactive ingredients with drug-like benefits from natural products have been aided greatly by the availability of natural product-derived libraries (collection of crude mixtures, fractions, and purified compounds). In this thesis, a library of extracts derived from 4,200 plants native to Korea was exploited to identify candidates for anti-osteoporosis agents and anti-melanogenic agents.

The approach to discover candidates for anti-osteoporosis agents involves a series of assays that utilize biomarkers for osteoclast and osteoblast differentiation: the library was screened for the ability to inhibit RANKL-induced NF-κB (nuclear factor–kappa B) expression in RAW 264.7 osteoclatic cells, to modulate the activity of alkaline phosphatase in MC3T3-E1 osteoblastic cells, and to enhance the deposition of extracellular calcium in osteoblasts *in vitro*. These efforts in conjunction with a dereplcation technology led to identification of *Edgeworthia papyrifera* and edgeworoside A which exhibited a desired bioactivity profile *in vitro*. In an animal model of post-menopousal osteoporosis, *E. papyrifera* was demonstrated to improve all of the osteoporosis relevant parameters, suggesting that *E. papyrifera* and edgeworoside A may be used as functional ingredients in health supplements to increase bone strength and as therapeutics to treat osteoporosis.

Identification of candidates for anti-melanogenic agents involves a series of tests that utilize α-MSH-stimulated melanogenesis *in vitro* and

quantification of tyrosinase and TRP1 expression in B16F1 cells. The efforts led to identification of *Rhizoma arisaematis* that inhibited biosynthesis of melanin and expression of tyrosinase and TRP1 in α-MSH-treated B16F1 cells. The anti-melanogenic effect of *R. arisaematis* was mediated through activation of autophagy in B16F1 cells, and pharmacological inhibition of autophagy reduced the anti-melanogenic activity of *R. arisaematis* in α-MSH-treated B16F1 cells. Further analyses of *R. arisaematis* using three-dimensional skin substitutes and in a human clinical trial revealed that it significantly suppressed pigmentation and exerted whitening effects on human skin. These observations serve as a basis for further elaboration of *R. arisaematis* for the development of functional skin care products.

Key words: *Edgeworthia papyrifera*, edgeworoside A, osteoporosis, osteoclast, osteoblast, ovariectomized, drug candidate, functional ingredients, *Rhizoma arisaematis*, Autophagy, Melanogenesis

Student ID: 2008-30925

CONTENTS

Chapter 2

LIST OF TABLES

LIST OF FIGURES

Chapter 1

Literature review

1.1. Overview of natural products from plants

1.1.1. Natural products from plants

Natural resources, especially from native plants, have long been used as pharmaceuticals, cosmetics, functional health foods, and foods for daily consumption. As the social and market demands for a better quality of life and improvements in the safety of food, cosmetics, and drugs have increased, the need for research into and the commercialization of natural products has also increased. In addition, “natural” is usually used as a synonym for “pure” or “non-artificial” products for the purposes of marketing in cosmetics, health foods, or supplements.

In recent years, as global agreements, conventions, and regulations for the sustainability of biological diversity have been reached, research and development of natural products has been strengthened and expanded. The Convention on Biological Diversity (CBD) entered force on 29 December 1993. The purpose of the CBD was divided into three main objectives: 1) the conservation of biological diversity, 2) the sustainable use of the components of biological diversity, and 3) the fair and equitable sharing of the benefits that arise from the utilization of genetic resources. The aspect of benefit sharing (ABS, the Nagoya Protocol for the access to genetic resources and the fair and equitable sharing of

benefits arising from their utilization) is a supplementary agreement to the CBD that came into effect in Korea on August 17, 2017. This protocol is expected to cause significant damage to the domestic bioindustry, especially in the fields of pharmaceuticals, cosmetics, and health functional foods. Although the era of natural royalties is imminent, the preparations of small and medium-sized domestic companies are inadequate. If the protocol is put into effect, an annual damage of 1,550 billion won is expected. Korea relies on imports for 80% of its natural resources and foreign natural products account for 60% of cosmetic ingredients. Thus, the screening and exploration of new natural resources from native plant products, including research into potential drugs, functional health foods, and cosmetic ingredients, are not only of research value, but they may also provide means to repair the damage caused to the bioindustry by the CBD and ABS. These could include import substitutions and the development of high value-added products, among others.

"Natural" refers to something that exists in or is produced by nature, and is not artificial or synthesized. Products of natural origin which can be called "natural products" include whole organisms, such as plants, animals, or microorganisms or parts of them, and any extracts or pure isolated compounds derived from them (Samuelsson, 1999; Spainhour,

2005). However, the term “natural products” is generally understood to refer to herbs, herbal concoctions, and traditional or alternative medicines (Holt, 2002). Plant extracts and products are used in the major industries of food production, cosmetics, pharmaceuticals, and flavorings and are believed to aid human health, quality of life and wellbeing. A “native plant” is one that is able to grow in its natural state without being artificially protected in a defined area. There are approximately 100,000 plant species in Korea, of which approximately 8,000 are classified as herbal plants. However, only approximately 500 of these, accounting for only 5% of the total herbal resource, have been scientifically studied, and less than 50 native herbal plants are cultivated in domestic areas. Of the 5,379 species of native plants that grow in Korea, 2,998 are classified as dicotyledonous plants, 924 as bryophyte plants, and 293 as fern. KRIBB, which has managed the plant extract bank of Korea for 10 years, has played an important role in the collection and supply of Korean natural plant extracts. In thesis, I used the KRIBB native plant library, as well as the in-house library of Gyeonggi Bio-Center, to search for possible applications of natural extracts from 4,200 natural Korean plants.

1.1.2. Natural products as drugs and ingredients for health foods and cosmetic

Natural products have been investigated and utilized to treat diseases since early human history. Their therapeutic usage dates back approximately to the third millennium BC. In the 18th and 19th centuries, many compounds discovered during the study of plant extracts became important for medicines, such as digoxin from foxgloves (1785), morphine from poppies (1806), and aspirin from the salicylic acid in willow bark (1897). These natural drug substances provided a pivotal impulse for the formation of the modern pharmaceutical industry. In the early 1900s, 80% of medicines were obtained directly from various parts of plants, such as the roots, bark, or leaves. At that time, fluid extracts were fashionable and the public usually used natural products as teas, tonics, and liquid medicines. In the mid-1900s, natural products continued to be of major importance, with endogenous chemicals such as steroids, prostaglandins, and peptide hormones providing the pharmaceutical industry with additional inspiration for natural drug discovery. In the final quarter of the 20th century, as the understanding of enzymology and receptor pharmacology advanced, the role of functional proteins in biology and in the biochemical pathways of disease became clearer. With the help of functional cellular assay tools and animal models of disease, medicinal chemists could synthesize and

screen small molecules to develop an understanding of the structure-activity relationships vital to optimizing the potency and selectivity of medicinal compounds. Natural molecules frequently provided inspiration for the design of receptor binders, for example, the nicotinic and muscarinic receptors. Antibiotics and antineoplastic agents were also developed as selective toxins with the use of selective cytotoxicity assays and tumor models (Rishton 2008). More recently, natural products have continued to provide a significant number of new drugs and leads. Their dominant role is evident in the fact that approximately 60% of anticancer compounds and 75% of drugs for treating infectious diseases are either natural products or natural product derivatives (Newman et al., 2003; Cragg et al., 2005). Despite this success, research on natural products has experienced a steady global decline over the past couple of decades. The introduction of high-throughput synthesis and screening, molecular modeling, and combinatorial chemistry, with their promises of a seemingly inexhaustible supply of compound libraries, has contributed to reduced interest from the pharmaceutical industry in natural product screening. Although these approaches provide rapid, large-scale, and easy screening methods to search for drug-like synthetic compounds, they require excessive follow-up procedures, such as the confirmation and optimization of hit compounds and the adaptation of medicinal chemistry for the lead generation. Recently, interdisciplinary research

and the emergence of biochemical screening and analysis technologies have provided solutions to many obstacles that have been present for several decades in the process of natural product drug discovery. Technological improvements in prefractionation and chemical conditioning have enhanced the effectiveness of the biochemical assays used in the screening of natural extracts and active phytochemicals from natural plant extracts offer effective resources for fragment-based target identification in molecular modeling. Moreover, plant extract libraries have been expanded and diverted to include possible adaptations for high-throughput screening (HTS). The supply problems of natural products have also been solved through a combination of synthetic and process chemistry. In addition, natural products, especially phytochemicals, have lately been combined with antibodies and various chemicals to improve the activity and target specificity of current drugs.

Changes in social and commercial environments, such as limitations to compound libraries, decreased approval of new drugs, and social demands for natural products, have stimulated research into new natural products for use as health foods, cosmetic ingredients, and drugs. With an aging population, natural products used in the treatment of musculoskeletal disorders would be a useful resource and could easily become a high-value market. Osteoporosis and hypertension are two

common diseases in aging populations, but natural products are rarely used as drugs or active ingredients in the treatment of musculoskeletal disorders. In addition, only eight kinds of natural products are approved as health functional foods in Korea and their market has been gradually diminished owing to the lack of emergence of any new natural products for 10 years. In the cosmetic industry, natural plant products for whitening are popular in Korea and Asia; the limitations of the mode of action of current agents, focused on tyrosinase, have encouraged new mechanisms based on natural whitening products. Therefore, anti-osteoporotic and whitening agents from natural Korean products should be developed, explored, and commercialized as soon as possible.

1.2. Osteoporosis and plant natural products

1.2.1. The nature of osteoporosis

The word osteoporosis, which literally means porous bone, indicates that bone density is low, and that the bones are thin. However, bone does not fracture as a result of thinness alone. In the early 1990s, a consensus meeting of the World Health Organization (WHO) defined osteoporosis as: “A systemic skeletal disorder characterized by a low bone mass and by microarchitectural deterioration of bone tissue, with a subsequent increase in bone fragility and susceptibility to fracture”. The first Consensus Conference on Osteoporosis of the new millennium proposed a new definition: “A skeletal disorder characterized by compromised bone strength predisposing the bones to an increased risk of fracture.” However, in order better to understand the etiology of osteoporotic fractures and the effects of therapy on the risk of fracture occurrence, it is essential to recognize the factors that govern bone strength. The strength of an individual bone depends on the mass, shape, and the quality of the bone itself.

Since the 1950s, primary osteoporosis has been characterized into two separate entities, one related to menopausal estrogen loss and the other to aging. Riggs (Riggs, Wahner et al. 1982) elaborated on this concept

by suggesting the terms Type I osteoporosis, which signified the loss of trabecular bone after the menopause, and Type II osteoporosis, which represented the loss of cortical and trabecular bone in men and women as the end result of age-related bone loss. In the above classifications, the Type I disorder directly results from a lack of endogenous estrogen, whereas the Type II osteoporosis reflects the composite influences of long-term remodeling inefficiency, reflecting inadequacies in dietary calcium and vitamin D, intestinal mineral absorption, and parathyroid hormone (PTH) secretion. Although there may be a heuristic value to define subsets of patients in this manner, the model is compromised as it does not account for the complex and multifactorial nature of the disease. Bone mass at any time in adult life reflects the peak value of bone minerals at skeletal maturity minus that which has been subsequently lost. A adolescent girl who has experienced the interruption of menses, extended bed rest, or systemic illness might enter adult life having failed to achieve the bone mass that would have been predicted from her genetic profile. The need to understand the nature of skeletal fragility more fully and overcome the limitations of bone mineral density (BMD) measurements, has brought renewed attention to the broader array of factors that influence skeletal fragility (Bouxsein 2003, Seeman and Delmas 2006). In support of this view, osteoporosis was defined at the 2001 Consensus Development Conference as “a disease characterized by

low bone strength, leading to enhanced bone fragility and a consequent increase in fracture risk" (Nih Consensus Development Panel on Osteoporosis Prevention and Therapy 2001). This definition underscores the role of bone strength and implies that understanding bone strength is the key to understanding fracture risk.

The enhanced fragility associated with osteoporotic fractures has been attributed to several factors, chief among them being low bone mass and microarchitectural deterioration. For many years, the prevailing view has been that osteoporosis develops through an excessive loss of bone. Only recently has attention been drawn to the possibility that abnormalities in bone acquisition during early life could form a basis for later bone fragility. In other words, properties other than bone mass and BMD may contribute to skeletal fragility.

Bone remodeling, specifically the balance between formation and resorption, is the biological process that mediates changes in the traits that influence bone strength. Thus, any diseases and drugs that have an impact on bone remodeling will influence the resistance of bone to fracture. Owing to a combination of changes in the structural and material properties of bone, whole bone strength declines markedly with age. Several important concepts must be considered when assessing these determinants of bone strength. Unlike most engineering materials,

bone continually adapts to changes in its mechanical and hormonal environment, and is capable of self-renewal and repair via the process of remodeling. Thus, in response to increased mechanical loading, bone may adapt through alterations to its size, shape, matrix properties, or any combination of these. For example, in a mouse model of osteogenesis imperfecta, a defect in collagen that leads to increased bone fragility can be compensated for by a favorable change to bone geometry which preserves whole bone strength. Thus, the loss of bone strength with age likely reflects the ongoing skeletal response to changes in its hormonal and mechanical environments.

Worldwide, over 200 million people are thought to have osteoporosis; it is by far the most common bone disease and is responsible for over 9 million fractures annually. With one in three women and one in five men over 50 years old at risk, osteoporosis causes significant mortality (20–30% associated with first hip fractures) and morbidity in elderly individuals. Given the aging population, the annual healthcare cost of osteoporotic fractures is predicted to reach $25.3 billion by 2025 in the USA alone.

The primary causes of osteoporosis are related to intrinsic age-related changes in bone metabolism, which have been historically associated with postmenopausal estrogen deficiency in women and decreased

testosterone production in men. A growing number of underlying diseases (e.g., congenital connective tissue defects, metabolic and hematologic disorders, hypogonadal states, and inflammatory diseases), nutritional deficiencies (e.g., vitamin D deficiency and malabsorption), and drugs (e.g., corticosteroids and thyroid replacement drugs) are recognized as secondary causes of osteoporosis and may be key etiological factors in premenopausal cases. The cellular mechanism of osteoporosis can be simply explained by the orchestrated balance between bone resorption by osteoclasts and bone formation by osteoblasts, which maintain a relatively stable bone mass in adulthood. In osteoporosis, accelerated osteoclastic resorption overwhelms compensatory bone formation, leading to net bone loss.

Most of the currently approved drugs for osteoporosis treatment focus on bone resorption by osteoclasts. An exception is the PTH analogues, but they have the disadvantages of inconvenient administration and several undesired side effects. Moreover, most health food ingredients designed to strengthen bone act indirectly on bone or as a supplement to calcium. Therefore, the discovery and development of new natural plant-based products for use as anti-osteoporotic agents should be prioritized and commercialized. A more precise description of the drugs and

ingredients used for the treatment of osteoporosis, and their mode of action, are mentioned in subsequent chapters.

1.2.2. Drugs and Osteoporosis

Osteoporosis is often called a “silent disease,” because bone loss occurs without symptoms. It is characterized by low bone mass and the microarchitectural deterioration of bone tissue, which leads to bone fragility and increased risk of fracture. The global osteoporosis market is expected to reach USD 16 billion by 2015. This significant growth is primarily attributed to the effective treatment options currently available in the market, as well as strong pipeline products.

Fosamax was the undisputed global market leader of osteoporosis drugs until 2007, when it had a market share of almost 37%. However, this had declined to 5% by 2015 owing to patent expiry and competition from cheaper generics. The osteoporosis market offers multiple opportunities for current and future market players. In addition to increasing awareness of diagnosis and treatment, there is a need to develop new drugs that promote bone building. As the market awaits new growth driven by the launch of several promising pipeline drugs, companies are looking for innovative ways to maximize revenues from products approaching the end of their lifecycles. This thesis has developed a drug-like new natural

plant product that not only preserves bones, but also helps bone formation, to keep pace with market trends. This chapter will attempt to provide a comprehensive summary of the effects of approved osteoporosis drugs on human iliac bone. Two categories of drugs will be considered: anti-catabolic, also known as antiresorptive, and anabolic.

1.2.2.1. Anti-catabolic drugs

The tissue and cellular mechanism of bone loss in postmenopausal women with osteoporosis result mainly from an imbalance in bone remodeling, with bone resorption exceeding bone formation. The higher the turnover and the more negative the bone balance, the greater the loss of bone mass and structural integrity. In the prevention and treatment of osteoporosis, anti-catabolic therapies suppress bone resorption through a decrease in the number, activity, and life span of osteoclasts, which reduces the bone turnover rate. This reduction may also be accompanied by an improvement in the bone balance in each basic multicellular unit (BMU). Through these actions, anti-catabolic therapies are capable of maintaining or increasing bone mass, maintaining bone microarchitecture, and improving bone mineralization and mechanical properties, which ultimately result in a decreased fracture risk.

Calcitonin is a polypeptide hormone secreted by the parafollicular cells of thyroid gland in mammals and by the ultimobranchial glands of birds

and fish. Calcitonin nasal spray, a synthetic polypeptide of 32 amino acids in the same linear sequence as calcitonin of salmon origin, has been approved by the US Food and Drug administration (FDA) for the treatment of postmenopausal osteoporosis. Calcitonin increases bone mass in the spine and modestly reduces bone turnover in postmenopausal women with osteoporosis. Intranasal calcitonin has been shown to reduce the risk of vertebral fractures, but efficacy on nonvertebral fractures has not been confirmed. The effects of calcitonin on iliac bone have been reported in numerous studies of patients with osteoporosis and in one study of patients with rheumatoid arthritis (Gruber, Ivey et al. 1984, Kroger, Arnala et al. 1992, Chesnut, Majumdar et al. 2005). However, no significant change was observed in osteoclast number compared with the baseline (Marie and Caulin 1986, Palmieri, Pitcock et al. 1989, Gruber, Grigsby et al. 2000).

HT (hormone therapy), including estrogen therapy and combined estrogen / progesterone therapy, was approved by the FDA for the treatment of osteoporosis in postmenopausal women. There have been numerous reports on the effects of HT on iliac crest bone in postmenopausal women with osteoporosis, yielding sufficient evidence to conclude that the beneficial skeletal effects of HT predominantly result from the suppression of bone turnover and the resulting

preservation of bone volume and structure in cancellous and cortical bone (Steiniche, Hasling et al. 1989, Holland, Chow et al. 1994, Vedi and Compston 1996, Eriksen, Langdahl et al. 1999). Similarly, some reports revealed that 2 years of HT reduced resorption cavity size (Vedi and Compston 1996). However, they found a reduction in wall width, which was interpreted as a compensatory response to the reduction in erosion depth. Generally, HT did not significantly reduce the bone resorption, and it increased the risk of cardiovascular disease, breast cancer and stroke. The women's health initiative (WHI) suggested that the bone-friendly aspect of HT was limited in clinical practice as possible adverse effects outweighed possible benefit (Oz, Zhong et al. 2012)

Selective estrogen receptor modulators (SERMs) are steroid analogs that have been developed to exert tissue-specific action, rather than systemic effects, and thus avoid some of the adverse effects associated with HT. In some studies, the effects of raloxifene on bone were compared directly with those of HT; the two agents were shown to be similar (Weinstein, Parfitt et al. 2003). In addition, the combination therapy of raloxifene and HT was examined and exhibited a positive effect on the rabbit model of the menopause (Yang, Hu et al. 2011).

Bisphosphonates, analogs of inorganic pyrophosphate, are potent inhibitors of bone remodeling and are used extensively in the prevention

and treatment of osteoporosis (Giuliani, Pedrazzoni et al. 1998). Histomorphometric data are available for a number of bisphosphonates, including alendronate, risedronate, pamidronate, clodronate, ibandronate, and zoledronate.

The effects of alendronate have been investigated in patients with postmenopausal (Bone, Downs et al. 1997, Chavassieux, Arlot et al. 1997, Arlot, Meunier et al. 2005) or glucocorticoid-induced (Chavassieux, Arlot et al. 2000) osteoporosis. Evidence for the suppression of bone remodeling after alendronate treatment comes from data that indicate a reduction in osteoid surface and thickness, surface mineralization, bone formation rate, and activation frequency. There were currently studies on the effect of various bisphosphonates, zoledreonic acid and teriparatide, on Paget disease and osteonecrosis of the jaw (Doh, Park et al. 2015).

Denosumab is a human monoclonal antibody with high affinity and specificity for the receptor activator of nuclear factor kappa B ligand (RANKL), an essential mediator of the formation, activity, and survival of osteoclasts. Through the neutralization of RANKL activity, denosumab inhibits osteoclastic bone resorption and reduces bone turnover, consequently increasing BMD and reducing the risk of new

vertebral, nonvertebral, and hip fractures (Cummings, San Martin et al. 2009).

Although above effective drugs are available for treatment of osteoporosis, emerging therapies, such as parathyroid hormone-related protein (PTHrP) analogue (Abalopararie) and cathepsin K inhibitor (Odanacatib), have been developed for gaining more effective anti-catabolic drugs (Schultz, Wurzel et al. 2015). Unfortunately, Odanacatib was discontinued further development due to the risk of stroke after a phase III trial (Mullard 2016). Recently, the needs of new candidates, especially from natural resource, for anti-catabolic agents on osteoporosis have been growing

1.2.2.2. Anabolic drugs

In late 2002, the first anabolic therapy for osteoporosis was introduced in the form of parathyroid hormone (PTH) (1-34) or teriparatide. Anabolic therapies operate through a fundamentally different mechanism of action to anti-catabolic agents (Riggs and Parfitt 2005). Instead of reducing the activation frequency of bone remodeling, they increase it. In each remodeling transaction, the amount of new bone formed exceeds that which was removed. As a result, anabolic agents rapidly increase bone mass and have the ability to improve, rather than simply maintain, cancellous and cortical bone microarchitecture. The effects of teriparatide monotherapy on iliac crest bone biopsies were also studied in a subset of patients who participated in a fracture prevention trial (Neer, Arnaud et al. 2001, Jiang, Zhao et al. 2003, Dobnig, Sipos et al. 2005, Paschalis, Glass et al. 2005, Ma, Zeng et al. 2006). Moreover, to investigate the cellular mechanisms underlying the early actions of teriparatide on bone, a study was conducted in a small cohort of patients with postmenopausal osteoporosis who were treated with teriparatide in the presence or absence of concomitant antiresorptive therapies (Lindsay, Cosman et al. 2006).

The differential effects of teriparatide and bisphosphonates, such as alendronate or zoledronate, on iliac bone were compared in

postmenopausal women with osteoporosis enrolled in two separate trials (Dempster, Zhou et al. 2012). Finally, teriparatide, which was approved by the FDA as an anti-osteoporosis therapy for only postmenopausal women and men with osteoporosis, was tested in a cohort of premenopausal women with osteoporosis (Cohen, Dempster et al. 2011).

The clinical efficacy of strontium ranelate has been demonstrated through fracture risk reduction for postmenopausal women by 41% in vertebral fractures, 16% in nonvertebral fractures, and 36% in hip fractures after 3 years of treatment in the Spinal Osteoporosis Therapeutic Intervention (SOTI) and the Treatment of Peripheral Osteoporosis (TROPOS) (Reginster, Seeman et al. 2005, Reginster, Felsenberg et al. 2008) studies. Data on the impact of strontium ranelate on human bone material quality in transiliac bone biopsies from women with postmenopausal osteoporosis have been reported by several groups. Roschger and his colleagues investigated BMD, strontium concentration, the collagen crosslink ratio, and indentation modulus in the iliac crest biopsies after 3 years of strontium ranelate treatment. Anabolic agents found that after treatment, strontium was heterogeneously distributed in bone and preferentially present in bone packets formed during treatment. However, the mean thickness and length of the plate-shaped bone mineral crystal were not affected by strontium ranelate treatment. Similar

findings were also reported by another groups (Recker, Marin et al. 2009, Boivin, Farlay et al. 2010). Furthermore, Roschger also suggested that the effect of strontium ranelate on BMD appeared to predominantly result from the uptake of strontium and not from changes in the bone calcium content. Additionally, in another study that compared strontium ranelate to PTH (1-84), significant increases in B-cell-specific activator protein (BSAP) were seen for PTH (1-84) after 24 weeks of treatment, but not for strontium ranelate (Keller and Kneissel 2005).

These data suggested that the effect of strontium ranelate on bone remodeling is modest and its effects on fracture reduction may be predominantly mediated through a different mechanism than that observed with anabolic or more potent antiresorptive agents; the increased effect may be mediated by changes in the material properties of the matrix.

Table 1.1 Drugs and functional foods for the management of Osteoporosis

Drugs	Functional ingredients
Catabolic	**Approval type**
Bisphosphonates	*Siberian ginseng , Rosa canina L.*
- Alendronate	*Perilla frutescens* , Pananx Notoginseng
- Ibandronate	Fatty Acid Complex, N-acetylglucosamine
- Risedronate	FattyAcidComplex,N-acetylglucosamine
- Zoledronate	Hop extract
Denosumab	*Scutellaria baicalensis*
Raloxifene (SERM)	Isoflavone
Estrogen	Polycan,
Calcitonin	Green mussels oil
Anabolic	**Notification type**
Teriparatide	Vitamin D, Vitamin K, Calcium
Strontium Ranelate	Mucopolysaccharide-protein, manganese

1.2.3. Mechanism of Osteoporosis

Bone cell biology significantly progressed in a short time; the concept of intercellular communication between bone cells is now beyond dispute. By 2000, it was known that bones cells, including, but not limited to, all stages of the osteoblast and osteoclast lineages, communicate with each other through many local signaling processes. Furthermore, each of the cell lineages is subjected to influences from cells of the immune and nervous systems, which allows the very tight control of bone modeling and remodeling that is necessary to preserve the structural integrity and form of the skeleton and enable injury repair.

In the adult human skeleton, between approximately 5% and 10% of the existing bone is replaced every year by bone remodeling. The remodeling process, which continues throughout adulthood, is an integral part of the calcium homeostatic system and provides the mechanisms for the resorptive removal of old bone, adaptation to mechanical stress, repair of microdamage, and replacement of that bone by bone formation. In order to achieve this, bone is continuously resorbed and reformed at approximately 1–2 million microscopic remodeling foci per adult skeleton. Within each of these BMUs, focal resorption is performed by osteoclasts, requiring approximately 3 weeks

per site, whereas the refilling of lost bone by osteoblasts requires approximately 3–4 months.

The nature of the remodeling process, occurring as it does in different parts of the skeleton at different times, highlights the importance of locally generated and regulated factors in ensuring the appropriate communication mechanisms among the participating cells. The initiation of the cycle, for example by mechanical strain, damage, or signals from cytokines or systemic factors, generates local signals that lead to collagenase digestion of the thin layer of nonmineralized matrix under the lining cells to expose the mineralized matrix that osteoclasts can resorb (Chambers and Fuller 1985, Delaisse, Eeckhout et al. 1988, Henriksen, Sorensen et al. 2006). In addition to RANKL production by osteoblast lineage cells in response to cytokines and systemic factors, osteocytes are likely an important source of signaling to surface cells for the need either to increase bone formation or to initiate resorption (Robling, Bellido et al. 2006, Bonewald and Johnson 2008, Kogianni, Mann et al. 2008). According to this model of initiation of resorption, osteoclasts or their late precursors near to final maturation and activation must be available close to their required sites. In 2009, evidence was obtained for this possibility, with the discovery of the “osteoclast niche” - cell cycle-arrested quiescent osteoclast precursors (QuOPs) that was

shown RANK and c-fms positive and detected along bone surfaces close to osteoblasts (Mizoguchi, Muto et al. 2009). QuOPs are capable of rapid differentiation into osteoclasts, but also require the supplementation of replenished precursors from the blood.

There is ample evidence that in bone remodeling, bone formation is coupled to bone resorption. The maintenance of trabecular and cortical bone mass and architecture in accordance with loading requirements demands that bone resorption and formation are coordinated, given that a high or low level of focal resorption is usually associated with similar, but not necessarily identical, changes in the level of focal bone formation in the cells of the BMU (Fig 1.1). The theory that resorption is followed by an equal amount of bone formation came to be known as "coupling." The coupling of osteoblast-mediated bone formation to bone resorption requires an understanding of how osteoblast lineage cells, forming bone within the BMU during balanced bone remodeling, replace almost exactly the amount of bone that has been lost.

The coupling might be achieved by the activities of one or more growth factors released from the bone matrix during resorption (Mohan and Baylink 1991, Baylink, Finkelman et al. 1993). Indeed, a large number of substances can be extracted from bone matrix that are mitogenic to osteoblasts or stimulate bone formation *in vivo* (Tang, Wu et al. 2009).

Experiments in genetically manipulated mice suggested that the release of active transforming growth factor (TGF)-β1 during bone resorption might couple bone formation to resorption through the induction of the migration of bone marrow mesenchymal stem cells to sites that have been resorbed, making them available for differentiation and bone formation in remodeling (Wu, Pang et al. 2010). This would provide an explanation for the concept that in remodeling, osteoblasts are recruited from a pool of stem cells and need to be attracted to remodeling sites to be differentiated and replenish the osteoblast population.

Observations made in genetically manipulated mice and human genetics have suggested that the osteoclast itself could also be the source of an activity that contributes to the fine control of osteoblast function in bone remodeling. In mice deficient in c-src, cathepsin K, or tyrosine phosphatase epsilon, bone resorption, but not formation, is inhibited, and v-ATPase V_0 subunit D_2-deficient mice exhibit the failure of fusion of osteoclast precursors with concurrent increased bone formation (Grigoriadis, Wang et al. 1994). In these knockout mice, although resorption is greatly reduced, osteoclast numbers are not. A possible explanation for the normal level of bone formation in these mice is that these osteoclasts, although unable to resorb bone, are nevertheless capable of generating a contributory factor in bone formation. In

contrast, mice lacking c-fos, which are unable to generate osteoclasts, have reduced bone formation as well as resorption (Sims, Jenkins et al. 2004). Studies with other mutant mice, in which the specific inactivation of each of the two alternative signaling pathways through gp130 were investigated, led to the conclusion that resorption alone was insufficient to promote the coupled bone formation, but that active osteoclasts were the likely source (Martin and Sims 2005).

Several osteoclast-derived factors have been postulated as coupling factors. Cardiotropin-1 (CT-1), a member of the family of cytokines, which signal through the gp130 transducer, is expressed in differentiated osteoclasts, but not in the osteoblast lineage (Cornish, Callon et al. 1993). As well as the indirect stimulation of osteoclast differentiation through stimulation of RANKL production, CT-1, like the leukemia inhibitory factor (LIF) and interleukin-11 (IL-11) (Cornish, Callon et al. 1993), powerfully stimulates bone formation through a mechanism that begins with a rapid increase in expression of the C/EBPδ transcription factor (Pederson, Ruan et al. 2008). Unexpectedly, CT-1, like oncostatin (OSM), LIF, and PTH, also profoundly decreased sclerostin messenger ribonucleic acid (mRNA) expression by osteocytes (Zhao, Irie et al. 2006), which introduced the possibility that osteoclasts might communicate with the osteoblast lineage through direct signaling to

osteocytes. Other osteoclast-derived factors such as Wnt10b, BMP6, and sphingosine-1-phosphate can also enhance osteoblast differentiation *in vivo* studies (Allan, Hausler et al. 2008).

In a search for osteoclast products that might contribute to the coupling process, evidence was obtained, by using genetic and pharmacological approaches in mice, that osteoclast-derived ephrin-B2 acts through a contact-dependent mechanism on EphB4, its receptor in the osteoblast, to promote osteoblast differentiation and bone formation (van Bezooijen, Roelen et al. 2004). This forward signaling effect through EphB4 is less convincing than the inhibition of osteoclast formation that occurs by reverse signaling through ephrin-B2 in osteoclast precursors (Keller and Kneissel 2005). Another possible mechanism of ephrin/Eph within the osteoblast lineage arises from our finding that PTH and PTHrP promoted the production of ephrinB2 by osteoblasts, and that blockade of the interaction between ephrinB2 and receptor EphB4 impairs late-stage differentiation of osteoblasts (Bellido, Ali et al. 2005). Intracellular communication of these coupling factors might be an attractive method for the regulation of bone volumes formed in the BMU.

A further participant in these intercellular communication processes is the osteocyte. Mutations in the *sost* gene were found to be responsible for the rare sclerosing bone dysplasias, sclerosteosis and Van Buchem

disease, both of which are characterized by a greatly increased amount of bone. The *sost* gene product, sclerostin, is produced exclusively in bone by osteocytes, and acts as a negative regulator of bone formation. This inhibition occurs via Wnt signaling after binding to LRP5/6, which thereby prevents its participation in the receptor complex that activates the Wnt pathway and subsequent bone formation. The production of sclerostin by osteocytes is rapidly decreased by treatment with PTH or PTHrP (Verborgt, Tatton et al. 2002, Noble, Peet et al. 2003), mechanical loading, and the actions of cytokines including OSM, CT-1, and LIF. For each of these stimuli, the removal of sclerostin as a constitutive inhibitor of bone formation could at least partly explain the accompanying increased bone formation. Physiologically, rapid changes in the osteocyte production of sclerostin could signal to surface cells to limit the filling of remodeling spaces by osteoblasts, in addition to keeping lining cells in a quiescent state on non-remodeling bone surfaces. Several reports revealed that osteocyte-derived signals can contribute to the recruitment and formation of osteoclasts (Neer, Arnaud et al. 2001, Beral and Million Women Study 2003, Tatsumi, Ishii et al. 2007). When the dentin matrix protein-1 (DMP-1) promoter was used to generate mice expressing diphtheria toxin (DT) receptors specifically in osteocytes, and DT was used to kill the osteocytes, an increase in RANKL mRNA was detected in bones shortly after osteocyte death. This was associated with

increased osteoclast formation and bone resorption, and then viable osteocytes prevent osteoclast recruitment and activation, whereas the reverse accompanies osteocyte death. This osteocyte-mediated regulation of resorption was strengthened by reports that osteocytes are an abundant and necessary source of RANKL production.

Bone remodeling occurs at many discrete sites throughout the skeleton, but does so asynchronously, and in response to the requirements of responses to loading and unloading, damage repair, and the replacement of old bone. If PTHrP does indeed play a physiological role as a local participant in the control of bone remodeling, the generation and engagement of its receptor in response to local needs within BMUs, or systemic PTH administration, differs markedly. When PTH is used by intermittent injection to activate the PTHR1 in the bone, widespread activation of BMUs occurs. If elevated PTH levels are sufficiently prolonged, the dominant effect is increased osteoclast formation and bone resorption. If this portrayal of the PTH/PTHrP relationship holds true, it might be expected that the repeated generalized recruitment of BMUs by the daily injection regimen would increase remodeling activity to the extent that it would be reflected in increased circulating and excreted resorption markers.

Recently, a better understanding of the molecular mechanisms driving this multifactorial bone loss is moving away from an estrogen-centric paradigm to one that focuses on age-related changes within the bone microenvironment. Moreover, above mentioning local and systemic factors, acting in the process of bone remodeling and the osteoporosis, have been developed as the target of osteoporosis treatment. However most of developing candidates from these targets were dropped and shown undesired effects, like as side effect and low efficacy *in vivo* experiments. The following figure represents the cellular and hormonal mechanisms as the anabolic and catabolic action in bone remodeling (Fig 1.2).

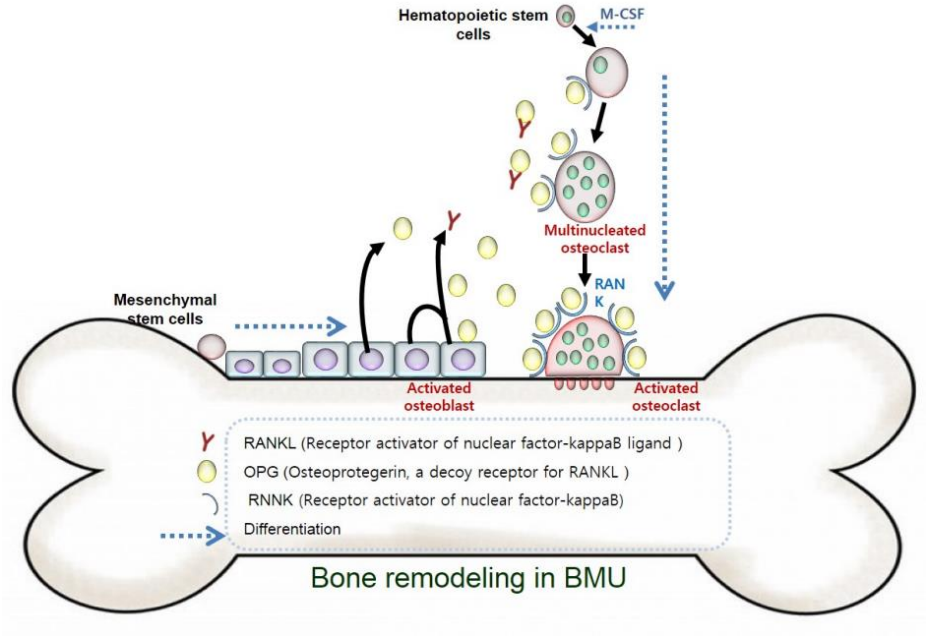

Fig 1.1 Bone remodeling in basic multicellular units (BMU) and Bone Modeling by Osteoblasts and Osteoclasts.

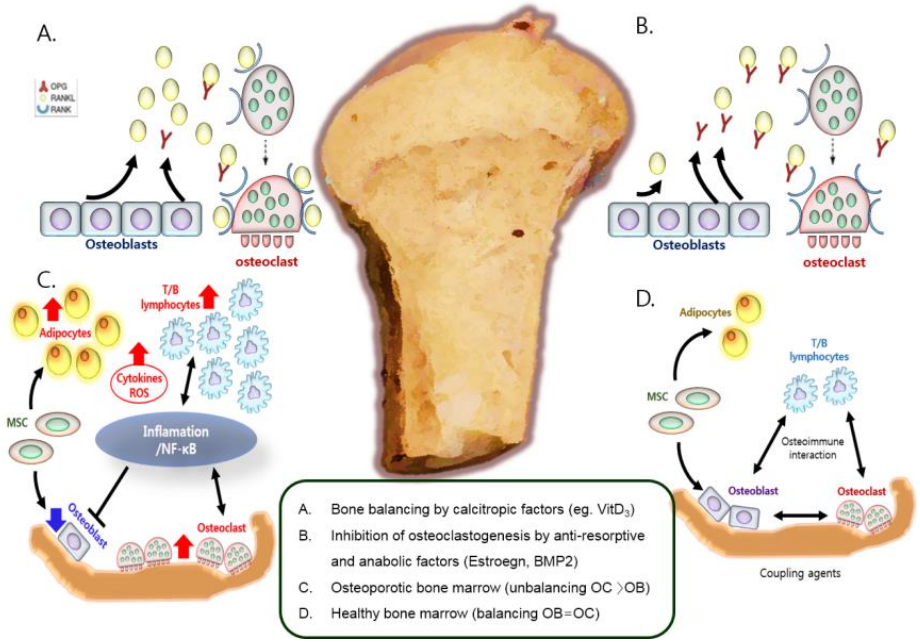

Fig 1.2 Control of Bone resorption by hormonal factors and aging.

1.2.4. Natural products used for the treatment of osteoporosis

The ideal strategy for the treatment of osteoporosis is the inhibition of bone resorption by osteoclasts and the increase of bone formation by osteoblasts. However, most of the current therapies focus only on the inhibition of bone resorption and there are only a few agents available that promote bone formation. The major treatments currently used for osteoporosis include hormone-replacement therapy, bisphosphonates, calcitonin, SERMs such as raloxifene and droloxifene, rhPTH, vitamin D analogs, and ipriflavone. The effect of these drugs in increasing bone mass or recovering bone loss is relatively minor, probably no more than 2% per year (Bilezikian 2008). However, conventional drug therapies have both positive and negative aspects. For example, although the estrogen replacement has produced positive results with respect to improved bone mineral density and reduced fracture incidence in early menopause, its prolonged use is restricted because of potential complications such as breast cancer, uterine bleeding, and cardiovascular events. One concern related to the usage of bisphosphonates is the complications of osteonecrosis of the jaw (ONJ). The incidence of ONJ is relatively low in patients administered oral bisphosphonates for osteoporosis or Paget's disease, but considerably higher in patients with malignancies that were administered high doses of intravenous

bisphosphonates (Black, Greenspan et al. 2003). Despite the excellent safety profile of PTH, concerns have arisen from its persistence after discontinuation without the sequential use of antiresorptive drugs (Finkelstein, Hayes et al. 2003). In addition, PTH is contraindicated for patients at risk of osteosarcoma. To date, most of the effective osteoporosis therapies reduce bone loss, but do not restore lost bone mass and strength. It is therefore desirable to have satisfactory bone building (anabolic) agents that stimulate new bone formation and correct the imbalance of the trabecular microarchitecture characteristics of established osteoporosis; these agents would offer a novel alternative for the treatment of osteoporosis (Xu, Lawson et al. 2005).

Plant natural products may provide solutions to the above-mentioned points, as they can be safer, show multi-target and multi-potent action, have the potential for long-term administration, and cause minimal side effects, compared with chemical and protein drugs. In recent years, interests in the treatment of osteoporosis with plant-based therapies have increased, particularly interests in traditional herbal medicines, for which extensive local knowledge has accumulated by observation over thousands of years. Herbal medicines have been widely used in clinical practice to prevent and treat bone diseases in many countries, because

they cause fewer adverse reactions and are more suitable for long-term use compared with chemically synthesized drugs.

1.2.4.1. Phytochemicals from natural products with osteoprotective and related activities

Icariin, the main active flavonoid glucoside isolated from *Epimedii folium*, has been reported to enhance bone healing and reduce the occurrence of osteoporosis. Treatment with icariin was found to increase COL I and alkaline phosphatase (ALP) mRNA expression in osteoblastic MC3T3-E1 cells in a dose-dependent manner (Song, Zhao et al. 2013). The signaling mechanism of icariin was also reported to exert osteogenic effects through the induction of BMP-2 and NO synthesis and the subsequent regulation of Cbfa1/Runx2 and osteoprotegerin (OPG)/RANKL gene expression (Li, Zeng et al. 2011). Naringin, a polymethoxylated flavonoid, was shown to increase BMP-2 expression and enhanced ALP activity, osteocalcin (OC) level, osteopontin (OPN) synthesis, and cell proliferation in primary cultured osteoblasts (Paschalis, Glass et al. 2005). Neoeriocitrin, a new dihydroflavonoid recently isolated from *Drynariae rhizoma*, significantly improved cell proliferation and ALP activity in addition to the upregulation of Runx2, COL I, and OCN expression in MC3T3-E1 cells (Li, Zeng et al. 2011).

Poncirin, a flavanone glycoside isolated from the fruit of *Poncirus trifoliata*, inhibited cytoplasmic lipid droplet accumulation and PPAR-γ and C/EBP-β mRNA expression in the murine pluripotent mesenchymal cell line C3H10T1/2. By contrast, poncirin enhanced the expression of Runx2 and transcriptional coactivator with PDZ-binding motif (TAZ). It also enhanced ALP and OCN mRNA expression, and increased mineral nodule formation in primary bone marrow mesenchymal stem cells (BMMSCs) (Yoon, Yun et al. 2011). Quercetin and rutin are common flavonoids found in fruits and vegetables. Both compounds were found to upregulate the osteoblast differentiation of BMMSCs in a dose-dependent manner. Quercetin and rutin increased ALP activity and demonstrated mineralization rates of up to 110 and 200%, respectively, compared to the control. Further, both of them were also found to increase the expression of OPN, Osx, Runx-2, OPG, and OCN (Srivastava, Bankar et al. 2013). Sweroside is a bioactive herbal ingredient isolated from *Fructus corni* and was shown to significantly increase the proliferation of human osteoblast-like MG-63 cells and rat osteoblasts. Additionally, sweroside increased ALP activity and OCN expression, and attenuated and inhibited apoptosis (Sun, Li et al. 2013). Ugonin K, a flavonoid isolated from the roots of *Helminthostachys zeylanica*, significantly increased ALP activity, expression of Bone sialoprotein (BSP) and OCN, and the mineralization of MC3T3-E1 cells.

Neobavaisoflavone and isoflavone, isolated from *Psoralea corylifolia*, concentration-dependently promoted osteogenesis in MC3T3-E1 cells.

Salvianolic acid B is a phenolic acid isolated from *Salvia miltiorrhiza*. A study by Xue indicated that salvianolic acid B promoted the osteogenesis of human mesenchymal stem cells (hMSCs) through the activation of the ERK signaling pathway, and salvianolic acid B supplementation (5 μM) increased ALP activity, OPN, Runx2, and Osx expression, and mineralization in hMSCs (Xue, Wang et al. 2014).

Costunolide is an active sesquiterpene lactone isolated from the roots of *Saussurea lappa*. The effect of costunolide on the function and growth of MC3T3-E1 cells was mediated through estrogen receptors (ERs), PI3K, ERK, protein kinase C (PKC), and mitochondrial ATP-sensitive K+ channels (Choi and Lee 2011).

Imperatorin and bergapten are two furanocoumarins isolated from *Cnidium monnieri*. Both compounds enhanced the phosphorylation of SMAD 1/5/8, p38, and ERK, and enhanced ALP activity, COL I synthesis, and bone nodule formation in primary cultured osteoblasts (Ma, Zeng et al. 2006). Psoralen, a coumarin-like derivative extracted from *Psoralea corylifolia*, was found to upregulate the expression of *BMP-2* and *BMP-4* genes, and to enhance the expression of Osx, the direct target gene of BMP signaling in primary mouse calvarial

osteoblasts. Osthole, a coumarin-like derivative extracted from *Fructus cnidii*, was reported to activate Wnt/β-catenin signaling, increase BMP-2 expression, and stimulate osteoblast differentiation (Lindsay, Cosman et al. 2006).

Kim et al. demonstrated that kirenol was capable of the promotion of osteoblast differentiation in MC3T3-E1 cells through the activation of the BMP and Wnt/β-catenin signaling pathways (Kim, Song et al. 2014). Emodin is a naturally occurring anthraquinone present in the roots and bark of numerous plants of the genus *Rhamnus*. A low concentration (5 μM) of emodin was found to strongly induce the mRNA expression of BMP-2 in MC3T3-E1 cells (Dempster, Zhou et al. 2012).

Acerogenin A, a diarylheptanoid isolated from *Acer nikoense* Maxim., increased BMP-2, BMP-4, and BMP-7 mRNA expression levels in MC3T3-E1 cells. However, noggin, a BMP antagonist, was found to inhibit the acerogenin A-induced increases in OCN, Osx, and Runx2 mRNA expression (Dobnig, Stepan et al. 2009). Genistein can induce ERα gene expression via the activation of MAPK/NF-κB/AP-1 and accordingly stimulates differentiation-related gene expression and osteoblast mineralization (Bonewald and Johnson 2008). Resveratrol, a polyphenol in red grapes and berries, stimulates the differentiation of human bone marrow stem cells and increases ALP activity (Kogianni,

Mann et al. 2008). However, most of these phytochemicals are similar in structure to isoflavone or flavonoids, and have not been shown to have meaningful efficacy as drugs in *in vivo* experiments (Table 1.2). Consequently, techniques for the screening of natural plant products and the identification of diverse phytochemical candidates with potential anti-osteoporotic properties should be developed and examined.

Table 1.2 The category, source, structure and mechanism of 36 natural compounds on osteoblast-mediated bone formation

Category	Compound name	Source	Structure	Mechanism
Flavonoid glucoside	Icariin	Herba epimedii	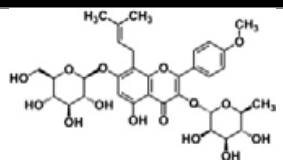	↑(ALP, COL I, bone nodule); ER-mediated ERK and JNK signal pathway ↑(BMP-2, NO,Cbfa1/Runx2,OPG/RANKL) PI3K–AKT–eNOS–NO–cGMP–PKG signal pathway ↑(BMP-2, SMAD4, Cbfa1/Runx2, OPG/RANKL) ↑(ALP, OPG/RANKL); ligand independent activation of ERα

Category	Compound name	Source	Structure	Mechanism
Flavonoid glucoside	Baohuoside-I, epimedin B Sagittatoside A	Herba epimedii	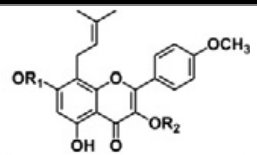	↑(ALP, OPG/RANKL); ER-dependent osteoblastic functions; Sagittatoside A: ligand-independent activation of ER α
Flavonoid	Poncirin	Poncirus trifoliata	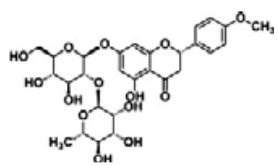	↓(PPAR-γ, C/EBP-β); ↑(Runx2,TAZ, ALP, OCN)

Category	Compound name	Source	Structure	Mechanism
Flavonoid	Rutin	Fruits and vegetables	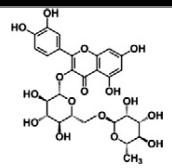	↑(ALP, OPN, Osx, Runx2,OPG, OCN)
Flavonoid	Quercetin	Fruits and vegetables	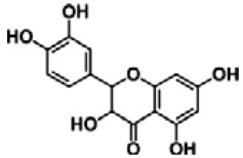	↑(ALP, OPN, Osx, Runx2,OPG, OCN) ↑(BSP, OCN); ↓(RANKL)

Category	Compound name	Source	Structure	Mechanism
Flavonoid	Taxifolin	Fruits and vegetables	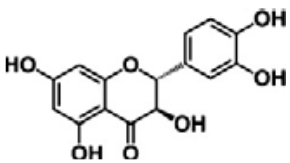	↑(BSP, OCN); ↓(RANKL)
Flavonoid	Ugonin K	Helminthostachys zeylanica	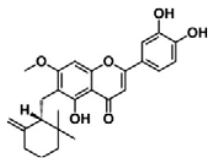	↑(ALP, BSP, OCN, Runx2, Osx); p38 MAPK- and ERK-mediated pathway; ER-dependent non-classical Src pathway and classical pathway

Category	Compound name	Source	Structure	Mechanism
Flavonoid	Genistein	Sophora japonica L.	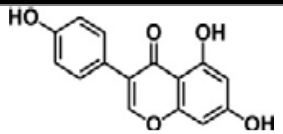	↑(ALP, COL I, OCN, BSP, Runx2 and Osx); p38-dependent pathway
Dihydro-flavonoid	Neoeriocitrin	Drynaria Rhizome	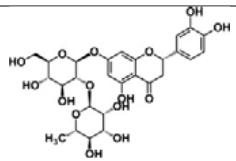	↑(ALP, Runx2, COL I, OCN)
Dihydro-flavonoid	Naringin	Drynaria Rhizome Citrus fruits	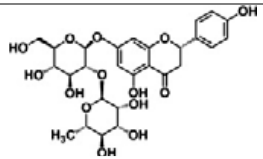	↑(ALP, Runx2, COL I, OCN) BMP-2; PI3K, Akt, c-Fos/c-Jun and AP-1 pathway

Category	Compound name	Source	Structure	Mechanism
Isoflavone	Neobavaisoflavone	Psoralea corylifolia	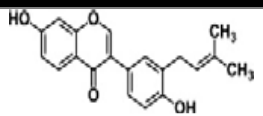	↑(ALP, COL I, OCN, BSP, Runx2 and Osx); p38 dependent pathway
Isoflavone glycoside	Puerarin	Pueraria mirifica	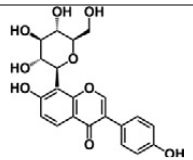	ER-dependent MEK/ERK and PI3K/Akt activation ↑(ALP, OPG/RANKL); ER-dependent
Phenylpropanoid Glycoside	Salidroside	Rhodiola rosea L.	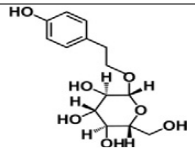	↑(ALP, OPN, Runx2, Osx, BMP-2, BMP-6, BMP-7, phosphorylation of SMAD 1/5/8 and ERK1/2); BMP signaling

Category	Compound name	Source	Structure	Mechanism
Phenylethanoid glycoside	Echinacoside	Cistanche tubulosa (Schrenk) R. Wight stems	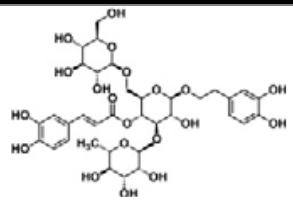	↑(ALP, COL I, OCN, OPG/RANKL)
Iridoid glycoside	Sweroside	Fructus Corni	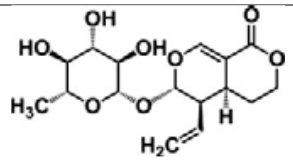	↑(ALP, OCN); inhibit apoptosis

Category	Compound name	Source	Structure	Mechanism
Phenolic glycoside	Gastrodin	Gastrodia elata	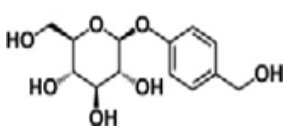	↑(ALP, OCN, COL I, OPN); ↓ROS
Steroidal saponin	Ophiopogonin D	Radix Ophiopogon japonicus	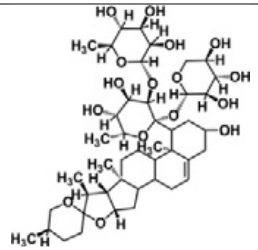	↑(ALP, OCN, COL1A1, OPN); ↓ROS; the FoxO3a-β-catenin signaling pathway

Category	Compound name	Source	Structure	Mechanism
20(S) protopanaxadiol glycoside	Ginsenoside-Rb2	Ginseng	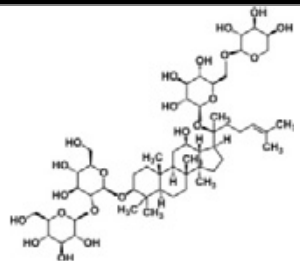	↑(ALP, COL I, OCN, OPN);↓(RANKL, IL-6, ROS)
Polyhydroxystilbenes(glycoside)	2,3,5,4′-Tetrahydroxystilbene-2-O-β-D-glucoside	Polygonum multiflorum Thunb	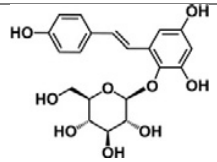	↑(ALP, COL I, OCN); ↓(RANKL,IL-6, ROS, MDA)

Category	Compound name	Source	Structure	Mechanism
Furanocoumarins	Imperatorin	Cnidium monnieri (L.) Cuss	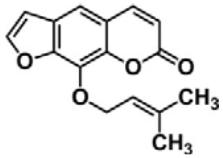	↑(ALP, COL I, bone nodule,BMP-2, phosphorylation of SMAD 1/5/8); p38 and ERK-dependent pathway
Coumarin-like derivative	Psoralen	Psoralea corylifolia	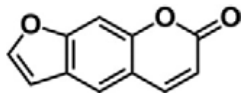	↑(ALP, COL I, OCN, BSP, Osx, BMP-2, BMP-4, phosphorylation of SMAD 1/5/8); BMP signaling

Category	Compound name	Source	Structure	Mechanism
Coumarin-like derivative	Osthole	Cnidium monnieri (L.) Cusson	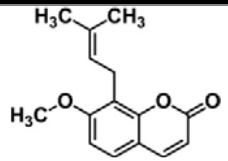	↑BMP-2; Wnt/β-catenin signaling
Sesquiterpene lactones	Costunolide	Saussurea lappa	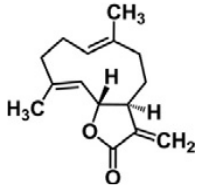	ER, PI3K, ERK, PKC, p38, JNK, and mitochondrial ATP-sensitive K+ channel

Category	Compound name	Source	Structure	Mechanism
Monoterpene	Albiflorin	Paeonia albiflora Pall	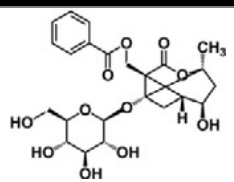	protect against oxidative stress-mediated toxicity
Diterpenoid	Kirenol	Herba Siegesbeckia	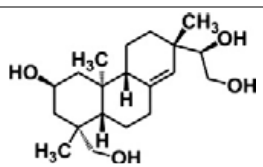	↑(ALP, COL I, OPN, OPG/ RANKL, BMP-2, Runx2, Osx; LRP5, DVL2, β-catenin, CCND1); BMP and Wnt/β-catenin pathways

Category	Compound name	Source	Structure	Mechanism
Phenolic acid	Vanillic acid	Sambucus williamsii Hance	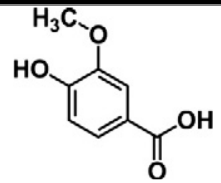	↑(ALP, Runx2, OCN, OPG/RANKL); MAPK (MEK/ERK)-mediated ER signaling pathway
Phenolic acid	Salvianolic acid B	Salvia miltiorrhiza	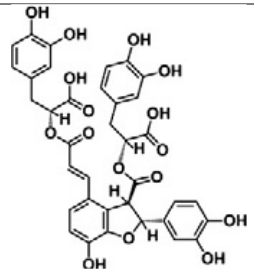	↑(ALP, OPN, Runx2, Osx); ERK signaling pathway

Category	Compound name	Source	Structure	Mechanism
Phenolic	Honokiol	Magnolia officinalis	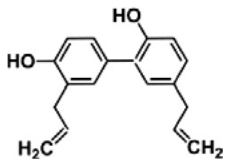	↑(ALP, COL I, OPG/RANKL, glutathione); ↓(TNF-α, IL-6, mitochondrial electron transport)
Polyphenol	Resveratrol	Red grapes and berries	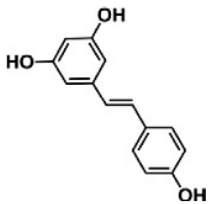	↑(ALP, Runx2/Cbfa1, Osx, OCN); ER-dependent ERK1/2 pathway

Category	Compound name	Source	Structure	Mechanism
Methoxy-substituted catechol	Apocynin	Picrorrhiza kurrooa Royle ex Benth	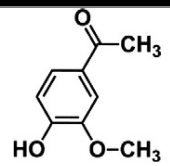	↑(ALP, COL I, OPG/RANKL);↓(ROS, TNF-α, IL-6)
Tetrameric stilbene	Kobophenol A	Caragana sinica Rhed	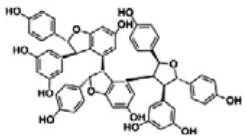	↓(NO-induced cell death); regulate JNK, NF-κB and AP-1 signaling pathways↑(ALP); ↓(ROS); p38 pathway

Category	Compound name	Source	Structure	Mechanism
Anthraquinone	Emodin	The genus Rhamnus	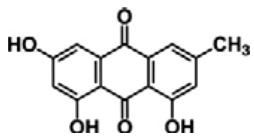	↑(BMP-2, ALP); PI3K, Akt and MAPK pathways
Diarylheptanoids	Acerogenin A	Acer nikoense Maxim	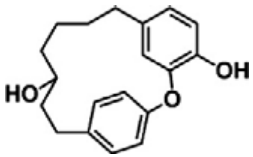	↑(OCN, Osx, Runx2, BMP-2, BMP-4, BMP-7)

1.2.4.2. Natural products with osteoprotective and related activities

Carthami flos, commonly known as safflower (Hong-Hua), is used in Chinese medicine to promote blood circulation, treat traumatic damage, and ease muscle pain. In Korean traditional medicine, the seeds of this plant are used to promote bone formation and prevent osteoporosis. Both crude and aqueous extracts promoted osteoblast differentiation in MC3T3-E1 cells. The osteoprotective properties of safflower were also associated with the inhibition of bone resorption related to the inhibition of Src kinases, the inhibition of osteoclast differentiation, and the suppression of RANKL-induced actin ring formation. The active ingredients of safflower seeds have been proposed to be the polyphenolic compounds tilianin, acacetin, and matairesinol, and their derivatives.

Cimicifugae rhizoma, known as "Sheng-Ma" in Chinese medicine, is renowned for its heat-repelling and detoxifying effects. Clinically, it is used in combination with other herbs to treat symptoms caused by excessive heat in the body, such as gum infections, mouth sores, sore throats, fevers, rashes, and skin diseases. Four triterpene compounds isolated from the extracts, namely cimicidol-3-O-β-xyloside, cimicidanol-3-O-xyloside, acetylacteol-3-O-arabinoside, and 7,8-didehydro-24-O-acetyl-hydroshengmanol-3-O-β-xyloside, were shown to decrease the circulating calcium levels in ovariectomized rats (Reeve,

Bradbeer et al. 1991). In a subsequent study, these three triterpenes were demonstrated to suppress the formation of osteoclast-like cells and their resorption activity.

Extracts of *A. heracleifolia* prevented the ovariectomy-induced elevation of serum alkaline phosphatase levels; it was able to preserve trabecular bone mass, bone volume, trabecular number, trabecular thickness, and the structure model index, as well as the BMD of the proximal tibia metaphysis and distal femur metaphysis in ovariectomized mice (Cummings, San Martin et al. 2009).

Actaea racemosa is a related species native to North America. The roots and rhizomes, known as black cohosh, are widely used for the management of symptoms associated with menopause. This natural product enhanced osteoblastic differentiation and increased the OPG/RANKL ratio in human osteoblasts. A standardized black cohosh preparation was found to prevent bone density loss at the distal end of the femur and to preserve the trabecular bone structure in the lumbar vertebra and femur of ovariectomized rats.

A triterpene saponin fraction of the plant extract was reported to be responsible for the osteoprotective effects. In mice, 25-O-acetylcimigenol 3-O-β-xylopyranoside was able to block *in vitro*

osteoclastogenesis induced by either RANKL or tumor necrosis factor (TNF)-α, and to attenuate TNF-α-induced bone loss.

Deoxyactein has also been isolated from black cohosh and was demonstrated to promote cell growth, ALP activity, collagen content, and the mineralization of MC3T3-E1 cells. In the presence of the reactive oxygen species (ROS) generator antimycin A, deoxyactein was able to suppress the production of ROS and osteoclast differentiation factors such as TNF-α, IL-6, and RANKL.

Cistanches herba, known in Chinese medicine as "Rou-Cong-Rong," is a kidney- and yang-tonifying drug that is believed to invigorate the essence of the body and blood. Common uses and indications include general physical weakness, fatigue, lower back pain, and joint weakness. In an early study, a monoterpene, 8-hydroxy-2,6-dimethyl-2-octenoic acid, was identified as an anti-osteoporotic compound from a related plant species, *C. salsa*. More recently, the plant has been revisited for its anti-osteoporotic potential.

An aqueous *Cistanches* extract dose-dependently enhanced BMD and bone mineral content, as well as improving bone biomechanical indices, such as maximum load, displacement at maximum load, and stress at maximum load, in ovariectomized rats (Reeve, Bradbeer et al. 1991). The extract was also reported to protect against ovariectomy-induced

bone degeneration through the regulation of bone metabolic genes, such as Smad1, Smad5, TGF-β1, and TIEG1 (Tang, Wu et al. 2009). An extract of *C. deserticola* was reported to promote osteoblast differentiation, as evidenced by increased alkaline phosphatase activity and mRNA expressions of BMP-2 and OPN.

Echinacoside, a phenylpropanoid glycoside also present in *Echinacea spp.*, has been isolated from *C. tubulosa* and was demonstrated to cause significant increases in MC3T3-E1 cell proliferation, ALP activity, collagen 1 secretion, osteocalcin levels, and mineralization (Li, Zeng et al. 2011). The authors concluded that OPG and RANKL may be involved in the anti-osteoporotic actions of echinacoside (Nakashima, Hayashi et al. 2011). In a follow-up *in vivo* study, the research team demonstrated the ameliorative effects of echinacoside against ovariectomy-induced damage, which led to improvements of BMD, bone biomechanical properties, microarchitecture, histomorphology, and uterus immunohistochemistry (Nakashima, Hayashi et al. 2011).

There have been many biological and pharmacological studies, both *in vitro* and *in vivo*, which have demonstrated that a wide variety of natural products possess potential beneficial effects on the maintenance or promotion of bone health. The information presented in Table 1.3 summarizes the Chinese herbal medicine sources of these bioactive

molecules. These substances may be useful as alterative medicines for osteoporosis, especially as preventive agents or as treatment at the early stages, along with exercise and calcium/vitamin D supplementation, to retard bone loss. Although many studies and investigations of anti-osteoporotic natural products, phytochemicals, and plant extracts, have been performed, few natural products are available on the market. This might be explained by the low efficacy demonstrated in *in vivo* osteoporotic models, the toxic ingredients found in many natural products, and the many obstacles to the identification of active phytochemicals. Therefore, the screening, exploration, and identification of new anti-osteoporotic natural plants and phytochemicals is important from both an academic and a commercial perspective.

Table 1.3 Botanical sources of natural products from Chinese medicinal herbs showing osteoprotective potential (Che et al, 2016)

Latin name	Chinese name	Plant part	Major active molecule
Actaea heracleifolia (Kom.) J. Compton;	Sheng-Ma	Rhizome	cimicidol-3-*O*-β-D-xyloside, cimicidanol-3-*O*-β-D-
Astragalus mongholicus Bunge	Huang-Qi	Root	formononetin
Carthamus tinctorius L.	Hong-Hua	Flower	matairesinol, tilianine, acacetin and their derivatives
Cistanche deserticola Y.C. Ma;	Rou-Cong-Rong	Stem	8-hydroxy-2,6-dimethyl-2-octenoic acid, echinacoside
Cordyceps sinensis (Berk.) Sacc.	Dong-Cong-Xia-		Cao cordycepin
Dioscorea spp.		Rhizome	Diosgenin, diospongins B and C, piperitol, sesqminone,
Dipsacus asperWall. ex C.B. Clarke;	Xu-Duan	Root	asperosaponins V and VI, hederagenin-3-O-(2-O-
Drynaria fortunei (Kunze ex Mett.) J. Sm.	Gu-Sui-Bu	Rhizome	naringin and other flavos
Eclipta prostrata L.	Mo-Han-Lian	Above-ground parts	diosmetin, 31-hydroxybiochanin A, 31-O-methylorobol
Epimedium brevicornum Maxim.;	Yin-Yang-Huo	Leaf	icariin, epimedins A, B and C, baohuoside-1,
Erythina variegate L.	Hai-Tong-Pi	Bark	6-prenylgenistein, 8-prenylgenistein, 6,8-

Latin name	Chinese name	Plant part	Major active molecule
Eucommia ulmoides Oliv.	Du-Zhong	Stem bark	geniposidic acid, geniposide, aucubin,
Ferula spp.	A-Wei	Resin	Ferutinin
Ligustrum lucidumW.T. Aiton	Lu-Zhen-Zhi	Fruit	oleanolic acid, ursolic acid,
Lycium babarum L.	Gou-Qi-zi	Fruit	polysaccharide
Morinda officinalis F.C. How	Ba-Ji-tian	Root	physicion, rubiadin, rubiadin-1-methyl ether, 2-
Ormosia henryi Prain	Lu-Mu	Root	isoformononetin
Oxytropis falcata Bunge	Lian-Xing-Ji-Dou	Whole plant	isoformononetin
Paeonia lactiflora Pall.	Bai-Shao	Root	6′-*O*-β-D-glucopyranosyl albiflorin
Panax spp.	Ren-Shen	Root	ginsenosides
Podocarpium podocarpum (DC.)	Yang et Huang	Whole plant	podocarnone, luteolin, astragalin, afzelin, kaempferitrin,
Polygonum cuspidatum Siebold & Zucc.	Hu-Zhang	Root and Rhizome	resveratrol
Psoralea corylifolia L.	Bu-Gu-Zhi	Fruit	psoralen, isopsoralen, psoralidin, corylin,
Pueraria lobate (Willd.) Ohwi	Ge-Gen	Root	isoformononetin,
Rehmannia glutinosa (Gaertn.) DC.	Di-Huang	Root	acteoside

Latin name	Chinese name	Plant part	Major active molecule
Salvia miltiorrhiza Bunge	San-Shen	Root/rhizome	salvianolic acids A and B,
Sambucus williamsii Hance	Jie-Gu-Mu	Stem	ficusal, ceplignan, dehydrodiconiferyl alcohol,
Sophora japonica L.	Huai-Jiao	Fruit, seed and root	genistein, 8-prenylkaempferol,
Sophora flavescens Aiton	Ku-Shen	Root	formononetin
Trifolium pretense L.	Hong-Che-Hou-	Inflorescence and twig	formononetin
Viscum coloratum (Kom.) Nakai	Hu-Ji-Sheng	Twig	(-)-syringaresinol 4-*O*-β-D-glucoside

1.3. Natural product from plants for whitening

1.3.1 Plant natural products used as cosmetic ingredients

Cosmetics are defined as “any substance or mixture intended to be placed in contact with the various external parts of the human body with a view to cleaning them, perfuming them, changing their appearance, protecting them, maintaining their good condition, or correcting the body.”. Cosmetics and personal care companies have had a long and significant interest in natural products; what was once a peripheral element of the industry has now become mainstream and continues to grow. Any natural products used as ingredients in marketed cosmetics should be reported and evaluated for their safety and modest bio-activity. The pharmaceutical industry uses several plants for drugs that are not suitable for use in cosmetic products. The 1989 Cosmetic Safety Act lists forbidden plant materials, which include belladonna (*Atropa belladonna*) and foxglove (*Digitalis purpurea*) (Dweck, 1996).

Natural molecules derived from plant extracts offer a particularly exciting avenue for further research. However, plant extracts are often poorly defined with respect to their method of extraction, plant-to-solvent ratio, and the content of active ingredients. Moreover, the

stability of the color, odor, transparency, and/or active ingredients over time is also often a limiting factor. Plant extracts differ from purified therapeutic agents in several aspects. First, they are more dilute than the pure chemicals that are familiar to us; second, herbs often contain additional active constituents that may be closely related both chemically and therapeutically to the primary active constituent. Natural plant “total extracts” as well as “selective extracts” are used in cosmetics. Total extracts are applied mainly according to the historical tradition of their use. In contrast, selective extracts are employed owing to investigations into their specific activities.

Major cosmetic companies continuously search for novel bioactive ingredients which are derived from the sea, the earth, and the plant kingdom. Popular ingredients include Chinese herbs, vitamins, minerals, antioxidants, enzymes, hormones, and a multitude of natural products. Plants were once the main source and foundation of all cosmetics, before methods were discovered to synthesize substances with similar properties. However, synthetic chemicals and extracts from other organisms, such as animals, have been gradually replaced by plant natural products, extracts, or phytochemicals. This is partly because of the poor reputation that animal-derived extracts have acquired over the past few years. Some animal-derived products need to be replaced, but

synthetic chemicals cannot always match their performance. Moreover, the use of natural ingredients in the cosmetics industry has grown significantly over the last 15 years, driven by growing consumer interests in health and well-being, as well as in organic and fair-trade products. This has led to an increased demand for botanical ingredients.

In an overview of natural products in the cosmetic market, skin care products are dominant (over 40%) and Asia represents the largest sales market for natural products (Fig 1.3). At present, various selective extracts are introduced for different effects in the modulation of skin properties, for example: licorice for skin irritations; ginkgo as a free radical scavenger; bearberry for skin lightening (complexion); walnut for skin tanning; and wheat germ for stimulating cell proliferation (Marks, 1997). Although, whitening and lightening effects are the most popular and expanding market in the skin care and color industry in Asia, limited natural products are currently used for whitening (Table 1.4). Therefore, for the discovery of new whitening natural products is important, not only academically, but also commercially.

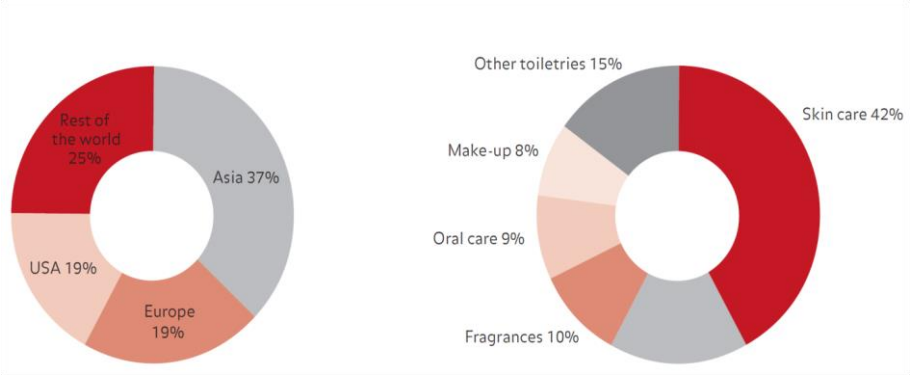

Fig 1.3. Sales of natural care products by region and product class, 2011 ("Access and benefit sharing in a time of scientific, technology and industry change: The Cosmetics sector", Rachel Wynberg and Sarah Laird, 2013)

1.3.2 Melanogenesis and whitening

Skin-whitening products are commercially available for cosmetic purposes to obtain a lighter skin appearance. They are also utilized for the clinical treatment of pigmentary disorders, such as melasma or postinflammatory hyperpigmentation. Whitening agents act at various levels of melanin production in the skin. Many of them are competitive inhibitors of tyrosinase, the key enzyme in melanogenesis; others inhibit the maturation of this enzyme, or the transport of pigment granules (melanosomes) from melanocytes to surrounding keratinocytes.

In the skin, melanocytes are situated on the basal layer that separates the dermis and the epidermis. One melanocyte is surrounded by approximately 36 keratinocytes. Together, they form the so-called epidermal melanin unit. The melanin produced and stored inside the melanocyte in the melanosomal compartment is transported via dendrites to the overlaying keratinocytes. The melanin pigment is a polymer synthesized from the amino acid L-tyrosine, which is converted by the enzyme tyrosinase into dopaquinone inside the melanosomes. Therefore, the most obvious cellular target for whitening agents is the tyrosinase enzyme.

Research efforts on synthetic and natural tyrosinase inhibitors have been recently reviewed in several papers (Goetz and Anderson 2010, Briscoe and Therond 2013, Nachury 2014). Tyrosinase inhibitors can be classified as competitive, uncompetitive, mixed type, or non-competitive inhibitors (Briscoe and Therond 2013). The nature of tyrosinase inhibition can be determined through the measurement of enzyme inhibition kinetics using Lineweaver-Burk plots with varying concentrations of L-3,4-dihydroxy-phenylalanine (L-DOPA) as the substrate. This can be seen, for example, in polyphenol extracts from acerola (West Indian cherry) or chalcone derivatives isolated from *Morus nigra* (black mulberry), which are described in the recent work of

Hanamura et al. and Zhang et al. (Gerdes and Katsanis 2008). The knowledge of the type of inhibition may be important for achieving optimal skin lightening effects as combined treatments may result in synergistic effects. This has been shown in a mixed treatment of the competitive tyrosinase inhibitor, arbutin, and the noncompetitive inhibitor, aloesin (Goetz and Anderson 2010, DeCaen, Delling et al. 2013).

Melanogenesis is the physiological production of melanin, a light-absorbing pigment that is responsible for the coloration of human skin and hair, together with three other biochromes (Liu, Zhi et al. 2015)**(**Fig 1.4**)**. This pathway was first reported by Raper in 1928 and later revised. It occurs in melanosomes, membrane-bound organelles located inside the melanocytes, from the base layer of the epidermis, also known as the stratum basale (Galluzzi, Baehrecke et al. 2017). Melanocytes constitute the second most important dermis cell lineage though keratinocytes represent 80% of the epidermis. Once melanin is produced, melanocytes transport the melanosomes, that have previously lost their tyrosinase activity, along their dendrites to reach the neighboring keratinocytes (Barmada, Serio et al. 2014). The keratinocytes are dispersed regularly and almost exclusively in the basal epidermis layer. The association of a melanocyte with 30–40 keratinocytes constitutes the epidermal unit in

which further reactions take place (Rich, Burkett et al. 2003, Onodera and Ohsumi 2005). Melanin then accumulates in the keratinocytes, where it conducts its preventive functions against photocarcinogenesis. The biosynthesis of this pigment plays a crucial role in skin protection by shielding it from sunlight damage (UV radiation absorption) and ion accumulation, and by trapping reactive oxygen species (Papandreou, Lim et al. 2008, Masini, Bugliani et al. 2009, Schneider and Cuervo 2014). Oxidative stress, a direct consequence of the environment (e.g., UV radiation and pollution) and lifestyle (e.g., cigarette smoking) of an individual, is implicated in skin pathogenesis and leads to alterations in connective tissues and the formation of lipid peroxides and reactive oxygen species harmful to the skin, and can lead to accelerated aging. Melanogenesis is a complex pathway regulated by several enzymes including tyrosinase, phenylalanine hydroxylase (PHA), and tyrosinase-related proteins (TRP-1 and TRP-2) (Fig 1.5). Tyrosinase, a glycosylated copper-containing polyphenol oxidase, is the key enzyme involved in the melanogenesis pathway. Tyrosinase is mainly involved in the initial rate-limiting reactions of melanogenesis, e.g., the hydroxylation of L-tyrosine (monophenolase activity) to L-3,4-dihydroxy-phenylalanine (L-DOPA) and its further oxidation (diphenolase activity) to produce L-dopaquinone. After L-dopaquinone synthesis, melanin biosynthesis diverges into two pathways, the eumelanin synthesis pathway and the

pheomelanin synthesis pathway. While pheomelanin and eumelanin are both found in human skin and hair, eumelanin is the dominant form and can be further divided into two types, brown eumelanin and black eumelanin. Insufficient eumelanin is the main cause of albinism. Pheomelanins chemically differ from eumelanins in that the oligomer structure of pheomelanins incorporate benzothiazine intermediate units, whereas eumelanins incorporate DHI and DHICA intermediate units (Greco, Panzella et al. 2012).

Table 1.4 The Korea Food and Drug Administration(KFDA) approved whitening cosmetics agents

No	Whitening functional ingredient	Content
1	Broussonetia Extract	2%
2	Arbutin	2~5%
3	Ethyl Ascobyl Ether	1~2%
4	Oil Soluble Licorice Extract	0.05%
5	Ascorbyl Glucoside	2%
6	Magnesium ascorbyl phosphate	3%
7	Niacinamide	2~5%
8	Ascorbyl Tetraisopalmitate	2%
9	Alpha isabolol	0.5%

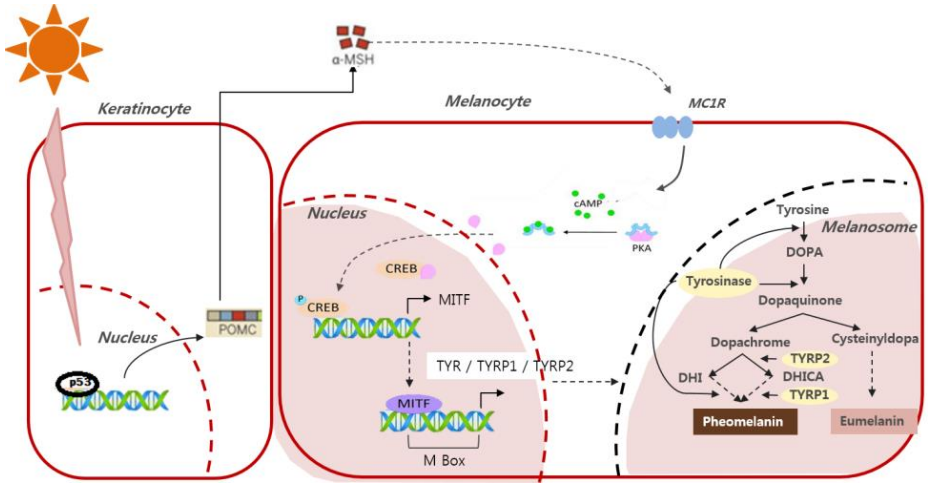

Fig 1.4 Melanogenesis pathway.

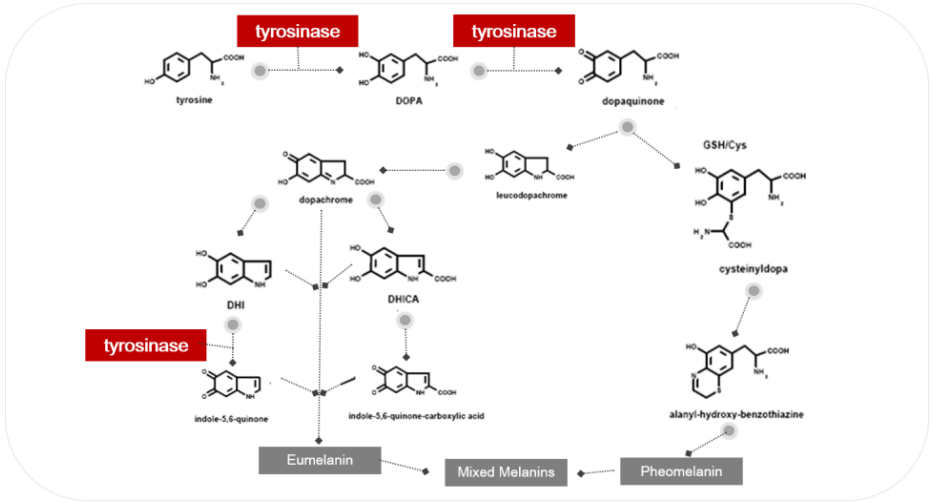

Fig 1.5 Melanogenesis complex pathway in melanosome.

1.3.3 Autophagy and whitening

Autophagy (from the Greek “self-eating”) is a conserved intracellular process for the degradation of proteins and organelles in lysosomes (Zhang and Baehrecke 2015) and this removal of damaged components, and continuous turnover to facilitate their renewal, is a cornerstone of the maintenance of cellular homeostasis (Mizushima 2005). The components awaiting recycling are sequestered into double-membrane vesicles, known as autophagosomes. Autophagosomes fuse with lysosomes, vesicle-shaped organelles with hydrolytic enzymes in their luminal region, which allows the degradation of the material enclosed within them (Liu, Zhi et al. 2015).

Cells use autophagy to maintain their physiological homeostasis; that is, for protein degradation, organelle recycling, and energy generation. Nevertheless, autophagy is also an inducible stress mechanism and increases in response to nutrient deprivation, bacterial infections, and protein misfolding to promote cell survival (Rich, Burkett et al. 2003, Onodera and Ohsumi 2005). Starvation is a strong selective pressure that has resulted in the evolutionary development of efficient nutrient sensing mechanisms in all organisms. Receptors and transporters located on the cell surface sense nutrient availability in the extracellular space and

transduce the information to the intracellular machinery responsible for energy production (Efeyan, Comb et al. 2015, Kaur and Debnath 2015). To maximize their sensory functions, most cell types present plasma membrane microtubule-based organelles known as primary cilia, which protrude from the cell surface and are rich with sensing and signaling receptors (Nachury 2014).

Cilia are composed of a central axoneme containing nine pairs of microtubules that grow through an assembly of tubular components, in a process known as ciliogenesis. The composition of the axoneme differentiates two types of cilia, namely the primary cilia (PC) and the motile cilia (MC), which feature an extra central pair of microtubules. Both MC and PC are rooted to basal bodies, structures that are derived from the centrioles after cell division. Defective or absent cilia cause pathologies, collectively known as ciliopathies, which range from polycystic kidney disease (PKD) to respiratory diseases, cognitive impairment disorders, and developmental disorders (Christensen, Pedersen et al. 2007). The unique morphology and positioning of the PC allows the activation of these pathways in response to extracellular changes or stresses. In recent years, changes in ciliary growth have been directly related to changes in autophagic activity. However, the complexity of this regulatory role has led to conflicting reports, whereby

blockage of autophagy can either increase or decrease ciliary length. Some of these opposing effects arise from the dual functionality of autophagy, which degrades both the proteins that contribute to ciliary growth (Pampliega, Orhon et al. 2013) as well as the regulatory proteins that block ciliogenesis (Tang, Lin et al. 2013).

Under nutrient-rich conditions, basal autophagy prevents continuous PC growth through the direct degradation of intraflagellar transport (IFT)20. However, upon serum removal, IFT proteins are required for ciliogenesis, and are thus spared from degradation. This switch from basal to induced autophagy promotes selective degradation of OFD1 and subsequent PC growth (Tang, Lin et al. 2013).

Recently, some reports have revealed the role of autophagy in the regulation of melanogenesis (Kim, Jo et al. 2013, Kim, Shin et al. 2013, Murase, Hachiya et al. 2013, Kim, Chang et al. 2014). Autophagy regulators control vesicle trafficking pathways, such as the biosynthetic pathways in melanogenesis, and play a key role in the regulation of melanocyte biology; therefore, they play an intimate role in controlling both the production of melanosomes and the transcription of MITF target genes. In addition to regulating melanosome formation, conventional autophagy participates in the removal of melanosomes in the context of

human diseases and melanomas. Recent studies have provided insight into the roles that different multiprotein complexes play in the regulation of autophagy and endosomal trafficking. Future studies should characterize the differential roles of multiprotein autophagy complexes in melanosome formation and destruction. (Hsiang Ho et al. 2011). The role of autophagy in the maintenance of cellular homeostasis is reportedly based on the degradation of useless proteins or damaged organelles in a lysosome-dependent manner (Kaur and Debnath 2015, Fullgrabe, Ghislat et al. 2016). Thus, autophagy functions as a cell-protective response to UV radiation (Klionsky, Abdalla et al. 2012). Although autophagy was considered to be a non-selective degradation pathway a decade ago, recent studies have shown that specific target organelles can be selectively eliminated. These selective pathways include mitochondrial autophagy (mitophagy) and peroxisomal autophagy (pexophagy) (Anding and Baehrecke 2017). Functional genome screening suggested that autophagy regulatory proteins, such as WIPI1 and Beclin1, are involved in pigmentation (Ganesan, Ho et al. 2008, Ho, Kapadia et al. 2011) and that autophagy contributes to skin color determination through the regulation of melanin degradation in keratinocytes (Murase, Hachiya et al. 2013) (Fig 1.6). Moreover, various autophagy regulators and the well-known whitening agent, resveratrol, increase melanin degradation via autophagy activation; the existence of

melanin in autophagosomes was shown by using EM analysis (Kim, Shin et al. 2013, Kim, Chang et al. 2014). Nonetheless, the role of autophagy in the regulation of skin pigmentation has not been well elucidated.

From a commercial viewpoint, the current whitening ingredients have focused on the inhibition of tyrosinase (Fig 1.7), which is a key enzyme in the melanin synthesis process. Therefore, if new whitening ingredients from natural plants or novel target-based agents were discovered, they would be remarkably shared and sales in the global market.

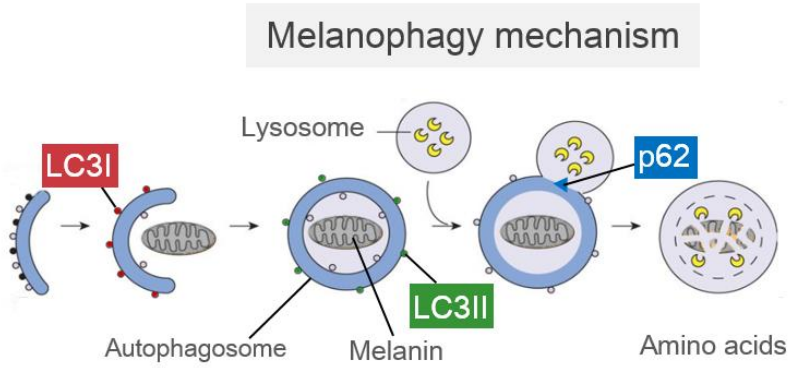

Fig 1.6 Modulation of autophagy regulators on melanosome formation and destruction

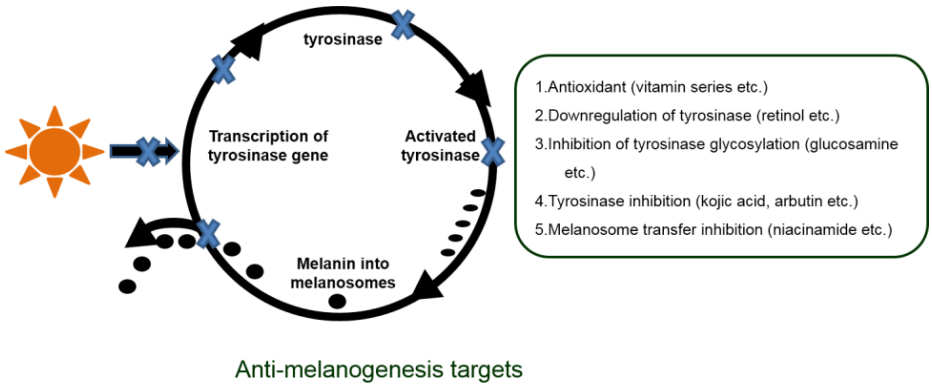

Fig 1.7 The mechanism of action of various pigmentation control targets and effective agents

1.4. Objectives of the dissertation

This dissertation focuses on the screening, evaluation, and selection of effective natural products and phytochemicals for the identification of potent anti-osteoporotic and anti-melanogenic agents. The specific objectives of this research are as follows:

1) Identification of plant extracts and their constituent phytochemicals effective as anti-osteoporotic drug candidates and preventive and therapeutic agents through *in vitro* and *in vivo* experiments.

2) Evaluation of natural anti-melanogenesis plant extracts *in vitro* and *in vivo* and the characterization of their actions as potent whitening agents.

Chapter 2

Effects of *Edgeworthia papyrifera* and edgeworoside A on osteoporosis as potent preventive and therapeutic agents

2.1. Summary

In this study, a library of extracts derived from 4,200 plants native to Korea was screened in a high throughput screening (HTS) system, which monitors NF-κB expression in RAW264.7 cells and ALP (Alkaline Phosphatse) activity in MC3T3-E1 cells. Then, the hits derived from these assays were further investigated in an osteoclastogenesis assay and AR-S (alizarin red staining) assay. The screening operations led to the identification of EP (*Edgeworthia papyrifera*) and DG (*Daphne genkwa*) as anti-osteoporotic agents. To evaluate their activities *in vivo*, both extracts were administered to ovariectomized mice. After 4 weeks, while the cortical bone thickness (Cbt) of ovariectomized mice was severely decreased compared to that of the sham group, the Cbt of the test groups administered the extracts remained similar to that of the control group. Other parameters that represent bone strength, such as Tbn (trabecular bone number) and Tbl (trabecular bone length), were also improved by the extracts.

To evaluate the therapeutic potential of EP, the extract was administered to ovariectomized rats for 9 weeks. Following this, the osteoclastogenic and osteogenic markers were each analyzed by using assay kits, and the trabecular bone was evaluated by micro CT.

Administration of EP to the ovariectomized animals resulted in a decrease in the levels of osteoclastic markers in the blood compared with the vehicle-treated group. In addition, the volume and structure of the trabecular bone was maintained as determined by micro CT imaging

To further investigate the extracts, the phytochemical constituents were identified by a dereplication method that involves ultra-high–performance liquid chromatography with high-resolution mass spectrometry (UHPLC-HRMS). From the results of the UHPLC-HRMS, 10 phytochemicals were identified, and the effects of each constituent on osteoclasts and osteoblasts were analyzed *in vitro*.

Among the target compounds tested, edgeworoside A showed dose-dependent inhibition of osteoclast differentiation and activation of osteoblast proliferation. To further evaluate this major constituent of *E. papyrifera*, the structure of the purified form was confirmed by high-resolution mass, MS/MS, and 1H-NMR spectrum analysis. As expected, the purified edgeworoside A also showed anti-osteoporotic activity *in vitro*, with an IC_{50} (half maximal inhibitory concentration) of 9.94 μM against osteoclastic inhibition.

Taken together, these results suggest that EP and its constituent edgeworoside A are promising drug candidates for the treatment of osteoporosis.

2.2. Introduction

Osteoporosis is one of the most common metabolic bone diseases. It is characterized by an imbalance of bone resorption over bone formation during the bone remodeling processes. This results in decreased bone mineral density and the disruption of the bone microarchitecture. The recent estimation by the IOF (International Osteoporosis Foundation) revealed that there are 200 million women who develop osteoporosis. The incidence of hip fracture is expected to rise from 1.66 million in 1990 to 6.26 million in 2050 (Cooper, Campion et al. 1992). Moreover, the cost of treating osteoporotic fractures in the United States would be tripled by the year 2040, compared with $19 billion in 2005 (Burge, Dawson-Hughes et al. 2007).

Bone remodeling is a key process of growth and maintenance of normal bone mass and strength, and it is tightly regulated by hormones, cytokines, and various external stimuli. The bone tissue continuously undergoes remodeling by bone resorption and bone formation, and the old bone is degraded by osteoclasts and replaced by osteoblasts (Hadjidakis and Androulakis 2006).

Osteoclasts, the bone resorbing cells, degrade the bone by secretion of acid and proteinases. For the maturation of osteoclasts, hematopoietic

stem cells differentiate into multi-nucleated osteoclasts by a fusion process which is induced by M-CSF (macrophage colony-stimulating factor) and RANKL (receptor activator of NF-κB ligand) (Lacey, Timms et al. 1998). M-CSF is important for the proliferation and survival of the osteoclast precursor cells, and RANKL is a cytokine from the TNF (the tumor necrosis factor) family that stimulates the differentiation of osteoclast precursor cells into mature osteoclasts (Kong, Yoshida et al. 1999).

Osteoblasts, the bone-forming cells, synthesize the matrix of the bone and control its mineralization. For the maturation of the osteoblasts, mesenchymal stem cells differentiate into preosteoblasts which show ALP (alkaline phosphatase) activity (Peng, Kang et al. 2004). The preosteoblasts then transform into mature osteoblasts, characterized by the secretion of bone matrix proteins, such as OCN and collagen type I, and attain a cuboidal shape.

Several drugs, including bisphosphonates (BPs), denosumabs, SERM (Selective estrogen receptor modulators), calcitonin, and teriparatide, are currently being used in clinical practice for the prevention and treatment of osteoporosis (Tabatabaei-Malazy, Salari et al. 2017). However, severe side effects and inconvenience in the administration of, and treatment with some of these currently available therapies provide the rationale to

explore newer candidates available in nature (Khajuria, Razdan et al. 2011).

Thus, these efforts on discovering new therapeutic agents have been fruitful—several plant extracts and phytochemicals have been found and utilized (Baek, Kim et al. 2014, Visagie, Kasonga et al. 2015, Zhang, Guan et al. 2015). *Berberis aristata* extract showed anti-osteoporosis activity in ovariectomized rats. Various Chinese and Korean traditional medicinal plants, such as *Achyranthes bidentata, Davallia formosana, Polygonatum sibiricum,* and *Carthamus tinctorius,* were also reported to exert anti-osteoporotic activity *in vitro* and *in vivo* (Yogesh, Chandrashekhar et al. 2011). Despite these efforts, the Korea Food and Drug administration has only permitted a limited number of functional ingredients to be used to improve bone health, including soy isoflavone, black yeast culture powder, and *E. senticosus* complex extract.

In this chapter, a library of 4,200 plant extracts was screened for the ability to inhibit osteoclast differentiation and stimulate the proliferation of osteoblasts. Selected plant extracts were evaluated in a preventive and therapeutic rodent model (ovariectomized model). After arriving at a candidate that showed potential as an anti-osteoporosis agent, its constituents were identified and their effects on osteoclasts and osteoblasts were investigated *in vitro*. The results suggest that the

identified plant extract and phytochemicals can be used as functional ingredients for the improvement on bone health and as drug candidates against osteoporosis.

2.3. Materials and methods

2.3.1. Reagents

A library of methanol extracts derived from Korean-native plants including *E. chrysantha* was provided by the plant extract bank at the Korea Research Institute of Bioscience and Biotechnology (KRIBB; Daejeon, Korea).

The compounds used were obtained from the following suppliers: edgeworoside A (Analyticon, NP-013336); Daphnoretin (Angene, AGN-PC-0QTRQJ); Tiliroside (Sigma 79257); Rutin hydrate (Sigma, R5143); Chlorogenic acid (Sigma, C3878). Chlorogenic acid methyl ester was synthesized in house.

2.3.2. Raw264.7 Cell Culture

Raw264.7 cell line (obtained from ATCC, ATCC® TIB-71™) was cultured in DMEM (Gibco, 11995-065) supplemented with 10% FBS (Gibco 19000) and 1% Penicillin-Streptomycin (Sigma, P4458) at 5% CO_2, 37 °C incubator.

2.3.3. NF-κB stable cell

Drug screening assays were conducted using RAW264.7 cells stably transfected with an NF-kB-driven luciferase reporter gene construct. To investigate the effect of Bay11-7082 on NF-kB activity, RAW264.7 cells stably transfected with an NF-kB-driven luciferase reporter gene were treated with 100 ng/mL RANKL (Pepprotech, 310-01) for 5 h following incubation with various doses of Bay11-7082 for 2 h. Luciferase activities were measured using a Envision Ultra Sensitive Luminescence mode.

2.3.4. High-throughput screening (HTS), NF-κB reporter gene assay

The cells were plated out onto 384-well white plates in 40 μL assay media at a density of 20,000 cells/well and incubated O/N at 37℃, 5% CO_2 incubator. The cell were treated with natural extracts or a reference (Bay 11-7082, 5 μM) compound using pintool (0.1 μL, final conc. 10 μM or 25μg/mL, DMSO 0.25%) for 2 h, and then were further incubated for 5 h following treatment with RANKL (final con. 100 ng/mL, 20 μL). Luciferase activity was measured with a Renilla-Glo™ (Promega, E2620) Luciferase assay reagent.

2.3.5. Tartrate-resistant acid phosphatase (TRAP) assay

Raw 264.7 cells were stimulated to differentiate into osteoclast-like cells with recombinant RANK-L (Pepprotech, 310-01). Raw 264.7 were seeded on a 96-well plate (corning costar 3599) at a density of 10^4 cells/well. After 2 h incubation, the culture medium was changed to osteoclast differentiation medium [α-MEM (Welgene, LM008-02), 10% FBS (Gibco, 16000-044), 1% Penicillin-Streptomycin (Sigma, P4458), 100 ng/mL RANK-L, and then either natural extracts, compounds, or controls were added to the cultures. The cells were cultured for 5 days with osteoclast differentiation medium. TRAP activity was measured using a TRAP kit (Kamiya, KT008) following the instructions from the manufacturer (Flexstation, Absorbance 540nm).

2.3.6. MC-3T3 Cell Culture

MC3T3-E1 cells (obtained from ATCC, CRL-2593, clone 4) were cultured in α-MEM (Welgene, cat.No. LM008-01) supplemented with 10% FBS (Gibco 19000) and 1% Penicillin- Streptomycin (Sigma, P4458) at 5% CO_2, at 37 °C incubator.

2.3.7. High-throughputs screening (HTS), Alkaline phosphatase (ALP) assay

MC3T3-E1 cells were seeded at a density of 200 cells/well in a 384-well plate (Greiner, 781091) and allowed to attach overnight. The next day, medium was changed to growth medium [α-MEM (Welgene, LM008-01), 10% FBS (Gibco, 16000-044), 1% Penicillin-Streptomycin (Sigma, P4458), 50 μM Ascorbic acid (Sigma A8960), 10 mM Glycerophosphate (Sigma G5422)], and either natural extracts, compounds, or controls were added to the cultures. The cultures were treated with natural extracts and 50 ng/mL of bone morphogenetic protein 2 (BMP-2, Pepprotech, cat.No. 120-02) using a pintool and the medium was replaced every three days. Alkaline phosphatase activity was measured using an Alkaline Phosphatase Assay Kit (Colorimetric) (Abcam, ab83369). After 14 days of culture, the cells were washed with 50 mM Tris-HCl and lysed in assay buffer for 1 h at 37 ℃. The lysates were incubated with 5 mM Nnpp (ρ-nitrosophenyl phosphatate) in the dark for 2 h at 25℃. The absorbance was then measured at 405 nm (Flexstation).

2.3.8. Alizarin Red S (ARS) Assay

MC3T3-E1 cells were seeded at a density of 10^4 cells/well in a 96-well plate (Corning costar 3599) and allowed to attach overnight. The next day, medium was changed to osteogenic differentiation medium [ODM, α-MEM (Welgene, cat.No. LM008-01), 1 μM Dexamethasone (Sigma D4902), 50 μM Ascorbic acid (Sigma A8960), 10 mM Glycerophosphate (Sigma G5422)], and then natural extracts, compounds, or controls were added to the cultures. Medium was replaced every three days with the appropriate treatment addition.

Mineralization of calcium deposits was assessed by Alizarin Red S staining. After 21 days, the cells were washed once with PBS, fixed for 20 min in ice cold 70% (v/v) ethanol, and rinsed once with deionized water. Cultures were stained for 15 minutes with Alizarin Red S (Sigma A5533), and then excess dye was removed gently using deionized water. For quantification of mineralization, the cells stained with Alizarin Red were lysed with 100 mM Cetylpyridinium chloride (Sigma C0732) and the absorbance at 540 nm was measured using a microplate reader (Flexstation).

2.3.9. Animals and Husbandry

To observe anti-osteoporotic potential of the natural products, ddY mice and Sprague-Dawley (SD) rats were used for the experiment at the Soonchunhyang University and Chosun University, respectively. Firstly, virgin female, specific pathogen-free outbred, Kwl: ddY mice (6-week old upon receipt) (Kiwa, Wakayama, Japan) were selected and allowed to acclimate for 7 days. The animals were maintained with a controlled temperature (22±2℃) and humidity (50~55%) under 12h: 12h (light: dark cycle). Normal diet (Harlan 2018S, USA) and tap water were given *ad libitum.* The animals were placed in individual cages and the food intake and water consumption were measured every 24 h during the experiment. All laboratory animals were controlled according to national regulations for the usage and welfare of laboratory animals and approved by the Institutional Animal Care and Use Committee (IACUC) in Soonchunhyang University prior to the experiments (Approval No. SCH2015-0036). Secondly, SD rats (virgin female, 24-week old) were selected and acclimatized for 7 days. The animals were housed with a controlled temperature (24±2℃) and humidity (50~55%) under 12 h: 12 h (light: dark cycle). During the study period, rodent normal diets and tap water were consumed *ad libitum.* The animals were placed in individual cages and the food intakes and water consumptions were

measured every 24 h during the experiment. All laboratory animals were controlled according to national regulations for the usage and welfare of laboratory animals and approved by the Institutional Animal Care and Use Committee (IACUC) in Chosun University prior to the experiments (Approval No. 2016-A0031). In addition, experiments on osteoporosis were performed based on United States Food and Drug Administration Guidelines.

2.3.10. Mice models for osteoporosis induction

In the present study, ddy mice (6 weeks old upon receipt) were prepared, and bilateral ovariectomy (OVX) was performed 7 days after acclimatization. Mice were anesthetized with intraperitoneal administration of 20 mg/kg of Zoletile (Zoletile 50TM; Virbac Laboratories, Carros, France) and maintained with 2.0 ± 0.5% isoflurane (Hana pharmaceutical Co., Hwasung, Korea) in a mixture of 70% N_2O and 30% O_2. Surgery was conducted according to the previously established method. In brief, mice were initially pre-anesthetized with 2% isoflurane (Hana Pharm. Co. Hwasung, Korea) in the chamber, and then maintained with 1~1.5% isoflurane in a mixture of 70% N_2O and 28% O_2. The OVX group were treated open surgery involving bilateral OVX through midline incision *linea alba* abdomen. Afterwards, the

incision was sutured by two layers. Muscular layers were sutured independently from other peripheral tissues using 3-0 silk sutures (Ailee Co. LTD., Busan, Korea) and the skin was closed by continuous sutures using 3-0 silk. The incisions at the non OVX control group were made along the *linea alba* abdomen and then stitched again, which did not perform bilateral OVX. In OVX and Sham control mice, only distilled water (vehicle) was orally administered in equal volumes and periods instead of the natural products (*Edgeworthia papyrifera* -OVX_EP group and *Daphne genkwa*-OVX_DG group) (20mg/kg), respectively. The schedule with this ddY mice OVX model is described in Fig 2.1A.

2.3.11. Rat models for osteoporosis induction

Forty female SD rats over 24 weeks of age were used at the estrogen deficiency through OVX-induced osteoporosis for investigating the natural compounds having therapeutic effects on anti-osteoporosis. The experimental groups for the study were summarized at Table 2.1.

The experimental animals were maintained in specific pathogen free conditions for at least one week for adaptation prior to surgery. In brief, both sides back of the SD rats were shaved and treated with iodine tincture prior to anesthesia. Oxygen containing 1.5 isoflurane was added to induce and maintain the anethesia during the surgery. Sterile surgical

blade (#15) was used for OVX at the lower part of both kidneys at the site of the rats about 3~5 mm. OVX was performed after the both uterine tubes was tied with a suture, and ointment treatment was conducted following suturing the incision site preventing from infectional inflammation and pain relief. The schedule with this SD rat OVX model is described in Fig 2.1B.

2.3.12. Physiological Data

2.3.12.1 Body weight

Mice. The body weights were measured daily before the oral administration of theplant extracts or compounds and the tendency of changes in body weight would be an important indicator of animal health conditions. Thus the data were carefully collected throughout the experiment. ***SD rats***. The collection of cumulative results for body weight is identical to that of the mice model described above.

2.3.12.2. Blood chemistry

For serum biochemistry, approximately 100 µl or 1 mL of whole blood was obtained from vena cava upon scarifying the mice and rats, respectively. The serum was separated from the blood by centrifugation

at 12,000 × g for 20 min at 4℃ using a clotting activated serum tube. All collected serum samples were frozen at –80℃ until they were assayed.

2.3.12.3. Selection of animals for estrogen deficient animals

Estrogen levels in the collected serum were analyzed to select the animals with osteoporosis. Serum estradiol levels were measured using the chemiluminescent immunoassay technique (ECLIA, Roche e411 immunoassay analyzer, Roche, Penzberg, Germany).

2.3.12.4. Verification of biomarkers for Bone resorption

PYD is released into the blood by collagen degradation during bone resorption and is almost metabolized in the body and excreted in the urine. To analyze PYD the urine of laboratory animals was separated and collected. The PYD concentration was measured by the method described in the ELISA kit (Rat Pyridinoline crosslinks (PYD) ELISA KIT, E02P0743). Activated osteoclast secretes various enzymes to absorb bone, and acid phosphatase reflects bone resorption as it is resistant to L-tartrate. Therefore, 0.2 mL of blood was collected from the tail vein of the experimental animals and centrifuged at 4,000×*g* for 10 minutes to separate plasma. The plasma was analyzed with a tartrate-resistant acid phosphatase (TRACP) & ALP assay kit (TAKARA,

MK301) according to manufacturer's protocol.

2.3.12.5. Analysis of the biomarkers related to bone formation

Since osteocalcin (OC) is a protein specific to bone and dentin, it is produced in osteoblasts. Therefore, an OC level can reflect the degree of osteogenesis. Thus, in order to measure OC in the plasma of isolated animals, rat glu-osteocalcin analysis was performed according to the analysis method provided by the High Sensitive EIA kit (TAKARA, MK146).

ALP is an enzyme secreted from osteoblasts and reflects the activity of osteoblasts. Therefore, the ALP values in the plasma of the animals were determined with TRACP & ALP assay kit (TAKARA, MK301) according to the method provided by manufacturer.

2.3.12.6. Analyses of Calcium and phosphate metabolism

The concentrations of calcium and phosphate in the blood after ovariectomy are reduced by calcitiropic hormone in the animals. Therefore blood calcium and phosphate concentrations were measured using a calcium detection kit and a phosphate assay kit, respectively.

2.3.12.7. Measurements of Bone Mineral Density (BMD)

The mean BMD of total body and the right femur were determined using the *in vivo* X-ray radiography micro-CT system (Korea Basic Science Institute, GwangJu Center; Quantume GX uCT, Perkin Elmer)

2.3.13. Bone Staining

The left sides of each mouse femur were removed and fixed in 10% neutral-buffered formalin, and then they were decalcified in decalcifying solution (24% formic acid and 0.5 N sodium hydroxidehydorixide) for three days (the solution was exchanged once a day for 3 days) at room temperature. Afterwards, the decalcified bone samples were embedded in paraffin sectioned about 4 μm, and stained with Hematoxylin & Eosin (Sigma-Aldrich, HHS32 & HT110232, Warrington, PA) and Masson trichrome staining kit (Polyscience, inc, 25088-1, St. Louis, MO).

2.3.14. Bone histomorphometry

Bone histomorphometry was performed using an automated image analyzing system under a microscopy (Olympus, BX-51, Japan) to examine bone mass, structure with bone resorption in a uniform area of epiphyseal or cortical bone regions of the femurs (growth plate areas were excluded). Cortical bone thinckness was measured in the mid-shaft regions of the femur, Trabecular bone volume (TV/BV, TBV; %),

thickness of trabecular bone (Tbt; μm/trabecular bone), number (Tbn; mean numbers of trabecular bone/epiphyseal areas), length (Tbl; mm/tranbecular bone) were measured for bone mass and structure, and osteocalst number (Ocn; mean osteoclast numbers/epiphyseal areas) and ratio (OS/BS; %) were measured on the bone surface (cortical bone), or the number of eroded surfaces as previously reported (Melton, Chrischilles et al. 2005).

2.3.15. Statistics analysis

Data are expressed as the means ± standard deviation (SD) or ± standard error of the values. Multiple comparison tests were performed a two-tailed test for the different dose groups. Variance homogeneity was examined using the Levene test. If the Levene test indicated no significant deviations from variance homogeneity, the data were analyzed using the one-way ANOVA test followed by the least-significant differences test to determine which group comparisons were significantly different. P value of <0.05 was considered statistically signicant.

2.3.16. Preparation and extraction of *E. papyrifera*

The dried extract of *E. papyrifera* was dissolved in 70% methanol, and 5 µL of sample was analyzed by LC-MS technique. All LC/MS analyses were carried out using an LTQ Orbitrap XL (Thermo Electron Co., USA) coupled to an Accelar ultra-high pressure liquid chromatography system (Thermo Electron Co., USA). Chromatographic separation of metabolites was conducted using a ACQUITY UPLC®BEHC_{18} column (2.1×150 mm,1.7 µm), operatedat 40°C and using mobile phases A (water) and B (acetonitrile with 0.1% formic acid) at a flow rate of 0.4 mL/min. The initial gradient composition (95% A/5% B) was held for 0.5 min, increased to 80% B in 10 min, decreased to 0% A in 10.01 min and held for 1.90 min. For recycling, the initial gradient composition was restored and allowed to equilibrate for 3 min. The LC-MS system consisted of a heated electrospray ionization probe (HESI-II) as the ionization source. HESI was operated at 300 °C with spray voltage of 5.0 kV. The nebulizer sheath and auxiliary gas flow rates were set at 50 and 5 arb, respectively. MS analysis was performed with polaritys witching, and the following parameters for MS/MS scan: *m/z* range of 100-1,000; collision-induced dissociation energy of 45%; data-dependent scan mode. The Orbitrap analyzer was used for high-resolution mass spectra data acquisition with a mass resolving power of 30,000 FWHM at *m/z*

400. The data-dependent tandem mass spectrometry (MS/MS) experiments were controlled using menu-driven software provided with the Xcalibur system. All experiments were performed under automatic gain control conditions.

2.3.17. Extraction and purification of phytochemicals

To obtain phytochemicals and secondary metabolites from *E. papyrifera,* dried twig and leaf (each 200 g) of *E. papyrifera* were extracted with MeOH for 24 h at room temperature and evaporated under reduced pressure at 40ºC to give residues (9.95 g and 19.69 g, respectively). Then the extract was diluted in 50% methanol (v/v in deionized water) to achieve concentrations of 540 mg/10 mL. Each extract was purified by high-pressure liquid chromatography (HPLC) on a Waters AutoPurification System (Waters, USA) with a QDa detector and a Waters Xbridge prep C_{18} Column (19 × 250 mm, 5 μm) with a gradient of A (0.1% formic acid v/v in deionized water) and B (acetonitrile) at flow rate of 25 mL/min. The initial gradient composition (90% A / 10% B) was held for 2.8 min, increased to 65% B in 43 min, and then decreased to 0% A in 45 min held for 5 min.

2.3.18. Nuclear magnetic resonance (NMR) analysis

^{1}H and ^{13}C NMR spectra were recorded on Bruker Avance II 400 (Bruker, USA) in MeOD solutions. Working frequencies were 400.1 and 101.0 MHz for ^{1}H and for ^{13}C, respectively.

2.4. Results

2.4.1. Development of HTS-compatible assays

During bone remodeling, osteoclasts (OC) are differentiated from the osteoclast precursors. This process is called 'osteoclastogenesis,' and the NF-κB signaling through TRAF6 induced by RANKL is the main signaling pathway for OC differentiation. Hence, a luciferase reporter gene under the control of the NF-κB site was constructed. In order to adapt the NF-κB reporter assay to an HTS system, a RAW264.7 cell line stably expressing the NF-κB reporter gene was established. The expression of the luciferase gene was increased by RANKL, and the RANKL-induced reporter gene expression was decreased by a reference compound Bay11-7082 (Fig 2.3A). The optimal dose and time for the treatment with a positive control (Bay11-7082) and RANKL, respectively, were determined as follows: 5 μM of Bay11-7082 for 2 h; 100 ng/mL of RANKL for 5 h (Fig 2.4A). Finally, the data derived from the negative control group (RANKL only) and the positive control group (Bay11-7082) were analyzed to calculate the z-score to confirm the significance and reproducibility of the results (Fig 2.4B).

Osteoblasts (OB), differentiated from mesenchymal stem cells, play a

key role in bone formation. ALP is the main marker for osteoblast differentiation and osteogenic activity of the OB. The ALP activity was measured by monitoring the amount of p-nitrophenol, which is produced by the hydrolysis of p-nitrophenyl phosphate (p-NPP) by ALP (Fig 2.3B).

The ALP assay was adapted to an HTS system that allows the identification of osteogenic inducers. In addition, it was confirmed the significance and reproducibility of the ALP HTS system using a reference compound (z' score = 0.4) (Fig 2.4D).

MC-3T3E1 cells were plated out to a 384-well plate and incubated for 18 h. The cells were treated with the extracts or a reference compound for 14 days, with replacement of the media every three days. The cultures were then analyzed for ALP activity as described in materials and methods.

2.4.2. Screening for potent anti-osteoclastic plant extracts

During the bone resorption process, NF-κB expression is induced by RANKL in osteoclasts, and thus the inhibitors of NF-κB expression prevent osteoclstogenesis (Jimi, Ikebe et al. 1996, Franzoso, Carlson et al. 1997, Bharti, Takada et al. 2004). As a mentioned above, Raw264.7

cells stably expressing the NF-κB-dependent reporter gene were established and treated with RANKL to activate transcription of the luciferase reporter gene. 4,200 extracts were screened for their ability to inhibit the RANKL-induced luciferase activity, and found 9 hit extracts (Table 2.2, Fig 2.5). These hit extracts were not cytotoxic as determined by the MTS assay (data not shown).

TRAP is a biomarker which is expressed during osteoclast differentiation. By measuring the TRAP activity, it was confirmed whether the 9 hit extracts could inhibit osteoclast differentiation. Raw264.7 cells were treated with 100 ng/mL RANKL and the extracts (0.78–12.50 μg/mL) for 5 days, after which the TRAP activity was measured. The results showed that 4 out of 9 hits were able to inhibit RANKL-induced TRAP activity in RAW 264.7 cells, suggesting that the extracts may inhibit osteoclast differentiation (Table 2.3, Fig 2.6).

2.4.3. Screening for potent osteogenic plant extracts

A library of 4,200 natural plant extracts was screened for the ability to enhance the differentiation of MC3T3-E1. The ALP activity was measured as a readout of MC3T3-E1 cell differentiation. The extracts were tested at a concentration of 25 μg/mL. Among them, 19 extracts enhanced ALP activity more than a 1.68-fold relative to the DMSO control (Fig 2.7, Table 2.4). They were not cytotoxic to MC3T3-E1 as determined by the MTS assay (data not shown).

Bone mineralization is the main process of bone formation, and calcification is an important marker for osteoblast differentiation and maturation. The degree of mineralization and differentiation can be measured with the use of alizarin red (AR), which is absorbed to calcium and quantified by measuring absorbance at 540 nm.

Optimizing the periods of differentiation which are suitable for AR staining was established. MC3T3-E1 cells were incubated with a reference (BMP-2) under differentiation conditions for increasing periods of time (7–28 days). The AR staining was evident at day 21. However, the staining appeared to diminish thereafter.

With the optimized conditions for AR-S assay, the effects of 19 hits on calcification in MC3T3-E1 were examined. The cells were treated with

increasing concentrations of the extracts (0.39–6.25 μg/mL) for 21 days, and the results showed that 6 of them did indeed increase the calcium mineralization in MC3T3-E1 cells (Fig 2.7, Table 2.5).

2.4.4. Selection of anti-osteoporotic plant extracts

For the selection of candidates as anti-osteoporosis agents, a series of assays were performed. First, a library of 4,200 natural extracts was screened for the ability to inhibit RANKL-induced NF-κB signaling. The hit extracts were then filtered to gain more effective extracts using the TRAP assay. Thereafter, 4 extracts were selected as candidate anti-osteoclastogenesis agents (Table 2.3).

In addition, the extract library was tested using the ALP assay to identify osteogenic agents, and the primary hits were then evaluated using the AR-S assay. A total of 6 extracts with the ability to increase calcium mineralization were found (Table 2.5).

However, some of the selected extracts were not considered appropriate for further evaluation *in vivo* due to their cytotoxicity and limited commercial availability. Consequently, two plant extracts, EP and *Daphne genkwa*, were selected as viable candidates (Table 2.6, Fig 2.9).

2.4.5. Preventive effect of *E. papyrifera* and *D. genkwa* extracts on ovariectomized mice

The selected natural products, DG and EP extracts were subjected to rapid evaluation of their anti-osteoporosis efficacy in an OVX mice model.

The animals were divided into the following groups: a control group to which only the vehicle (Veh) was administered; the Non_Veh group, which was subjected to abdominal incision to expose the ovaries and administered the vehicle; the NON_P group which was subjected to abdominal incision to expose the ovaries and administered DG or EP extract; the OVX_Veh group, which was ovariectomized and administered the vehicle alone, and the OVX_P group which was subjected to ovariectomy and administered the DG or EP extract (Fig 2.1A). For the sham operation, the surgical abdominal incision was closed with sutures without removing the ovaries.

As described in Fig 2.2., the animals were sacrificed to assess the anti-osteoporotic potential of both substances after administration of DG and EP according to the experimental schedule.

2.4.5.1. Examination for gross morphological abnormalities

After sacrificing the animals, all organs were examined by stereo-microscopy (Olympus, model SZ61®, Japan) to assess any gross morphological abnormalities. The microscopic observation detected diffuse nodules in the small intestine of most of the animals administered with the DG extract. In contrast, the animals administered with the EP extract did not show any abnormal morphology in any organ (Fig 2.10).

2.4.5.2. Histopathologic evaluation of the bones

The histopathological evaluation was performed using hematoxylin-eosin (H&E) and Masson's trichrome (MT) staining. (Fig 2.11, Fig 2.12). H&E staining is generally the most basic method for histopathological evaluation, while MT has different specific applications. The latter is more suitable for distinguishing cells from surrounding connective tissue. Therefore, most recipes produce red keratin and muscle fibers, blue or green collagen and bone, red or pink cytoplasm, and dark-brown to black cell nuclei. This method is very useful for the pathological evaluation of bone, and is a widely used dyeing method.

As shown in Fig 2.11A and Fig 2.12A**,** bone loss was evident in the OVX_Veh group as compared to that in the sham and Non_Veh groups.

However, the ovariectomy-induced bone loss was significantly prevented in the OVX_P group administered with DG or EP

2.4.5.3. Histomorphometry of the bones

The bone histomorphometric parameters were analyzed, including trabecular bone volume (%), trabecular bone number (Tbn, #/epiphyseal), trabecular bone length (Tbl, longitudinal thickness; μm), trabecular bone thickness (Tbt, cross thickness; μm), cortical bone thickness (Cbt, cross thickness; μm) and osteoclast cell number (Ocn, osteoclast cell number; #/Epiphyseal). The results showed that the DG and EP extracts significantly prevented OVX-induced osteoporosis and suggest that repeated administration of DG and EP could be very useful for the prevention of osteoporosis (Fig 2.11B and Fig 2.12B).

2.4.6. Therapeutic effects of the *E. papyrifera* extract on ovariectomized rats

Both, DG and EP extracts, showed excellent anti-osteoporotic effects. However, as shown in the previous studies **(**Fig 2.10), the use of DG caused abnormalities such as diffuse nodules in the small intestine in the previous OVX mice model. In addition, the use of DG extract was finally excluded from further validation in the light of reports of possible safety

issues with human use (Geng, Ma et al. 2013, Qiao, Zhao et al. 2014). As described in the Materials and Methods, animals were divided into 5 groups (n=6 in each group): naive; sham; OVX; OVX+EP (26.25 mg/kg/day); OVX+EP (56.5 mg/kg/day)

2.4.6.1. Body weight gain

Data were collected on weight gain of the experimental groups during the 9 weeks to assess the anti-osteoporotic effect of EP extract. The sham group showed similar weight gaining behavior as the naïve control group during the experimental period. In addition, the ovariectomized group administered with vehicle only showed similar weight gaining behavior as the ovariectomized group administered with extracts. However, the ovariectomized groups (OVX and OVX + EP) tended to gain more weight than did naive and sham groups.

2.4.6.2. Biomarker analysis of pyridinoline for bone resorption

Pyridinoline (PYD) is released into the blood by collagen degradation during bone resorption and almost metabolized in the body and excreted in the urine of the animals. Therefore, urine from the experimental

animals was collected and analyzed by the PYD ELISA. The result was shown in the Fig 2.13. The PYD concentrations were obtained according to the equation gained from the standard line (Fig 2.13A). As shown in Fig 2.13B, while sham-operation had no effect on the level of PYD as compared to naïve control, ovariectomization led to a significant increase in the level of PYD ($p < 0.01$ when compared to the sham-operated group). An OVX-induced increasement of the concentration of PYD was reduced by 25.6% in the group of OVX+EP (52.5 mg/kg).

2.4.6.3. Analysis of TRACP in serum

TRACP, an enzyme present in the osteoclasts, was secreted to absorb bone, this acid phosphatase reflects the bone resorption. As shown in Fig 2.14, the TRACP concentrations in the plasma of the naive and sham control groups after 9 weeks of oral administration were 2.26 ± 0.43 μg/mL and 2.50 ± 0.22 μg/mL, respectively ($p=0.08$). However, the level of TRACP was significantly increased by ovariectomization and was higher than the respective level in the sham-operated group ($p < 0.01$). The results also showed that an OVX-induced increase in the levels of TRACP were reduced by 52.5 mg/kg EP.

2.4.6.4. Analysis of serum osteocalcin

Serum OC concentrations are significantly correlated with bone growth, and are elevated in puberty. Its increase is detected after menopause for early diagnosis of postmenopausal osteoporosis.

Analyzed in Fig 2.15, OC concentrations in the naive and sham control groups were 4.84 ± 0.39 μg/mL and 4.98 ± 0.25 μg/mL, respectively, and ovariectomization led to a significant increase in the level of OC ($p < 0.01$ when compared to the sham-operated group). However, OVX-induced increase in the level of OC was not reduced by 52.5 EP administration.

2.4.6.5. Analysis of serum ALP

The ALP level is known to have a significant correlation with bone growth, and hence used for the early diagnosis of postmenopausal osteoporosis as its concentration increases after menopause. As shown in Fig 2.16., ovariectomization led to a significant increase in the level of ALP ($p < 0.01$ when compared to the sham-operated group). However, EP had no significant effect on the level of ALP in ovariectomized animals.

2.4.6.6. Serum calcium concentrations measured by calcitrophic hormone metabolism in the animals

In animal studies, the concentrations of calcium and phosphate in the blood after ovariectomy are reduced by calcitropic hormone. As shown in Fig 2.17**,** serum calcium concentrations of the naive and sham groups were 2.25 ± 0.085 mM and 2.29 ± 0.28 mM, respectively, and sham-operation did not appear to affect a serum calcium level. However, the serum calcium concentration was significantly reduced by ovariectomization (1.84 ± 0.07 mM). It is of note that an OVX-induced decrease in calcium level was recovered by EP administration (52.5 mg/kg) to a level similar to that observed in the sham control.

2.4.6.7. Measurement of estrogen concentration to determine the success of the OVX surgical outcome

Estrogen plays a crucial role in bone homeostasis and its deficiency cause both the early and late forms of osteoporosis in postmenopausal women. This hormone induces the synthesis of active vitamin D and indirect inhibition of bone resorption. Therefor hormone replacement therapy and SERM have been used to treat osteoporosis in postmenopausal women. Thus, it is necessary to analyze the changes in estrogen concentrations following ovariectomization.

As shown in Fig 2.18**,** serum estradiol concentrations in the naive and sham groups were 5.53 ± 0.26 pg/mL and 5.64 ± 0.38 pg/mL, respectively. As expected, the serum estradiol concentration was significantly reduced by ovariectomization (4.09 ± 0.16 pg/mL) However, an OVX-induced decrease in estradiol level was not recovered by EP administration.

2.4.6.8. Bone fracture risk verification by *in vivo* X-ray radiography micro CT

Bone mineral density can be expressed as a measure of bone strength and fracture latitude, and the lower the bone density, the greater the risk of fracture. In thesis, the right femur of the experimental animals was removed and *in vivo* X-ray radiography was performed. According to the Fig 2.19, it was observed that the trabecular bone which is generally broad and compact over the area from mid-shaft to epiphyseal region as seen in the naive and sham groups, was different in the OVX group. The trabecular bone was not only very small in size, but also had a very small distribution over the bone area at 9 weeks after oral administration. This can be examined in more detail through the horizontal view and the sagittal view, as provided in Fig 2.19. Although animals progressed to osteoporosis after ovariectomy, in the case of OVX+EP (26.25

mg/kg/day and 52.5 mg/kg/day), which were repeatedly treated for 9 weeks, the density and volume of the trabecular bone were significantly increased compared to that of the OVX animals treated with only the vehicle. This is consistent with the results for the test materials in the other effects. It has been demonstrated in this experiment that sustained oral administration of EP has a therapeutic effect sufficient to inhibit osteoporosis in the OVX-induced osteoporosis animal models.

2.4.7. Identification of phytochemicals in *E. papyrifera*

Table 2.7 shows the phytochemicals identified in the extract from *E. papyrifera*. Analysis of the extracts using ultra-high–performance liquid chromatography with high-resolution mass spectrometry (UHPLC-HRMS) revealed 10 phytochemicals. The high-resolution mass and MS/MS spectral characteristics of phytochemicals were compared to commercially obtained standards and published data. After extraction by ion chromatography (XIC), the LC-MS data were manually sorted to list the information provided, such as the retention time, the m/z values for [M+H]+, and the MS/MS fragmentation pattern, from the base-peak chromatograms (Table 2.7). Each high-resolution MS spectrum and MS/MS spectrum peak were identified using the natural-product database available online and in-house MS/MS spectral library.

Searchable MS/MS spectra libraries based on the results of the liquid chromatography coupled with electrospray ionization (ESI) and tandem mass spectrometry (LC-MS/MS) with data-dependent acquisition using an ion trap mass spectrometer were compiled with respect to the identification and confirmation of phytochemicals, as secondary metabolites from *E. papyrifera*.

The main compound was identified as rutarensin by searching the database and confirmed by comparison analysis with standard. The other peaks were detected before and after the major peaks (Fig 2.20A). The high-resolution mass spectrum showed an m/z 355.1031, 369.1189, 611.1617, 543.1292, 515.1192, 595.1453, 659.1616, 629.1302, 527.1340, and 353.0659 ([M+H]+), which was tentatively identified as based on the high-resolution mass and MS/MS production ions, respectively (Fig. 2.21C, Table 2.7). Thus, the LC-MS/MS analysis of EP identified 10 peaks as known or putative structures, including chlorogenic acid (4.86 min), chlorogenic acid methyl ester (6.29 min), rutin (6.95 min), daphnodorin B (8.34 min), daphnorin (8.81 min), tiliroside (9.35 min), rutarensin (9.48 min), edgeworoside A (9.98 min), daphnodorin A (10.34 min), and daphnoretin (11.18 min) (Fig 2.20B).

2.4.8. Effects of phytochemicals on the activity of osteoclasts and osteoblasts

Previous studies have revealed 10 phytochemicals from EP identified by UHPLC-HRMS. These compounds, except for those with low concentrations in the EP extract, were then tested in the TRAP assay for evaluating the effect of phytochemicals on osteoclastogenesis. A total of 6 phytochemicals, chlorogenic acid, rutin, tiliroside, rutarensin, edgeworoside A, and daphnoretin, were treated and evaluated for their inhibitory activity following the same procedure at the concentrations of 2.5–20 μM (Fig 2.21)

2.4.9. Identification and activity of purified Edgeworoside A

To obtain edgeworoside A, EP was extracted using methanol. The phytochemical was then purified using an AutoPurification System (Waters, USA) and a quantity of 2.11 mg was obtained (Fig 2.22). The purified samples were examined in a bioactivity assay and structure analysis was done by high-resolution mass, MS/MS and ^{1}H-NMR spectrum analysis. The high-resolution mass and MS/MS spectral characteristics of edgeworoside A were compared to commercially obtained standards (Fig 2.23A, B). The molecular formula of the purified sample was assigned as $C_{33}H_{24}O_{13}$ by high resolution mass spectra in

which the [M+H]+‡ peak was at m/z 629.1609. The ^{1}H- and ^{13}C-NMR assignments (Fig 2.23C, Table 2.7) were made by comparison with edgeworoside A. The presence of the sugar moiety D-fucose in the purified sample was confirmed by comparison of its ^{13}C-NMR resonances with standard reference data (Neuringer, Sears et al. 1979), and also by acid hydrolysis of purified sample to provide fucose. In the ^{1}H-NMR, the d at d 7.54 (J=9.5 Hz), 6.26 (J=9.5 Hz), 7.52 (J=9.6 Hz), and 6.30 (J=9.6 Hz) could be assigned to H-C(4'), H-C(3'), H-C(4''), and H-C(3''), respectively. The occurrence of the H-C(4)s downfield at d 7.78 revealed the presence of an O-substituent at C(3). The sugar moiety gave rise to the signals of an anomeric proton at d 5.50, the protons geminal to an OH group at d 3.89 ± 4.66, the anomeric C-atom at d 97.7, and further OH-bearing C-atoms at d 97.7, 72.2, 69.9, 68.8, 67.0, and 16.5. The α-D-configuration of the fucose moiety was confirmed by a small coupling constant for its anomeric proton (J=2.0 Hz). The position of the fucose moiety at C(7'), the O-linkage between C(3) and C(7''), and the C-C linkage between C(8) and C(8') were inferred by comparison of the 13C-NMR chemical shifts with those of edgeworoside (Li, Tong et al. 2014).

Next, the biological activities of the above purified and identified edgeworoside A on osteoclast were examined *in vitro* by a TRAP assay, AR_S test and proliferation of OB. Purified edgeworoside A (2.5–20

μM) decreased the activity of TRAP on the osteoclasts in a dose-dependent manner, and did not affect the viability of RAW267.4 cells at the same concentration. The IC_{50} of purified edgeworoside A based on the TRAP assay was < 5 μM (Fig 2.24A). To infer its effect on bone formation, its action on the proliferation and activity of osteoblasts was evaluated in the AR_S test. Purified edgeworoside A was revealed to have a positive effect on the proliferation of the osteoblasts (Fig 2.24C), although not on their activity. The MTS assay showed that purified edgeworoside A at concentrations of 5 ~ 20 μM led to an increase in cell viability (Fig 2.24D).

These results show that purified edgeworoside A is biologically and analytically equivalent to the standard and has the ability to act as a potent anti-osteoporotic drug and as a functional ingredient in health supplements.

2.5. Discussion

In this thesis, HTS-compatible assays were developed to monitor the NF-κB signaling in RAW 264.7 and ALP activity in MC3T3-E1. These assays were designed for the identification of anti-osteoporosis agents in an effective, easy, and quick manner. The use of HTS systems to search for anti-osteoporotic candidates has been previously reported, such as an osteogenic HTS system using human mesenchymal stem cells (hMSC) and ALP, and a proliferation HTS system for screening osteogenic (Abdelsayed, Vartanian et al. 2004) compounds (Alves, Dechering et al. 2011, Brey, Motlekar et al. 2011). Subsequently, a natural plant library consisting of 4,200 Korean natural plant extracts was screened for the desired bioactivity. The hit extracts were further evaluated for anti-osteoclastogenesis and osteogenic activities using a TRAP assay and an AR-S assay, respectively. After the *in vitro* screening campaigns, two kinds of natural extracts, *E. papyrifera* (EP) and *D. genkwa* (DG), were selected that showed anti-osteoclastogenesis activity in RAW264.7 cells and the potential to be developed as anti-osteoporotic agents (Fig 2.9, Table 2.6).

For evaluating the protective effect of these potent antiosteoporotic extracts on animal model, these extracts were treated on ovariectomized mice *in vivo.* The ovariectomized rodent model is a well-established and

widely known animal model of post-menopausal osteoporosis (Jee and Yao 2001, Sophocleous and Idris 2014).

With respect to efficacy, both extracts exhibited desirable bioactivity as anti-osteoporosis candidates. While the ovariectomized animal group showed a marked decrease in thickness, length, number, and volume of the trabecular bone, the group administered the extracts exhibited bone phenotypes similar to those of the control **(**Fig 2.10, Fig 2.11). However, although the extracts derived from DG were not cytotoxic to cultured cells *in vitro*, they induced abnormal tubercles in the small intestine. Even though the pharmacological effects of DG on arthritis(Zhang, Zhang et al. 2014), rheumatic arthritis*(Jiang, He et al. 2014),* inflammation, and allergy (Kai, Koine et al. 2004) have been reported, it is a known poisonous plant, especially the flower (Zhang, Zhang et al. 2014, Yun, Kim et al. 2015). It was therefore decided not to investigate *D. genkwa* further. Instead, only *E. papyrifera* was tested in a therapeutic rodent model; *E. papyrifera* has the ability to inhibit the differentiation of osteoclasts and activate calcium deposition in osteoblasts without any safety issues *in vitro* and *in vivo*. After administrating *E. papyrifera* to the ovariectomized animal group for 9 weeks, the serum, urine, and bone phenotypes were analyzed, and then compared with the data of the sham and control (OVX) groups. The results showed that administration of *E.*

papyrifera resulted in a significant change in the markers of bone resorption, including calcium, PYD, and osteocalcin. In addition, the OVX-induced bone loss was markedly prevented by the treatment with *E. papyrifera*, compared to that of OVX control group, as determined by imaging with X-ray radiography micro CT. These results suggest that *E. papyrifera* has the ability to prevent or delay osteoporosis and can be developed as an ingredient in health supplements and an anti-osteoporotic drug candidate.

E. papyrifera is well-known as a raw material for high quality paper. In traditional oriental medicine, the *Edgeworthia* species is used to treat traumatic injury, inflammation, and pain, in some localities of China and Korea (Hu, Jin et al. 2008). With respect to the pharmacology, some researchers have reported its effect on diabetes (Wang and Cheng 2006, Gao, Zhang et al. 2015). To explore the mechanism of action of *E. papyrifera*, its constituents were analyzed by UHPLC-HRMS, and 10 phytochemicals were identified (Table 2.7). Rutarensin was the most abundant; other phytochemicals including chlorogenic acid, tiliroside, edgeworoside A, and rutin were also detected. Some of the identified compounds were already reported by others previously (Hu, Jin et al. 2009, Li, Tong et al. 2014). The identified compounds were examined by using the TRAP assay and ARS test. As shown in Fig 2.21**,** 3 of the

phytochemicals exerted effective anti-osteoclastogenesis activity. At a concentration of 5 μM, rutin and daphnoretin inhibited the RANKL-induced TRAP activity by 48.52% and 51.33%, respectively. Their inhibitory activities on osteoclastogenesis have already been reported (Kyung, Lee et al. 2008); however, the anti-osteoporosis activity of edgeworoside A has not been previously reported. In addition, edgeworoside A showed the most potent inhibitory activity among the 6 phytochemicals in the TRAP assays (72.65% inhibition at 5 μM), and was the one that promoted osteoblast proliferation to the greatest extent. The inhibition activity of *E. papyrifera* extract against the differentiation of osteoclast was compared with that of commercially available extract and recently reported one, and the results are summarized in Table 2.8. *Scutellaria baicalensi*, approved as a bone strengthen ingredient from KFDA, was reported to inhibit TRAP activity by 21% at the concentration of 10 μg/ml. In addition, Chinese herbal medicines, *Cynanchum atratum, Corydalis turtschaninovii* and *Melia Azedarach* exhibited their inhibitory activities against the differentiation of osteoclast at the concentration range of 10 μg/ml ~ 100 μg/ml. In an *in vivo* study, *Berberis aristata* at doses of 100 ~ 500 mg/kg alleviated the negative makers of bone resorption in ovariectomized rats (Yogesh, Chandrashekhar et al. 2011), while *E. papyrifera* at dose of 52.5 mg/kg significantly improved all of the osteoporosis relevant parameters in this

thesis. These results suggest that that *E. papyrifera* has sufficient efficacy to be used as a functional ingredient.

While Edgeworoside A, identified from *E. papyrifera* in this thesis, showed a remarkable inhibition activity against osteoclastogenesis at the concentration of 2.5 μM, ipriflavone, approved as an osteoporotic drug in EU and Japan, was reported to inhibit osteoclastogenesis at 10 μM (Morita et al. 1992). Moreover, rutin and adiponectin which were recently reported to exhibit anti-osteoclastogenic activities demonstrated IC_{50} values of 3.22 μM and 3.84 μM, respectively against osteoclastogenesis. In the case of (-)-epigallocatechin gallate, it exhibited anti-osteoclastogenesis activity at the concentrations of 10~100 μM. However, IC_{50} of edgeworoside A was turned out to be 2.09μM, suggesting that it is an excellent candidate for anti-osteoporosis drug.

Hence, the existence and activity of purified edgeworoside A from *E. papyrifera* was precisely examined. First, I purified edgeworoside A from *E. papyrifera* using an AutoPurification System, and compared its mass spectrum, molecular weight, and retention time with a standard of edgeworoside A using UHPLC-HR-MS. The identity of edgeworoside A derived from *E. papyrifera* was finally confirmed by NMR analysis. Edgeworoside A was isolated previously from two species, *E. chrysantha*

(Yan, Tong et al. 2004) and *Daphne retusa* (Hu, Jin et al. 2009). This is the third report of edgeworoside A in this family. Moreover, it has not been reported from any other family. Thus, it might be a useful chemotaxonomic marker for the family *Thymelaeaceae*, family names of EP. Although a couple of studies have shown the pharmacological activities of coumarins such as the anti-inflammatory and analgesic activities from the traditional Chinese medicine 'Zushima', which is structurally similar to edgeworoside A (Li, Wu et al. 2002, Hu, Jin et al. 2008), its anti-osteoporotic activity was first revealed in this study.

In this thesis, *E. papyrifera* and edgeworoside A have both anti-osteoclastogenesis and osteogenic activities *in vitro*. It is noteworthy that *E. papyrifera* exerted preventive and therapeutic activities in mice and rodent osteoporotic models. Considering the anti-osteoclastogenesis activities of each compound, edgeworoside A, daphnoretin, and rutin appear to significantly contribute to the bioactivity of *E. papyrifera*. Hence, edgeworoside A can be considered a suitable candidate for the development of an anti-osteoporotic drug.

Table 2.1 The groups of SD rats used in OVX experiments

Group	Animals (n)	Descriptions
Naïve	6	Normal animals
Sham	6	Exposure of both sides of ovaries after incisions
Ovariectomy (OVX)	6	OVX performed, and same volumes of vehicle administrated orally only
OVX_SD (52.5 mg/kg)	6	administration of high concentration of EP (52.5mg/kg/day)
OVX_SD (26.25 mg/kg)	6	administration of low concentration of EP (26.25mg/kg/day)
Total	30 ± 4	Extra animals (4 animals) to prepare for experimental error

Table 2.2 Selection of hit extracts that inhibit RANKL-induced activation of NF-kB signaling pathway

Name	Part	Family
Daphne genkwa	stem, root	*Thymelaeaceae*
Alnus hirsuta var. sibirica	stem, duramen	*Betulaceae*
Acer tegmentosum	stem, bark	*Aceraceae*
Daphne genkwa	subterranean part	*Thymelaeaceae*
Euphorbia ebracteolata	aerial part	*Euphorbiaceae*
Euphorbia ebracteolata	subterranean part	*Euphorbiaceae*
Alnus pendula	stem, bark	*Betulaceae*
Lindera erythrocarpa	stem, bark	*Lauraceae*
Alnus hirsuta	leaf, stem	*Betulaceae*

Table 2.3 A list of Korean natural extracts that inhibited RANKL-induced TRAP activity in RAW 264.7 cells

Name	Part	Family
Daphne genkwa	stem, root	*Thymelaeaceae*
Daphne genkwa	subterranean part	*Thymelaeaceae*
Euphorbia ebracteolata	aerial part	*Euphorbiaceae*
Euphorbia ebracteolata	subterranean part	*Euphorbiaceae*

Table 2.4 A list of hit extracts that scored in ALP assay

Name	Part	Family
Daphne genkwa	stem, root	*Thymelaeaceae*
Torreya nucifera	leaf	*Taxaceae*
Euphorbia sieboldiana	total	*Euphorbiaceae*
Daphne genkwa	subterranean part	*Thymelaeaceae*
Sasa borealis	leaf	*Gramineae*
Caryopteris divaricata	subterranean part	*Verbenaceae*
Neoshirakia japonica	fruit	*Euphorbiaceae*
Fagus crenata var. multinervis	stem, bark	*Fagaceae*
Edgeworthia papyrifera	stem, duramen	*Thymelaeaceae*

Continue

Name	Part	Family
Gleditsia japonica var. koraiensis	stem, bark	*Leguminosae*
Maackia amurensis	leaf, stem	*Leguminosae*
Carex blepharicarpa var. insularis	total	*Cyperaceae*
Lonicera vesicaria	leaf, stem	*Caprifoliaceae*
Edgeworthia papyrifera	stem	*Thymelaeaceae*
Maackia amurensis	leaf, stem	*Leguminosae*
Staphylea bumalda	stem, bark	*Staphyleaceae*
Pueraria thunbergiana	branch, leaf	*Leguminosae*
Commelina communis	total	*Commelinaceae*
Iris netschinskia	total	*Iridaceae*

Table 2.5 A list of extracts that scored in AR-S assay

Name	Part	Family
Daphne genkwa	stem, root	*Thymelaeaceae*
Torreya nucifera	leaf	*Taxaceae*
Euphorbia sieboldiana	total	*Euphorbiaceae*
Daphne genkwa	subterranean part	*Thymelaeaceae*
Neoshirakia japonica	fruit	*Euphorbiaceae*
Edgeworthia papyrifera	stem, duramen	*Thymelaeaceae*

Table 2.6 A list of plant extracts that showed the ability to modulate osteoclastogenesis and osteoblastogenesis

Name	Part	Family	Osteoclastogenesis		Osteoblastogenesis		Known hazards
			NF-kB	TRAP	ALP	AR-S	
Daphne genkwa	Stem,Root	*Thymelaeaceae*	Effect	Effect	Effect	Effect	All parts, especially flower, of the pl ant are poisonous.
Daphne genkwa	Subterranean part	*Thymelaeaceae*	Effect	Effect	Effect	Effect	All parts, especially flower, of the plant are poisonous.
Torreya nucifera	Leaf	*Taxaceae*	no effect	no effect	Effect	Effect	None known (natural monument)
Euphorbia sieboldiana	Total	*Euphorbiaceae*	no effect	no effect	Effect	Effect	The sap is toxic on ingestion and high ly irritant externally, causing skin rea ctions and inflammation
Neoshirakia japonica	Fruit	*Euphorbiaceae*	no effect	no effect	Effect	Effect	The sap is poisonous.
Edgeworthia papyrifera	Stem, Duramen	*Thymelaeaceae*	no effect	Effect	Effect	Effect	None known
Euphorbia ebracteolata	Aerial part	*Euphorbiaceae*	Effect	Effect	no effect	no effect	-
Euphorbia ebracteolata	Subterranean part	*Euphorbiaceae*	Effect	Effect	no effect	no effect	-

Table 2.7 Identification of 10 compounds from *E. papyrifera* extract

RT (min)	Compound	$[M+H]^+$	Formula	Δppm	MS/MS fragment ion
4.86	chlorogenic acid	355.1031	$C_{16}H_{19}O_9$	0.515	163
6.29	chlorogenic acid methyl este	369.1187	$C_{17}H_{21}O_9$	0.496	177
6.75	Rutin	611.1617	$C_{27}H_{31}O_{16}$	0.819	303, 465
8.34	daphnodorin B	543.1292	$C_{30}H_{23}O_{10}$	1.209	255, 311, 373, 395, 407, 419, 525
8.81	Daphnorin	515.1192	$C_{25}H_{22}O_{12}$	1.587	315, 353, 424, 502
9.35	tiliroside	595.1453	$C_{30}H_{26}O_{13}$	1.130	121, 147, 152, 171, 182, 199, 213, 231, 241, 257
9.48	Rutarensin	659.1616	$C_{31}H_{30}O_{16}$	1.455	164, 178, 191,309,338
9.98	edgeworoside A	629.1302	$C_{33}H_{24}O_{13}$	2.007	189, 321, 427, 465
10.34	daphnodorin A	527.1340	$C_{30}H_{22}O_9$	0.666	152, 255, 281, 299, 311, 389
11.18	daphnoretin	353.0659	$C_{19}H_{12}O_7$	0.937	163, 179, 192, 208, 309, 334, 338, 343

* Commercial source

Table 2.8. Comparison of anti-osteoclastogenesis agents on the differentiation of osteoclast

Natural product of name	Effective concentration on osteoclastogenesis	Reference
Natural product (extract)		
E. papyrifera		in this thesis
S. baicalensis Georgi[1)]	10 μg/ml	(Im et al. 2011)
C. atratum and *M. azedarach*	10~100 μg/ml	(Mukudai, Kondo et al. 2014)
phytochemical		
Edgworiside A	2.09 uM (IC_{50})	in this thesis
rutin	3.22 uM (IC_{50})	in this thesis, (Kyung, Lee et al. 2008)
Daprorectin	3.87 uM (IC_{50})	in this thesis, (Huang, Feng et al. 2016)
Epigallocatechin gallate	10~100 uM	(Lin, Chen et al. 2009)
Drug		
ipriflavone	10 uM	(Morita et al. 1992)

[1)] *S. baicalensis* approved from KFDA as bone strengthen functional food ingredient

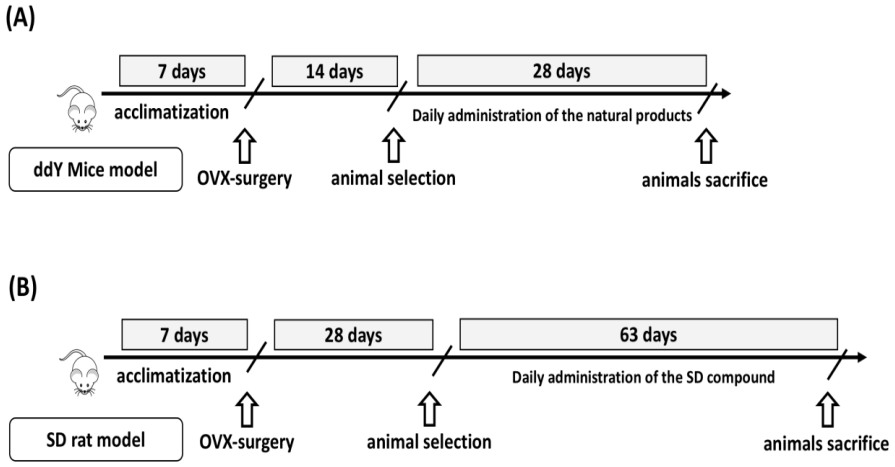

Fig 2.1 The experimental schedules for validation of natural products *in vivo*. (A) OVX in ddY mice was performed by surgical removal of ovaries after incision of abdomen. Following OVX, animals were recovered for 2-weeks, and then they were orally administered with EP and DG daily for 28 days in order to quickly validate the effects of the natural compounds. (B) OVX in SD rats was performed by surgical removal of ovaries after incisions of both sides of animal's back. Following OVX, animals were recovered and maintained for induction of osteoporosis. The selected animals were orally administered with EP daily for 63 days in order to validate the effects of EP.

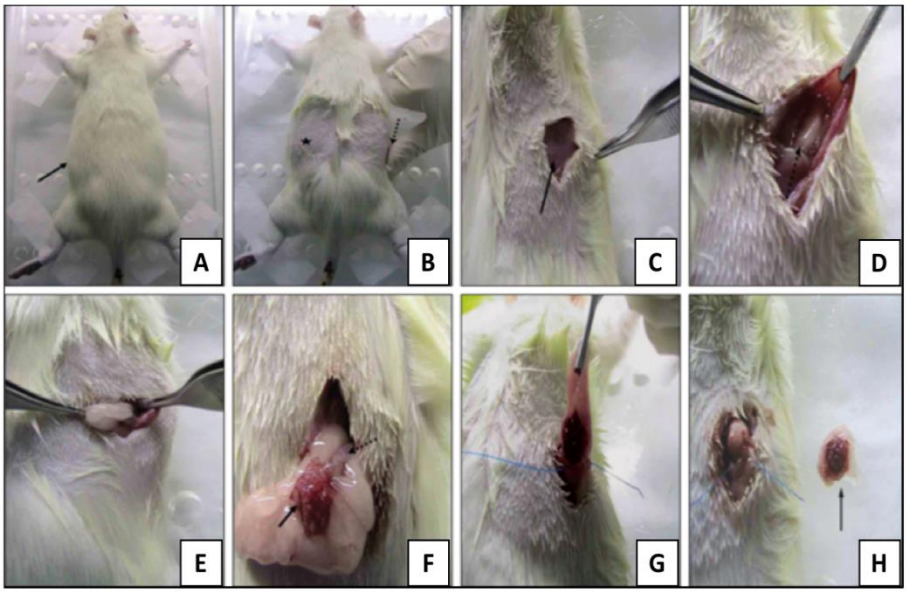

Fig 2.2 The surgical procedures for removing ovaries from female SD rats. (A) The location of kidney was indicated by an arrow. (B) The location of kidneys in the shaved animal was indicated by star (left side) and an arrow (right side). (C) The muscle layer is shown. (D) Upon incision of the muscle layer, the adipose tissues around the kidney are exposed. (E) The location of the ovaries was confirmed by adipose tissue. (F) Ovaries surrounded by adipose tissue were completely exposed. (G) Adipose tissues were eliminated for separating ovaries. (H) The ovaries were completely removed and the incision was sutured to complete the operation.

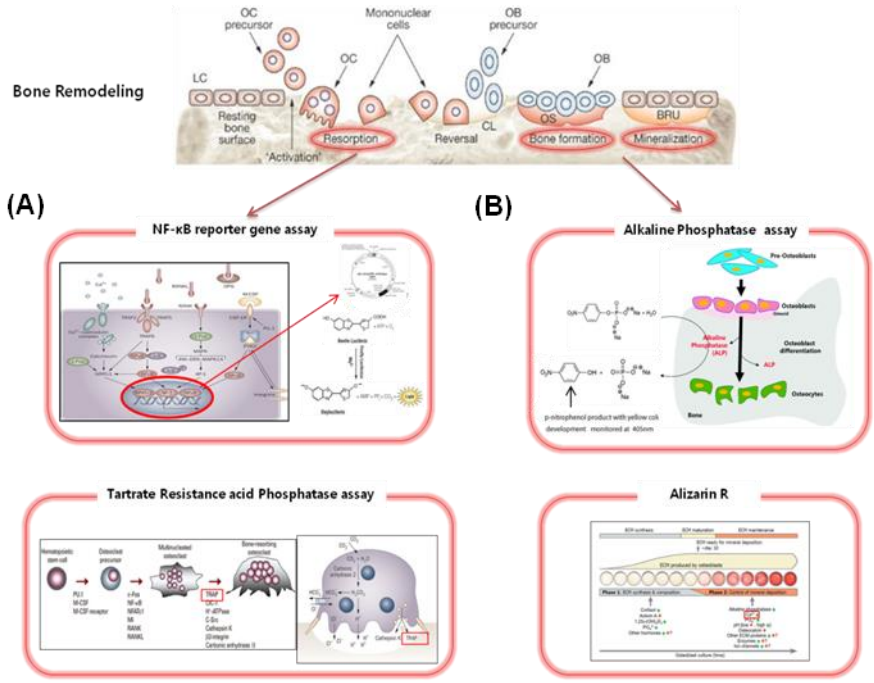

Fig 2.3 The molecular targets of bone remodeling and HTS-compatible assays for the identification of anti-osteoporotic agents. (A) NF-κB and TRAP are among well-known biomarkers for osteoclastogenesis, (B) ALP and mineralization are among well-known biomarkers for osteoblast differentiation.

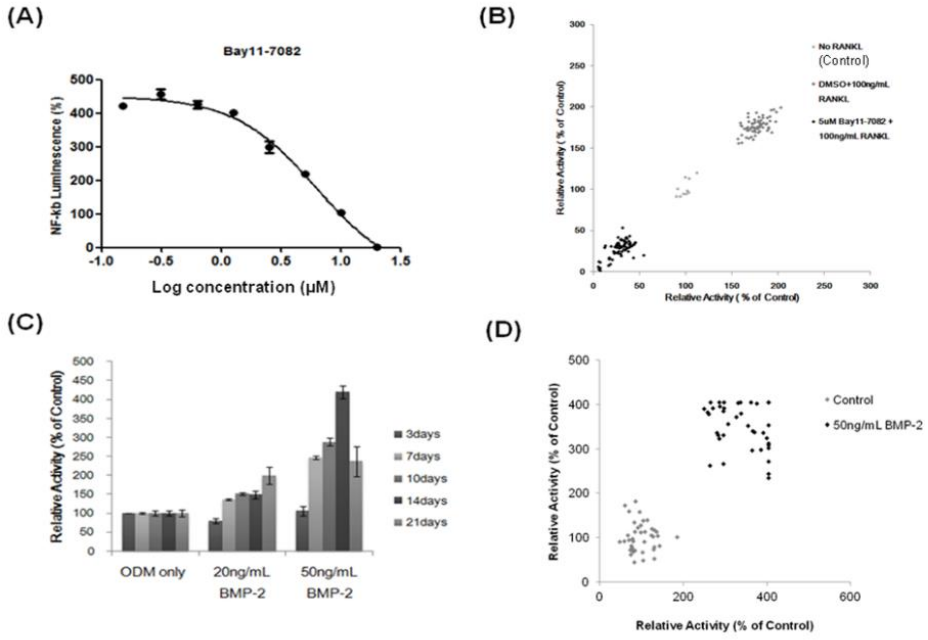

Fig 2.4 Development of HTS-compatible assays. (A) NF-κB reporter gene assay. RANKL-induced expression of reporter gene in the stable cell line was inhibited by a reference compound (Bay11-7082) in a dose dependent manner. (B) Validation of the reporter gene assay in HTS system. (C) The optimal dose and time for the treatment with positive control (BMP-2) in ALP assay using MC3T3-E1 cells. (D) Validation of the ALP assay in HTS system.

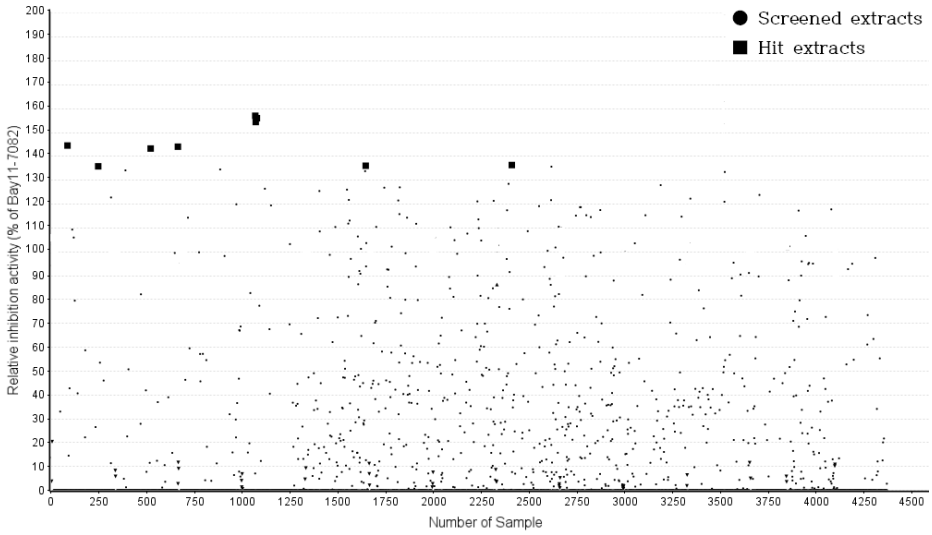

Fig 2.5 Screening of a plant extract library for inhibitors of RANKL-induced NF- κB signaling pathway. The cells were treated with either extracts (25 μg/mL) or a reference compound Bay11-7082 (5 μM) for 2 h, and then treated with RANKL (100 ng/mL). The luciferase activity was expressed as relative inhibition activity compare to inhibition activity of positive control, Bay11-7082 (100%).

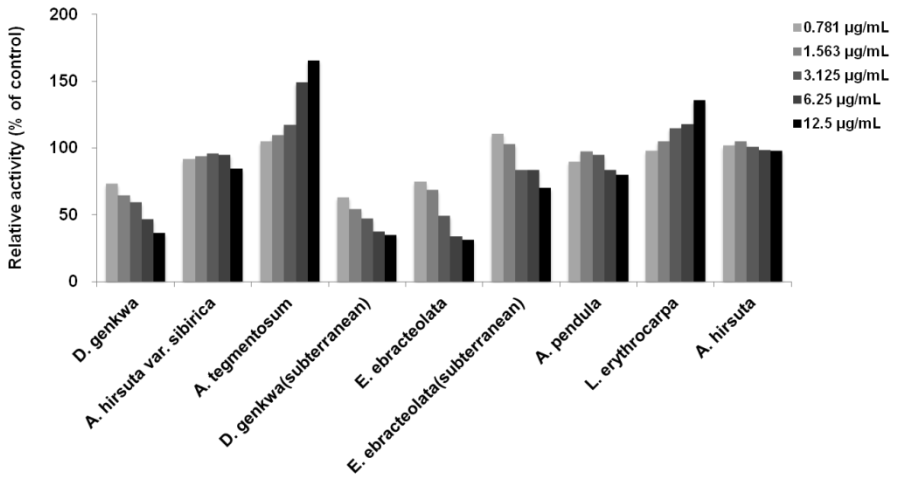

Fig 2.6 The effect of plant extracts on TRAP activity in RAW264.7 cell. Raw 264.7 were treated with indicated plant extracts upon stimulation with RANKL (100 ng/mL) for 5 days, and then TRAP activity was measured. Data are expressed as a percentage of DMSO controls (100%).

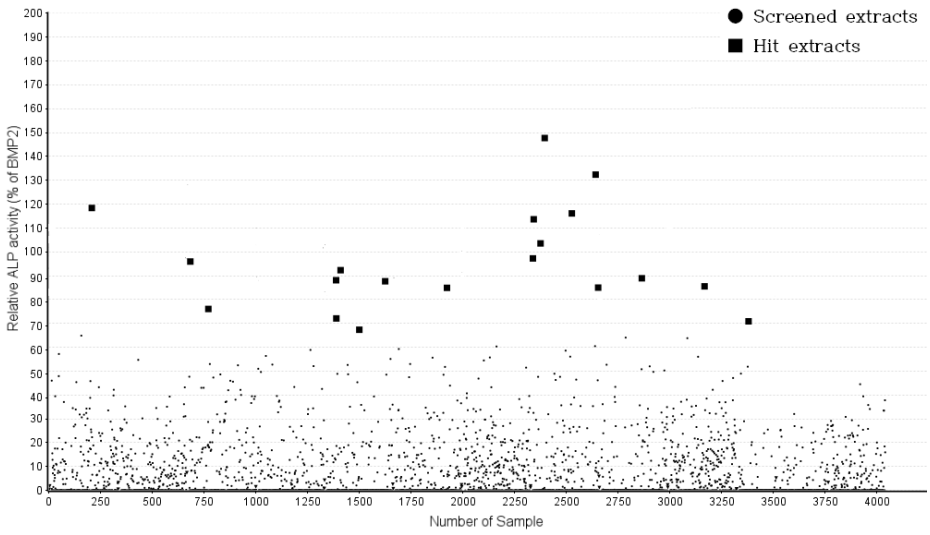

Fig 2.7 Screening of plant extracts library using an HTS-compatible ALP assay. MC3T3E1 cells were treated with either BMP-2 alone or extract (25 μg/mL) for 14 days with the replacement of media every 3 days, and then ALP activity was measured. Data are expressed as percentages of the data obtained for the BMP-2-treated cells (100%)

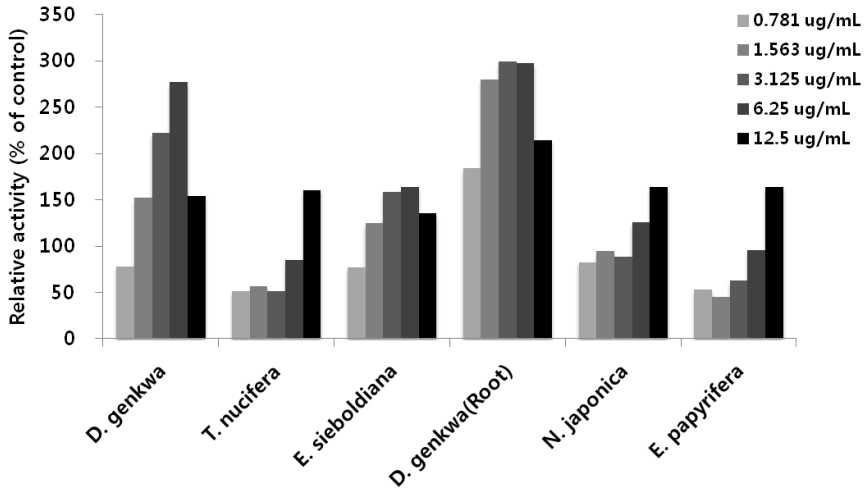

Fig 2.8 ARS assay with selected plant extracts. MC3T-3E1 cells were treated with increasing concentrations of the extracts for 21 days, and then mineralization of the cultures were quantified by ARS assay. Data are expressed as percentages of the data obtained for the DMSO-treated cells.

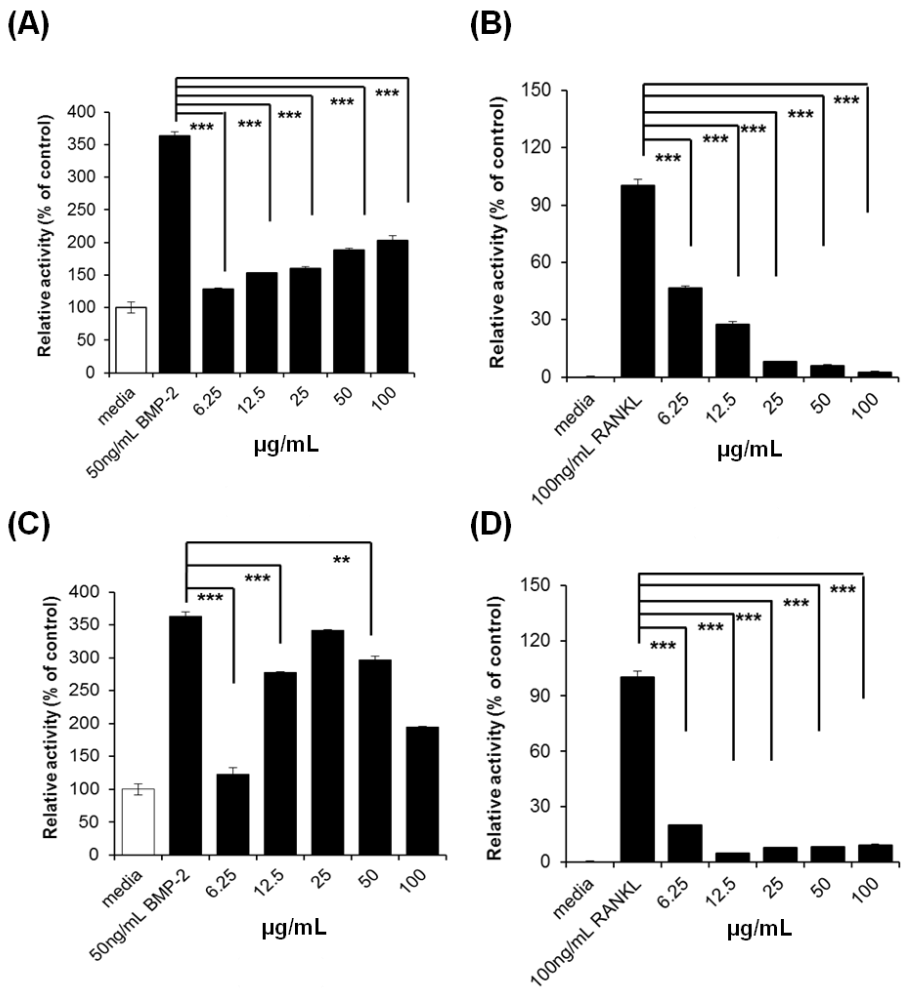

Fig 2.9 Effects of *E. papyrifera* (EP) and *D. genkwa* (DG) extracts on osteoclast and osteoblast. (A and B) The effects of EP on mineralization and TRAP activity are shown. (C and D) The effects of DG on mineralization and TRAP activity are shown. ** p-value < 0.005, *** p-value < 0.001 *vs*. control, BMP-2 or RANKL.

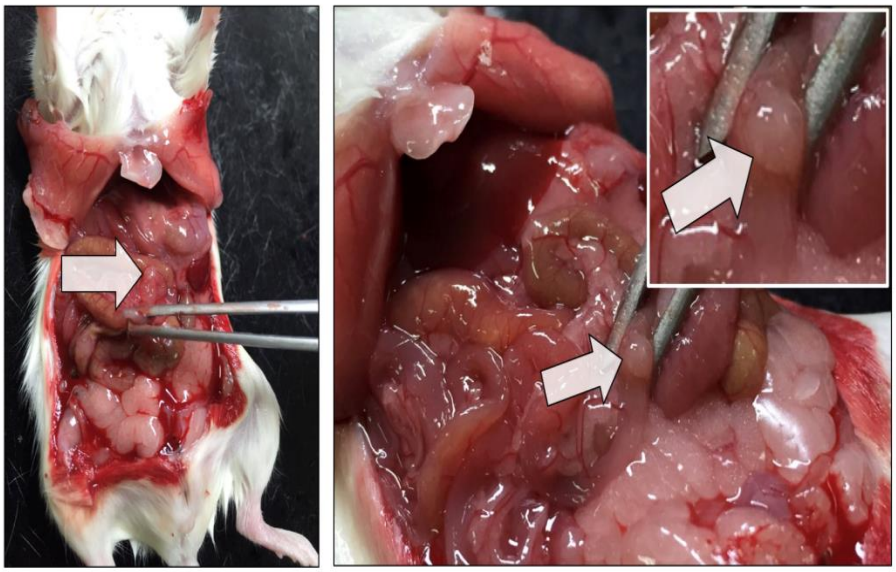

Fig 2.10 Observation of diffuse nodules in the small intestine of animals administered with *D. genkwa*. Animals were sacrificed and all the digestive organs were examined for gross abnormality. The circular diffuse tubercles (white arrows) were found in the small intestine of the OVX_P group. They were also observed in NON_P group which was subjected to abdominal incision only and was administered with DG. This may affect animal feed intake and body weight gain, and it may be pathogenic to digestive organs due to continuous use

(A)

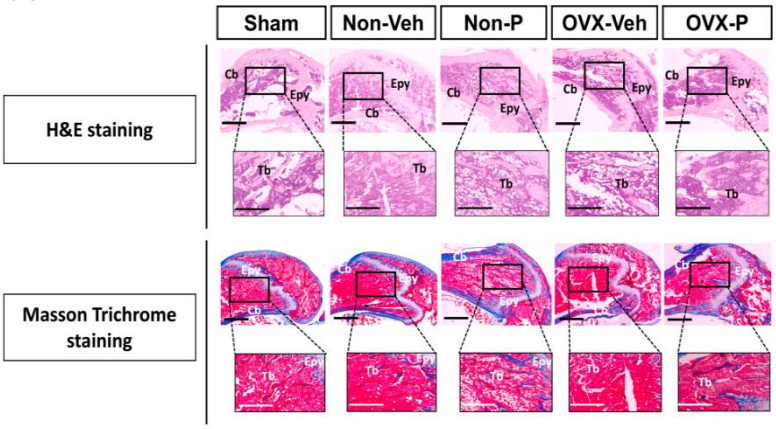

(B)

Groups	Bone mass and structure					Bone resorption
	TBV (%)	Tbn (numbers)	Tbl (mm)	Tbt (μm)	Cbt (μm)	Ocn (numbers)
Sham	35.32±4.21	18.01±1.01	1.09±0.43	46.18±10.16	196.14±19.18	2.71±1.50
Non_Veh	36.11±2.98	18.51±1.31	0.91±0.33	45.55±8.06	192.35±15.29	3.01±1.01
Non_P	39.91±6.81[b]	19.11±1.77[b]	0.80±0.11[b]	44.92±9.21[b]	194.82±10.95[a]	3.38±4.20[b]
OVX_Veh	19.39±4.61[a]	8.38±1.31[a]	0.43±0.19[a]	34.14±3.31[a]	119.35±12.01[a]	16.13±3.09[a]
OVX_P	31.08±2.17[b]	14.12±1.42[a,b]	0.63±0.26[b]	40.98±5.23[b]	192.18±15.20[b]	7.78±2.26[a,b]

Values are expressed mean ± S.D. of five mice.
[a] p<0.05 as compared with Sham by LSD test.
[b] p<0.05 as compared with OVX control by LSD test.
OVX = ovariectomy
TBV = Trabecular bone volume (%), BV/TV
Tbn = Trabecular bone number (N/epiphyseal)
Tbl = Trabecular bone length (Longitudinal thickness; mm)
Tbt = Trabecular bone thickness (Cross thickness; μm)
Cbt = Cortical bone thickness (Cross thickness; μm)
Ocn = Osteoclast cell number (N/epiphyseal)

Fig 2.11 Anti-osteoporotic effects on *D. genkwa*. (A) The left femurs were stained with H&E and MT. The demarcated area showing trabecular bone was magnified at the bottom of each image. Sham, Naive animal treated with vehicle only; Non_veh, abdomen incision and treated with vehicle only; Non_P, abdomen incision and treated with DG; OVX_Veh, OVX & treated with vehicle only; OVX_P, OVX & treated

with DG. It is evident that ovariectomy led to a decrease in trabecular bone volume and the thickness of cortical bone however the; ovariectomy-induced bone loss was prevented by the administration of DG. The collagen fibers and connective tissues were more clearly observed by the MT staining than H&E staining. Scale Bar = 200 ㎛. (B) Histomorphometry for the femur in the experimental groups: Trabecular bones; Values are expressed as mean ± S.D. (n = 5). It is evident that all of the osteoporosis relevant parameters were improved by the administration of DG. All abbreviations are spelled out at the bottom.

(A)

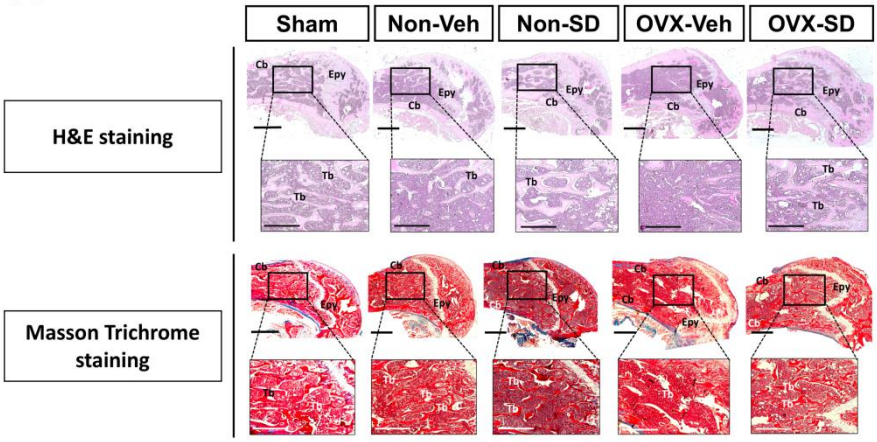

(B)

Groups	Bone mass and structure					Bone resorption
	TBV (%)	Tbn (numbers)	Tbl (mm)	Tbt (μm)	Cbt (μm)	Ocn (numbers)
Sham	39.74±4.38	17.11±1.01	1.09±0.13	47.14±11.06	194.14±18.28	2.61±1.20
Non_Veh	38.74±5.38	17.41±1.60	0.89±0.33	47.55±9.06	195.35±16.88	3.01±1.01
Non_SD	35.21±5.63[b]	18.25±1.67[b]	0.73±0.12[b]	43.92±8.93[b]	194.91±14.85[a]	3.38±4.20[b]
OVX_Veh	18.17±1.61[a]	7.88±1.25[a]	0.39±0.07[a]	33.05±4.31[a]	117.35±11.22[a]	15.13±3.09[a]
OVX_SD	33.78±3.47[b]	16.03±1.21[b]	0.73±0.16[b]	53.98±5.15[b]	193.18±15.30[b]	6.78±2.26[b]

Values are expressed mean ± S.D. of five mice.
[a] p<0.05 as compared with Sham by LSD test.
[b] p<0.05 as compared with OVX control by LSD test.
OVX = ovariectomy
TBV = Trabecular bone volume (%), BV/TV
Tbn = Trabecular bone number (N/epiphyseal)
Tbl = Trabecular bone length (Longitudinal thickness; mm)
Tbt = Trabecular bone thickness (Cross thickness; μm)
Cbt = Cortical bone thickness (Cross thickness; μm)
Ocn = Osteoclast cell number (N/epiphyseal)

Fig 2.12 Anti-osteoporotic effects on *E. papyrifera*. (A) The left femurs were stained with H&E and MT. The demarcated area showing trabecular bone was magnified at the bottom of each image. Sham, Naive animal treated with vehicle only; Non_veh, abdomen incision treated with vehicle only; Non_SD, abdomen incision and treated with EP; OVX_Veh, OVX & treated with vehicle only; OVX_SD, OVX & treated

with EP. It is evident that ovariectomy led to a decrease in trabecular bone volume and the thickness of cortical bone; however the ovariectomy-induced bone loss was prevented by the administration of EP. The collagen fibers and connective tissues were more clearly observed by the MT staining than H&E staining. Scale Bar = 200 ㎛. (B) Histomorphometry for the femur in the experimental groups: Trabecular bones; Values are expressed as mean ± S.D. (n = 5). It is evident that all of the osteoporosis relevant parameters were improved by the administration of EP. All abbreviations are spelled out at the bottom.

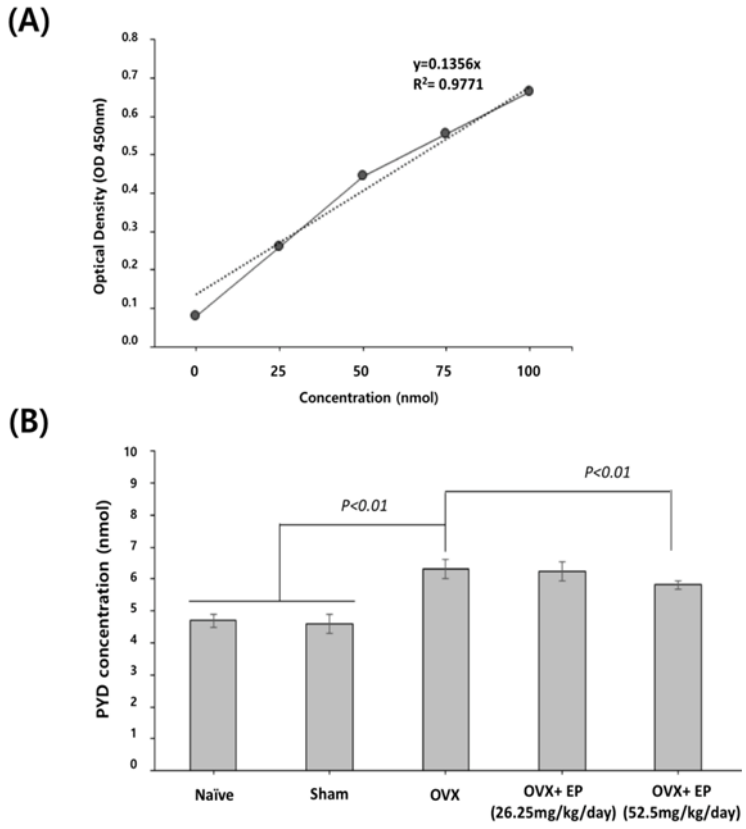

Fig 2.13 Analysis of a bone resorption biomarker (PYD). (A) The absorbance of increasing concentrations of PYD were measured and shown as a function of PYD concentration. A standard line of PYD is shown (dotted line). (B) Urines collected from each group were analyzed for PYD, and the PYD concentrations were calculated according to the standard line. Data are expressed as the mean ± S.D.

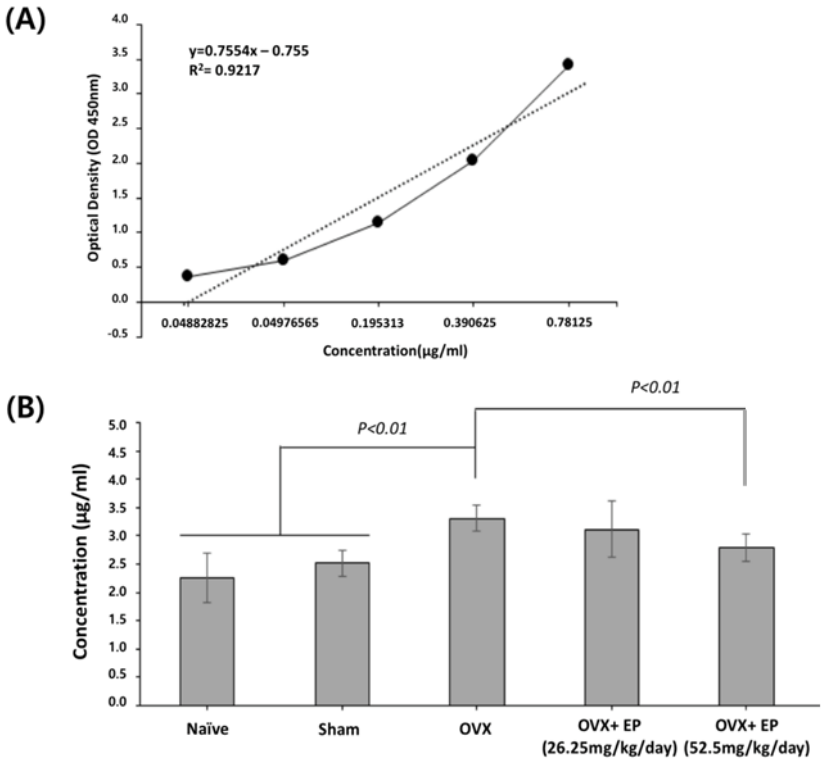

Fig 2.14 Analysis of TRACP (tartrate-resistant acid phosphatase) in serum. (A) The absorbance of increasing concentrations of TRACP were measured and shown as a function of TRACP concentration. A standard line of TRACP is shown (dotted line). (B) Blood samples collected from the tail veins of each group were analyzed for TRACP, and the TRACP concentrations were calculated according to the standard line. Data are expressed as the mean ± S.D.

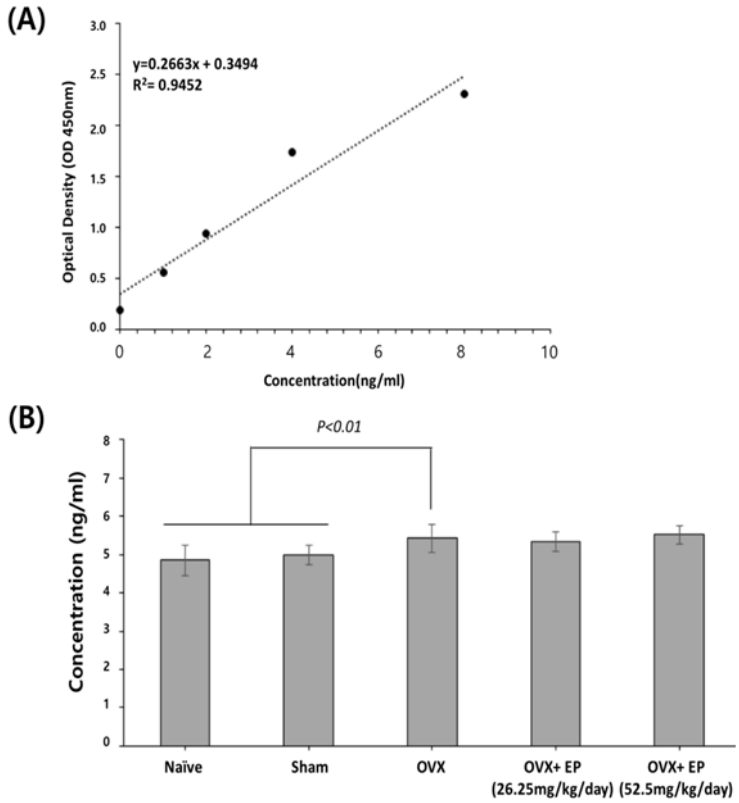

Fig 2.15 Analysis of serum osteocalcin. (A) The absorbance of increasing concentrations of osteocalcin were measured and shown as a function of osteocalcin concentration. A standard line of osteocalcin is shown (dotted line). (B) Blood samples collected from the tail veins of each group were analyzed for osteocalcin, and the osteocalcin concentrations were calculated according to the standard line. Data are expressed as the mean ± S.D.

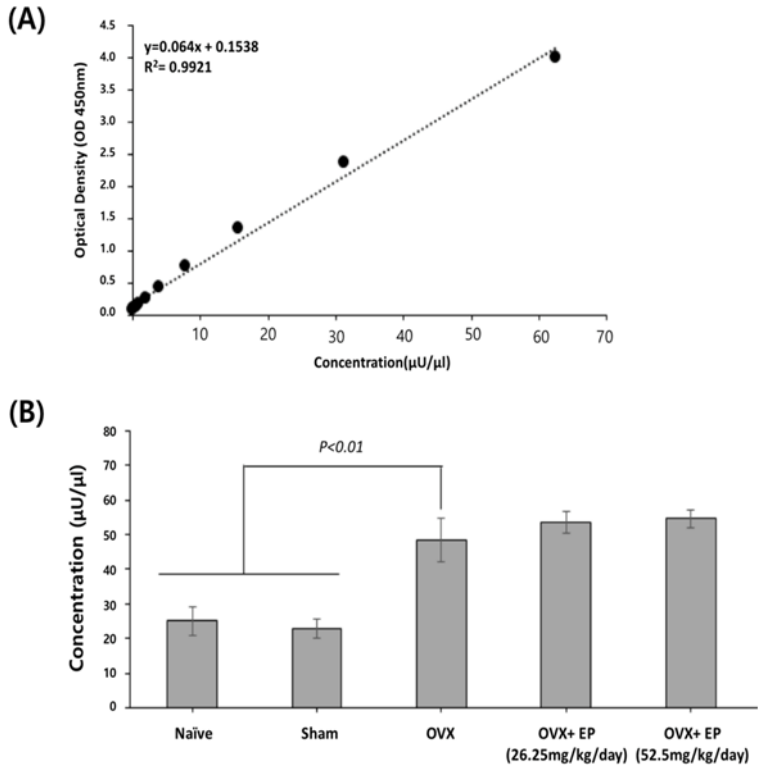

Fig 2.16 Analysis of serum ALP. (A) The absorbance of increasing concentrations of ALP were measured and shown as a function of ALP concentration. A standard line of ALP is shown (dotted line). (B) Blood samples collected from the tail veins of each group were analyzed for ALP, and the ALP concentrations were calculated according to the standard line. Data are expressed as the mean ± S.D.

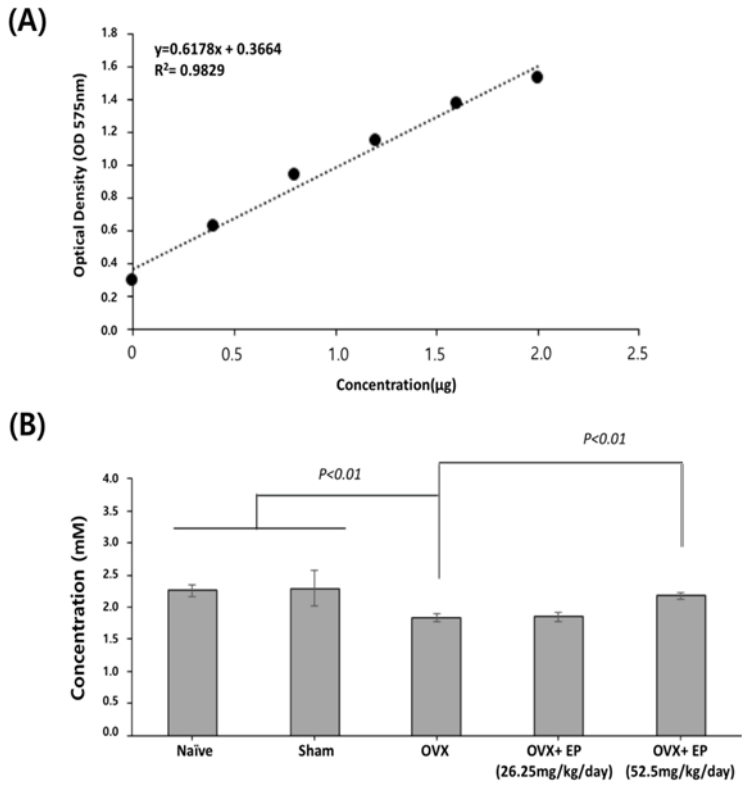

Fig 2.17 Analysis of serum calcium. (A) The absorbance of increasing concentrations of calcium were measured and shown as a function of calcium concentration. A standard line of calcium is shown (dotted line). (B) Blood samples collected from the tail veins of each group were analyzed for calcium, and the calcium concentrations were calculated according to the standard line. Data are expressed as the mean ± S.D.

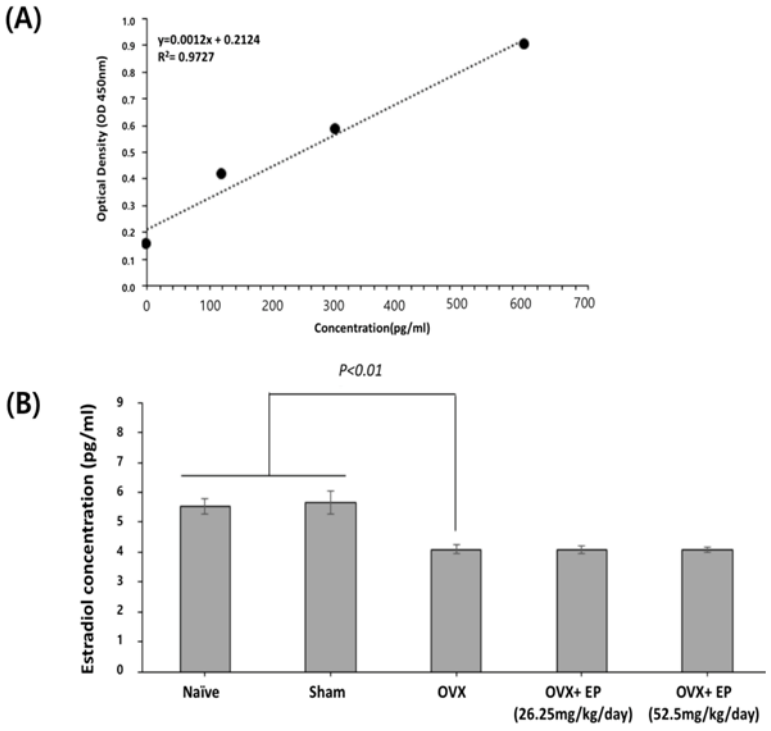

Fig 2.18 Analysis of serum estrogen. (A) The absorbance of increasing concentrations of estrogen were measured and shown as a function of estrogen concentration. A standard line of estrogen is shown (dotted line). (B) Blood samples collected from the tail veins of each group were analyzed for estrogen, and the estrogen concentrations were calculated according to the standard line. Data are expressed as the mean ± S.D.

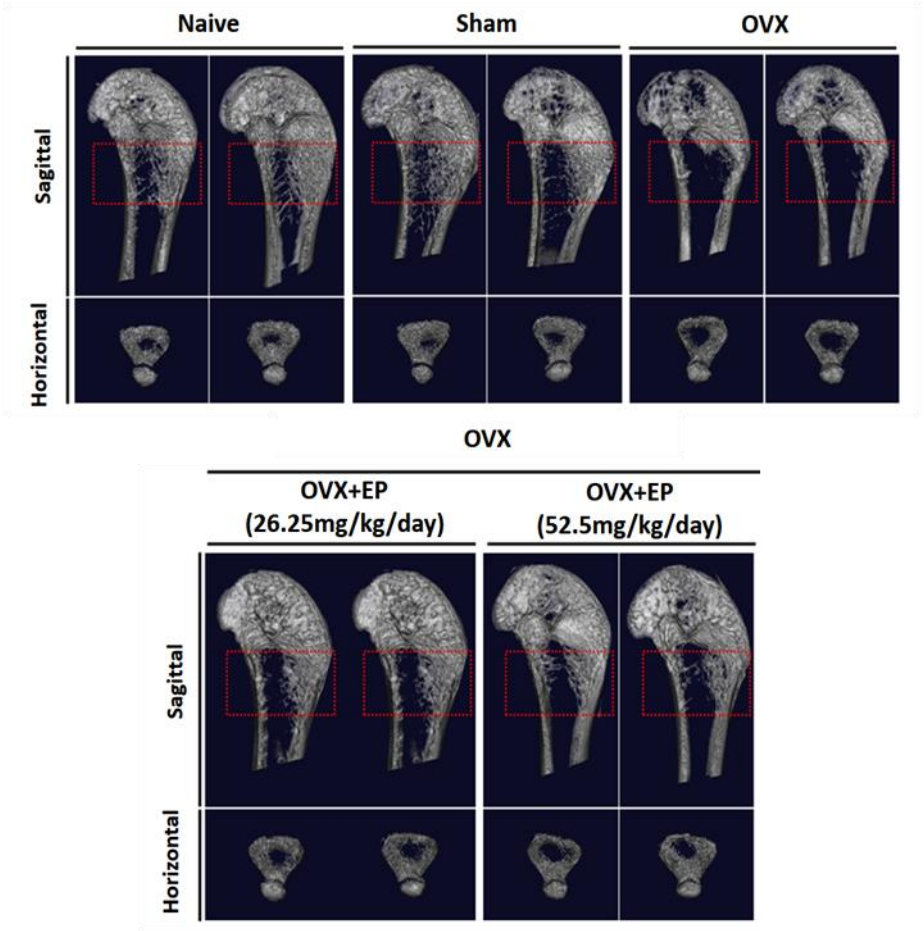

Fig 2.19 Analysis of bone mineral density by *in vivo* X-ray radiography micro-CT. The right femurs of the animals from each group were surgically removed and subjected to *in vivo* X-ray radiography micro-CT, and the representative horizontal and sagittal views are shown. The area between end of mid-shaft and the epiphyseal area is distinctly demarcated to emphasize the degrees of trabecular bone density and volume.

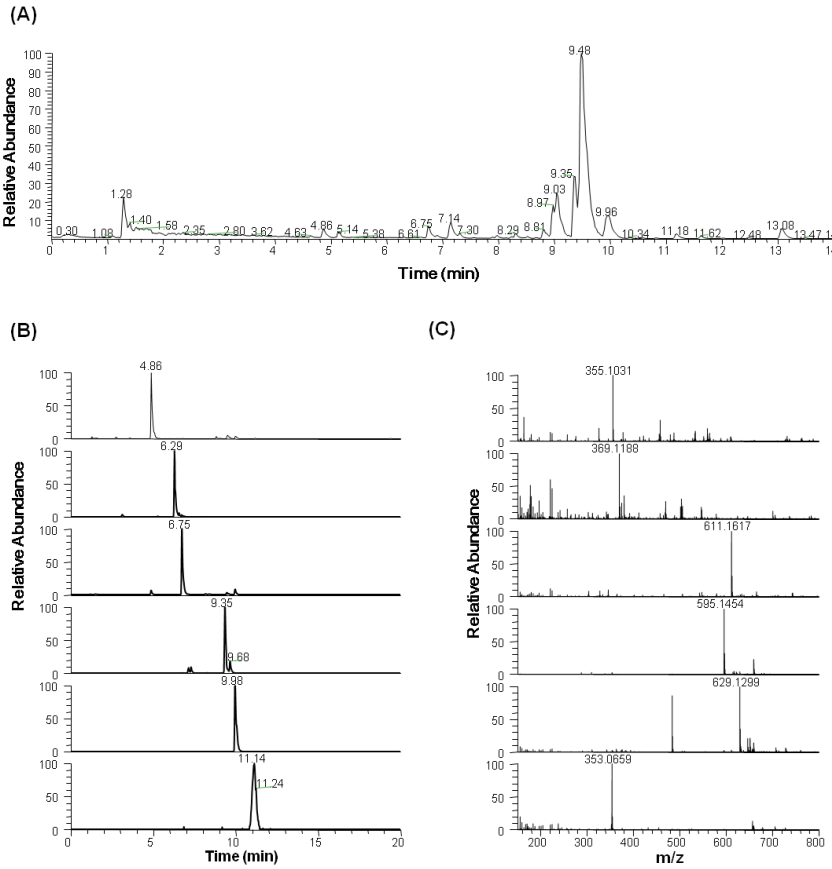

Fig 2.20 Ultra-high-pressure liquid chromatography (UHPLC) - high-resolution mass spectrophotometry (LC-HR-MS) analysis of the extract from *E. papyrifera*. (A) UHPLC chromatogram of the extract derived from *Edgeworthia papyrifera*. (B) The retention time of each of the identified main compounds is shown. Chlorogenic acid (4.86 min), chlorogenic acid methyl ester (6.29 min), rutin (6.75 min), tiliroside (9.35 min), edgeworoside A (9.98min), and daphnoretin (11.34 min). (C) High-resolution mass spectra of 6 main compounds.

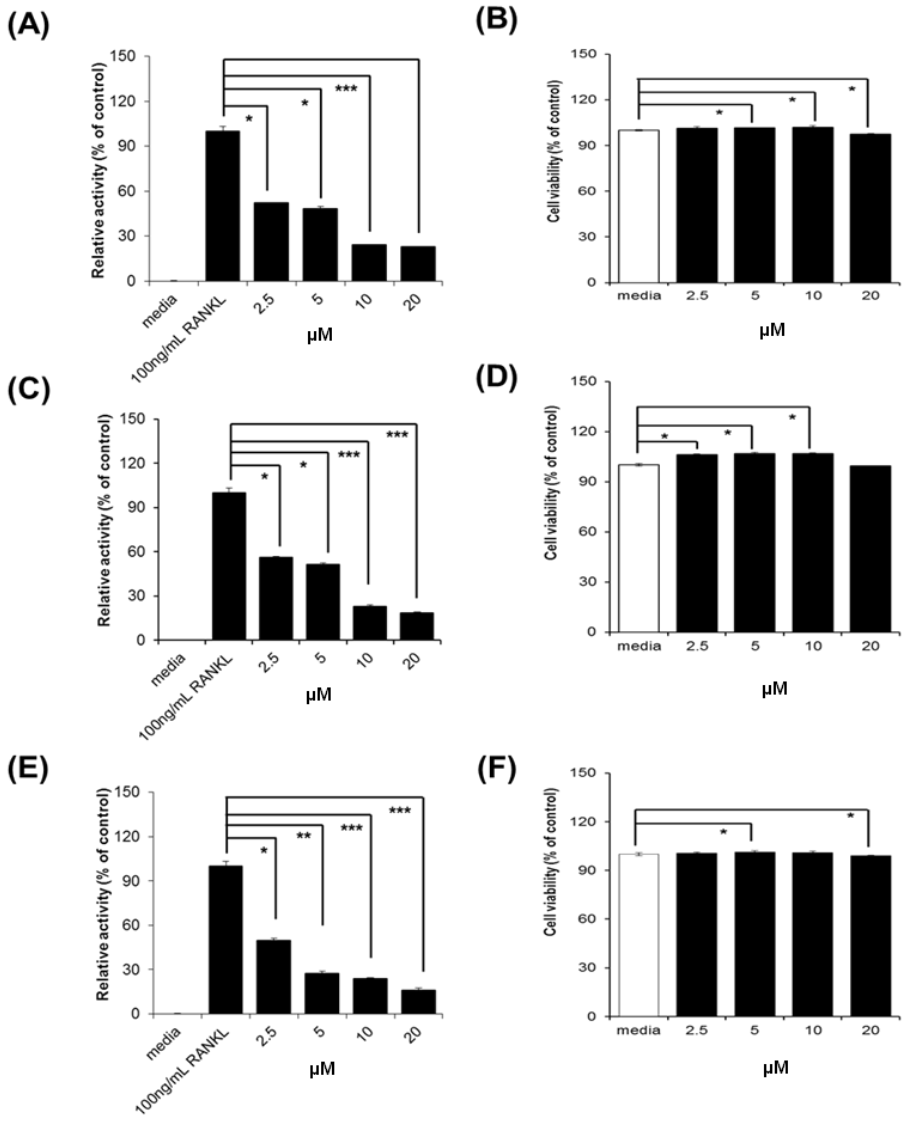

Fig 2.21 Effects of rutin, daphnoretin, and edgeworoside A on TRAP activity in RAW264.7 cells. Raw 264.7 were treated with either DMSO or compounds upon stimulation with RANKL (100 ng/mL) for 5 days, and then TRAP activity and cell viability of the cultures were measured. (A and B) Rutin. (C and D) Daphnoretin. (E and F) Edgeworoside A.

Data are expressed as a percentage of DMSO controls (100%). ** *p*-value < 0.005, *** *p*-value < 0.001 *vs.* control or RANKL.

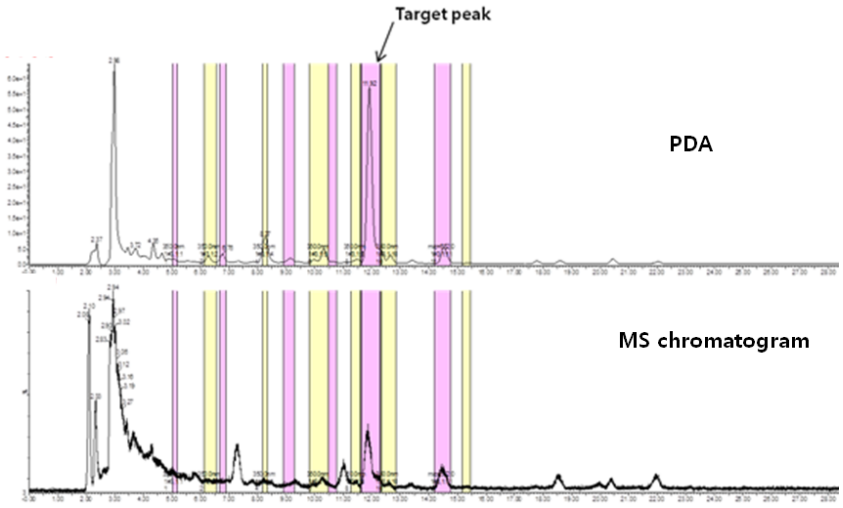

Fig 2.22 Purification of edgeworoside A from *E.chrysantha* by AutoPurification System. Edgeworoside A was purified by AutoPurification System with a QDa detector and Xbridge prep C_{18} Column with a gradient of A (0.1% formic acid v/v in deionized water) and B (0.1% formic acid v/v in acetonitrile) at flow rate of 25 mL/min. HPLC chromatogram (PDA) of edgeworoside A (upper) and MS chromatogram (lower).

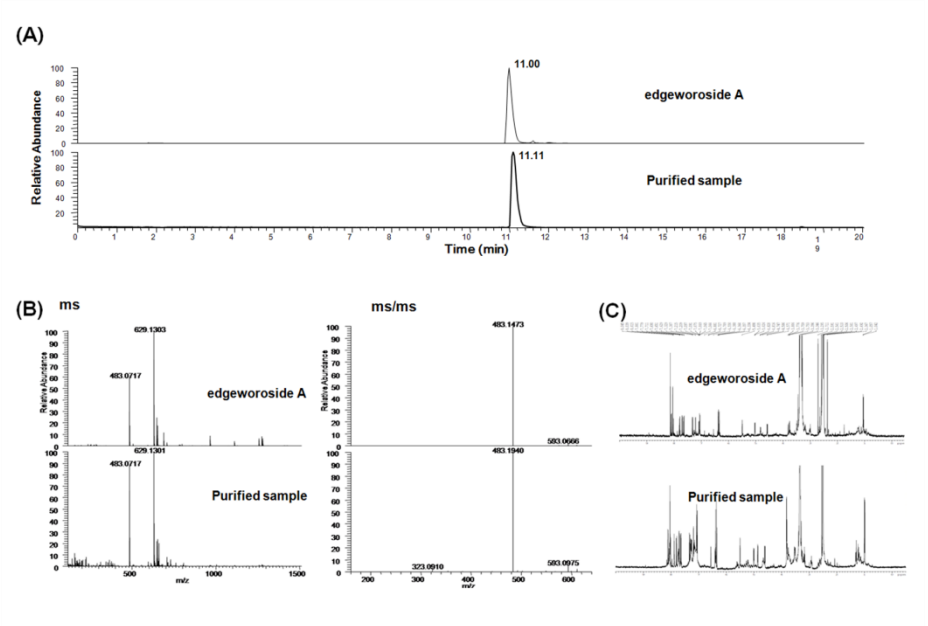

Fig 2.23 Confirmation the structure of commercial edgeworoside A and purified sample from *E. papyrifera* (A) UHPLC chromatogram of edgeworoside A (upper) and purified compound (lower). (B) The high resolution mass spectra (left) and mass/mass spectra (right); (C) ^{1}H NMR data of edgeworoside A (upper) and purified sample (lower).

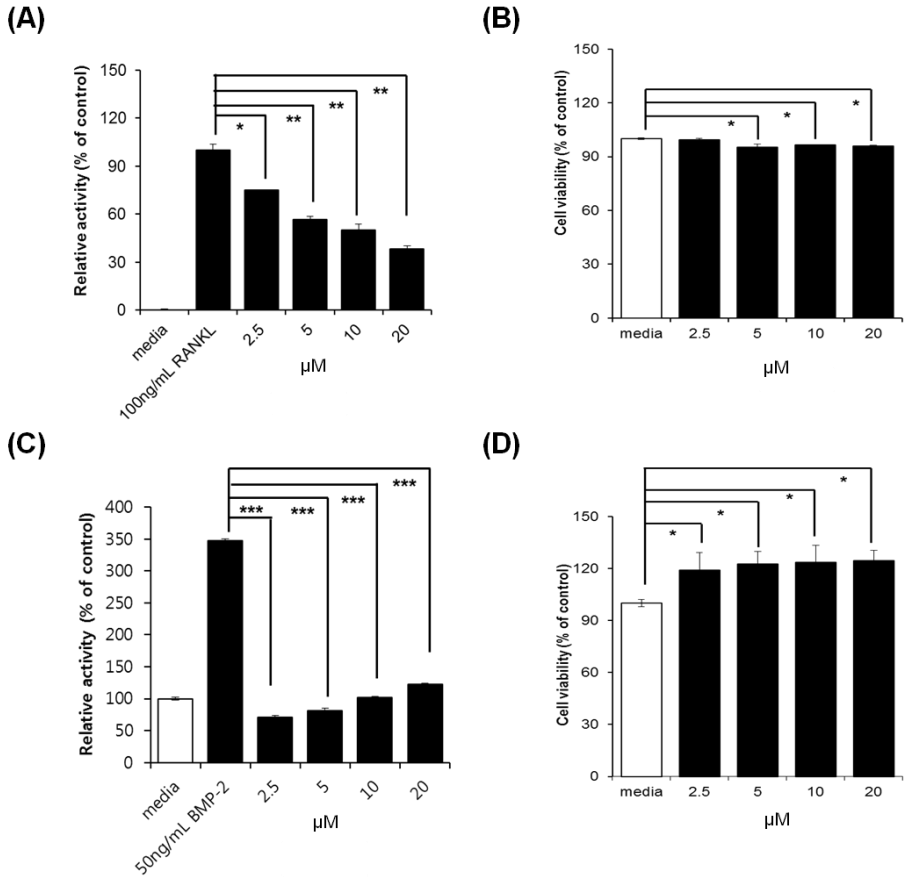

Fig 2.24 Effects of purified edgeworoside A on osteoclastogenesis and osteoblastogenesis. Raw 264.7 cells were treated with either DMSO or increasing concentrations of edgeworoside A upon stimulation with RANKL (100 ng/mL) for 5 days, and then TRAP activity (A) and cell viability (B) of the cultures were measured. MC3T-3E1 cells were treated with either DMSO, BMP-2, or increasing concentrations of edgeworoside A for 21 days, and then mineralization (C) and viability (D) of the cultures were quantified. ** p-value < 0.005, *** p-value < 0.001 *vs.* control, BMP-2 or RANKL.

Chapter 3

Whitening effect of *Rhizoma arisaematis* as functional cosmetic material

3.1. Summary

Skin pigmentation involves multiple processes including melanin synthesis, transport, and melanosome release. Melanin content determines skin color and protects against UV radiation-induced damage. Autophagy is a cooperative process between autophagosomes and lysosomes that degrades cellular components and organelles. This thesis investigates that the anti-melanogenic effects of *Rhizoma arisaematis* extract (RA) by regulating autophagy. RA treatment suppressed the α-MSH-stimulated increase of melanogenesis and down-regulated the expression of tyrosinase and TRP1 proteins in B16F1 cells. In addition, autophagy was activated in RA-treated cells. Inhibition of autophagy reduced the anti-melanogenic activity of RA in α-MSH-treated B16F1 cells. The anti-melanogenic potential of RA was confirmed in a human skin model. Treatment with RA suppressed pigmentation in 3-demensional human skin substitutes. Moreover, in a clinical trial, RA had a significant whitening effect on hyperpigmentations. Collectively, these results suggested that RA inhibits skin pigmentation through modulation of autophagy.

3.2. Introduction

Pigmentation of human skin is regulated by various stimuli, including ultraviolet (UV) radiation, microenvironmental stiffness, hormones, and inflammation (Ebanks, Wickett et al. 2009, Gillbro and Olsson 2011, Chen, Weng et al. 2014). Melanin is a biological pigmentation regulator that imparts color to the skin or hair (d'Ischia, Wakamatsu et al. 2015, D'Mello, Finlay et al. 2016). Melanogenesis involves multiple processes including melanin synthesis, transport, and melanosome release. Melanin protects the skin from UV radiation (D'Mello, Finlay et al. 2016). However, dysregulation of melanogenesis is linked to various skin diseases including acquired hyperpigmentation, melisma, and age spots (Lee 2015, Ainger, Jagirdar et al. 2017). Several melanogenic proteins have been identified as key players in melanogenesis (d'Ischia, Wakamatsu et al. 2015) . In response to UV radiation, alpha-melanocyte stimulating hormone (α-MSH) is produced and stimulates the melanocortin-1 receptor that activates a cyclic adenosine monophosphate (cAMP)-dependent pathway. Subsequently, the increased cAMP lead to activation of downstream protein kinases and upregulation of the expression of the microphthalmia-associated transcription factor (MITF) (Park, Kosmadaki et al. 2009, Hsiao and Fisher 2014). MITF is a master controller in the expression of

melanogenesis-related proteins such as tyrosinase and tyrosinase-related protein (TRP)-1/2 (Park, Kosmadaki et al. 2009, Hsiao and Fisher 2014). Tyrosinase (a copper containing enzyme) play a key role in the synthesis of melanin, as it catalyzes the two initial steps in melanin production: hydroxylation of tyrosine to 3,4-dihydroxyphenylalanine (DOPA) and oxidation of DOPA to dopaquinone. TRP1/2 catalyzes further oxidation steps in melanogenesis. Thus, tyrosinase activity is very important in controlling the synthesis of melanin. Approaches to inhibit these melanogenic enzymes have been used to skin hyperpigmentation conditions, such as melisma and age spots (Pillaiyar, Manickam et al. 2017). Examples of tyrosinase inhibitors used by the medical and cosmetic industries are arbutin, kojic acid, and resveratrol (Gunia-Krzyzak, Popiol et al. 2016, Pillaiyar, Manickam et al. 2017).

Recently, autophagy has been reported to play an important role in melanogenesis regulation in melanocyte and keratinocytes (Kim, Jo et al. 2013, Kim, Shin et al. 2013, Murase, Hachiya et al. 2013, Kim, Chang et al. 2014). Autophagy is important for maintenance of cellular homeostasis via degradation of useless proteins or damaged organelles in a lysosome-dependent manner (Kaur and Debnath 2015, Fullgrabe, Ghislat et al. 2016). Thus, autophagy functions as a cell-protective response in response to various cellular stress stimuli, such as starvation,

UV radiation, pathogen invasion, and oxidative stress (Klionsky, Abdalla et al. 2012). Autophagy has been considered as to be a non-selective bulk-degradation pathway. However, recent studies have shown that specific target organelles can be selectively eliminated; for example, mitochondrial autophagy is known as mitophagy, and peroxisomal autophagy as pexophagy (Anding and Baehrecke 2017). A recent functional genome screening study suggested that autophagy regulatory proteins such as WIPI1 and Beclin1 are involved in pigmentation (Ganesan, Ho et al. 2008, Ho, Kapadia et al. 2011). In addition, it was demonstrated that autophagy contributes to skin color determination by regulating melanin degradation in keratinocytes (Murase, Hachiya et al. 2013). Nonetheless, the role of autophagy in the regulation of skin pigmentation has not been well elucidated. Because an understanding of the mechanisms of melanogenesis can help explain pigmentation dysregulation and facilitate the development of potential cosmetic strategies, the effects of extracts from plants on melanogenesis were examined *in vitro* and *in vivo*, and the relation of anti-melanogenic activity of selected extract and activation of autophagy was explored in melanocytes.

3.3. Materials and methods

3.3.1. Cell culture

The B16F1 melanoma cell line was purchased from ATCC (Manassas, VA) and Melan-A melanocyte cell line was kindly provided by KHU skin biotechonology center (Suwon, Korea). B16F1 cells were maintained at 37°C in a 5% CO_2 humidified incubator and grown in Dulbecco's modified Eagle's medium (DMEM, Hyclone, Thermo Scientific, Logan, UT) supplemented with 10% fetal bovine serum (FBS) (Invitrogen, Carlsbad, CA) supplemented with 1% penicillin/streptomycin. To generate cells stably expressing GFP-LC3, B16F1 cells were transfected with pEGFP-LC3 using lipofectamine according to manufacturer's protocol (Invitrogen, Carlsbad, CA). Stable transfectants (B16F1/GFP-LC3) were selected by growing in selection medium containing 1mg/mL G418 for 7 days. After single cell cloning, stable clones were selected under a fluorescence microscope. Melan-A cells were maintained at 37°C in a 10% CO_2 humidified incubator and grown in RPMI-1640 (Sigma-Aldrich, St. Louis, MO, USA) supplemented with 10% fetal bovine serum (FBS, Gibco, Carlsbad, CA, USA), 1% penicillin/streptomycin (Gibco) and 200nM phorbol 12-myristate 13-acetate (PMA, Sigma-Aldrich). Three-dimensional human skin

substitute (MelanoDerm™, MEL-312-B) was purchased and maintained in EPI-100-NMM-113 media optimized according to the manufacturer's instructions (MatTek, Ashland, MA).

3.3.2. Reagents

α-MSH (alpha-melanocyte stimulating hormone), kojic acid, 3-methyladenine, bafilomycine A1, DMSO, glycerin, 1,3-butylene glycol, 1,2-hexanediol and resveratrol were purchased from Sigma-Aldrich (St. Louis, MO). A lyso-tracker probe was purchased from Invitrogen, The expression plasmid pEGFP-LC3 was kindly provided by Noboru Mizushima (Tokyo Medical and Dental University, Japan). For cream formulation, montanov™ 202 (arachidyl alcohol, behenyl alcohol and arachidyl glucoside), Sepiplus™ 400 (polyacrylate-13, polyisobutene, polysorbate 20) and Simulsol™ 165 (PEG-100 stearate and glyceryl stearate) were purchased from SEPPIC (France). Dragoxat® 89 (ethylhexyl isononanoate) was purchased from Symrise (Germany). Miglyol® 8810 (butylene glycol dicaprylate/dicaprate) was purchased from IOI Oleo GmbH (Germany). DC200 (dimechicone) was purchased from Dow corning (USA). Kalcol® 6850 (cetearyl alcohol) was purchased from Kao chemicals (Japan).

3.3.3. Plant material preparation and extraction

Dried Rhizoma *arisaematis* roots were purchased from Kyeong-Dong local market, Seoul, South Korea. Samples were authenticated. A voucher specimen was deposited at the Herbarium of the National Arboretum, Gyeonggi-do, Korea. Dried roots were ground in an FM-909T grinder (Hanil Co., Seoul, Korea) and then sieved through standard 80-mesh sieve. These samples were used for the experiments. A sample (50 g) was mixed with 950 g of 80% ethyl alcohol in a round flask. After mixing, the flask was extracted in a reflux extractor (GLMMD-F, Global LAB, Korea) with a refrigerant condenser for 3 h at 80 °C. After extraction, the extract was passed through 1.2 and 0.45 μm membrane filters. The filtered extract was evaporated in an NE-1001SD rotary evaporator (Eyela, Tokyo, Japan) and then lyophilized in FD8512 freeze dryer (Ilshin Lab Co. Ltd., Seoul, Korea) at -80 °C. The obtained powder was stored in a desiccator (Dry Keeper) at 1% relative humidity for analysis.

3.3.4. Screening of anti-melanogenic substances

Melan-A cells were lysed in lysis buffer (10 mM sodium phosphate [pH 6.8], 1% NP-40) and centrifuged and supernatant was used as the enzyme source. L-DOPA was dissolved in assay buffer (10 mM sodium

phosphate [pH 6.8]) at 1 mg/mL and used as a substrate by filtering. Extracts were prepared in an assay plate, enzyme and substrate were added, reaction was carried out at 37 °C. The amount of melanin produced was measured using plate reader (Flexstation, Molecular Devices).

3.3.5. Determination of melanin content

Melanin content was determined using a slight modification of a previously described method (Kim, Jo et al. 2013). B16F1 cells were treated with α-MSH for 24 hr. Then the cells were exposed to RA for additional 24 hr. To measure melanin content, cells were harvested by trypsinization and dissolved in a soluble buffer (1N NaOH containing 10% DMSO) at 100 °C for 30 min, and then, relative melanin content was determined by measuring absorbance at 415 nm using an ELISA plate reader (Victor X3, Perkin Elmer). The change in lightness (ΔL) value of the skin model was calculated from the L value (lightness index) measured by a colorimeter (CR-300; Konica Minolta, Tokyo, Japan), as follows: $\Delta L = L$ (treatment skin) − L (control skin) at 12 days (Choi, Shin et al. 2016). An increase in ΔL value indicates the chemical-induced hypopigmentation of the skin.

3.3.6. Cream formulations for clinical test

Two cream formulations (control cream and RA cream) were prepared for clinical tests (Table 3.1). Both A and B phases were heated separately to 80 °C. The B phase was slowly added to the A phase using a homo-mixer (MarkII, Primix, Japan) at 4,000 rpm for 30 min. After homogenization, the creams were cooled to room temperature.

3.3.7. Clinical study on hyperpigmentation

In this clinical study, we examined a depigmentation effect on hyperpigmentations following the NIFDSE (National institute of food and drug safety evaluation) guideline (Dorato et al. 2011). Twenty-two hyperpigmented volunteers were evaluated in the clinical study. All volunteers were female, and the average age was 47. This study was approved by the Institutional Review Board (IRB) of hospital (KDRI-IRB-16923). Volunteers applied the RA cream to one cheek and the control cream to the other cheek for 4 weeks. The pigment density of the patients was evaluated using a Mexameter (MX 18, CK electronic GmbH, Germany) and Janus facial analysis system (PSI, Korea) every 2 weeks.

3.3.8. Cell viability and autophagy analysis

Cell viability was determined through the reduction of WST-8 [2-(2-methoxy-4-nitrophenyl)-3-(4-nitrophenyl)-5-(2,4-disulfophenyl)-*2H*-tetrazolium, monosodium salt] to water soluble formazan using a Cell Counting Kit-8 (CCK-8) (Dojindo Laboratories, Kumamoto, Japan). CCK-8 was added to each well at 1/10 the volume of the media in the well. Cells were incubated at 37°C for 30 min. The absorbance change was measured at 450 nm using a microplate reader (Victor X3, Perkin Elmer). To assess autophagy activation, B16F1/GFP-LC3 cells were treated with RA and the cells with autophagy were determined by counting the number of cells with GFP-LC3 punctate structures under a fluorescence microscope (IX71, Olympus, Japan).

3.3.9. Western blot analysis

Proteins were isolated from cells using 2 x Laemmli sample buffer (Bio-Rad, Hercules, CA). After separation by 10-15% SDS-PAGE, proteins were transferred to polyvinylidene fluoride (PVDF) membranes (Bio-Rad, Hercules, CA). Membranes were blocked with 5% skim milk in TBST for 1 hr and then incubated with specific primary antibodies overnight at 4°C. Anti-LC3 (NB100-2220) antibody was purchased from NOVUS Biologicals (Littleton, CO); anti-p62 (sc-28359) antibody was

purchased from Santa Cruz Biotechnology (Santa Cruz, CA); anti-Actin (MAB1501) antibody was purchased from Millipore (Temecula, CA). Details of the anti-tyrosinase and anti-TRP1 antibodies are described in a previous study (Kim, Jo et al. 2013). For protein detection, membranes were incubated with HRP-conjugated secondary antibodies and signals were detected using the Super-signal West Dura HRP detection kit (Pierce, Rockford, IL).

3.3.10. Statistical analysis

Results are expressed as means ± S.E.M. The significance of differences between experimental groups was determined by Student's *t*-test. A *p*-value <0.05 was considered to indicate statistical significance. All clinical results were expressed as means ± standard deviation (S.D.) and analyzed using Minitab 17 (Minitab® 17.3.1, Minitab Inc.). The Ryan-Joiner Normality test was used for statistical analysis. To determine if differences between periods were significant, the paired t-test and Wilcoxon signed rank tests were performed. Statistical differences between experimental groups were determined by Welch's t-test and Mann-Whitney U test. A *p*-value <0.05 was considered statistically significant.

3.4. Results

3.4.1. Screening of potent anti-melanogenic plant extracts

In an effort to discover an anti-melanogenic substance, 303 herbal extracts derived from South Korea were screened for the ability to inhibit melanogenesis. The crude extracts were tested at a concentration of 200μg/mL, and those extracts which inhibited the enzyme activity greater than 20% as compared to the DMSO control were subjected to melanin contents assay in Melan-A to confirm the desired activity profile. Finally, two extracts, *Rhizoma arisaematis* extract (RA) and *Cassia herba* extracts (CH) were selected through this screening system (Table 3.2).

3.4.2. Effect of *R. arisaemaits* on pigmentation in normal human epidermal melanocytes and human skin

The effect of RA on a human artificial skin model was assessed. 3-Dimensional human skins were treated with kojic acid, RA or CH for 12 days, and the pigmentation were measured by differences of lightness value. As shown in Fig. 1A, pigmentation was reduced by treatment of RA in the human artificial skin model (Fig 3.1A, B). Then the effects of RA were examined on human skin directly. The RA-containing skin

cream was formulated and treated to human facial skin. Notably, it showed that the melanin value of human facial skin was significantly reduced in the RA cream-treated group compared with the control group (Fig 3.1C, D). These results from human skin models strongly indicate that RA has a depigmentation effect on human skin.

3.4.3. Confirmation of anti-melanogenic effects in B16F1 cells

To identify molecules capable of regulating skin pigmentation, a natural product library was screened and then *R. Arisaematis* extract was identified as a potent anti-melanogenic regulator. It has been reported that RA has a toxic effect on cancer cells, thus the cell viability of B16F1 melanoma cells treated with RA was also examined. As shown in Figure. 1A, RA had no significant cytotoxic effect in B16F1 cells up to a concentration of 1 mg/mL, while cell proliferation was slightly enhanced (Fig 3.2A). Therefore, 0.5 mg/mL RA was treated for further experiments. To examine the effect of RA on melanin generation, B16F1 cells stimulated with α-MSH were treated with either RA or resveratrol, a well-known inhibitor of skin pigmentation. Treatment with α-MSH strongly induced melanin synthesis. However, excessive melanin production by α-MSH was efficiently suppressed in RA-treated cells (Fig 3.2B, C). Expressions of specific melanogenesis-related proteins were

evaluated in RA-treated cells. Expression levels of both tyrosinase and tyrosinase-related protein-1 (TRP1), which were elevated by α-MSH treatment, decreased to the same levels in RA-treated cells as those measured in resveratrol-treated cells (Fig 3.2D).

3.4.4. Role of *R. arisaemaits* in activation of autophagy in B16F1 cells

Activation of autophagy inhibits skin pigmentation in melanocytes was reported previously (Kim, Jo et al. 2013). Therefore, the role of RA in activation of autophagy was examined. To investigate the effect of RA on autophagy, B16F1 cells stably expressing the GFP-fused LC3 protein, which is generally used as an indication of autophagy activation were exposed to RA. As shown in the Fig. 3.3A and B, the formation of punctate GFP-LC3 proteins was notably increased (Fig. 3.3 A, B). In addition, treatment with RA decreased levels of the p62 protein, a substrate for autophagy-mediated degradation but increased LC3 II conversion, suggesting that RA induces activation of autophagy (Fig 3.3C). To examine autophagy flux in response to RA treatment, B16F1 cells were incubated with RA with or without bafilomycin A1 which inhibits fusion of autophagosome to lysosome. The level of LC3 was higher in the cells treated with RA and bafilomycin A1 than the cells treated with either of these compounds individually (Fig 3.3D). I further

assessed lysosome activation following RA treatment. B16F1 cells were treated with RA for 24 hr and then stained with a lysotracker (red) dye. As shown in Fig. 3E, treatment with RA resulted in increased lysosome activity compared with the control cells (Fig 3.3E). Taken together, these results suggest that RA induces autophagy in B16F1 cells.

3.4.5. Effect of autophagy inhibition in *R. arisaemaits*-mediated anti-melanogenic activity in B16F1 cells

The effect of inhibition of autophagy in RA-treated cells was investigated. Several phosphoinositide 3 (PI3) kinase inhibitors, such as 3-methyladenine (3MA) inhibit the early step of autophagy activation. Thus, 3MA was used to inhibit autophagy action in RA-treated cells. Consistently, treatment of 3MA in B16F1/GFP-LC3 cells significantly suppressed autophagy activation induced by RA treatment (Fig 3.4A). Some reports have revealed the evidences that autophagy is involved in melanosome destruction and biogenesis (Kim, Jo et al. 2013, Murase, Hachiya et al. 2013), hence the effect of autophagy inhibition on melanin synthesis after RA treatment was tested. Notably, inhibition of autophagy by 3MA treatment sufficiently reduced the anti-melanogenic effect of RA in α-MSH-treated cells (Fig 3.4B, C). The effect of suppression of autophagy on ARP101-mediated anti-melanogenesis was confirmed by

Western blotting analysis with key melanogenesis regulators as tyrosinase and tyrosinase-related protein 1 (TRP1). Consistent with the melanin content results, treatment of cells with 3MA allowed the recovery of the RA-reduced protein levels of tyrosinase and TRP1 in α-MSH-stimulated cells (Fig 3.4D). These results suggest that autophagy activation contributes to the anti-melanogenic effect of RA.

3.5. Discussion

In thesis, *R. arisaematis* (RA) identified as a novel anti-melanogenic agent by screening a natural product library. RA is a well-known traditional oriental medicine that is used to treat convulsions, inflammation, and cancer (Shen, Zhang et al. 2014). In addition, RA has been shown to influence lipid and glucose metabolism in a high fat diet model (Lee, Kim et al. 2007). Although the pharmacological effects of RA in cancer and inflammation have been studied the effect of RA on melanogenesis has not been investigated. Here, the anti-melanogenic effect of RA was explored. Treatment with RA efficiently inhibited hyper-melanogenesis in α-MSH-treated cells (Fig 3.1). In addition, RA reduces melanogenesis in human skin models (Fig 3.2). Previously, it was reported that RA had a cytotoxic effect on cancer cells (Li 1998, Huang, Yang et al. 2011). Combination of RA with ginger juice or bile juice efficiently reduces its toxicity, suggesting that different progressions attenuate the toxicity of RA (Chen, Xu et al. 2012). Therefore, the cytotoxic effect of RA in B16F1 cells was tested and then treatment of these cells with RA did not induce cell death and toxicity at the tested-dosages (0.1 ~ 1 mg/mL). These results suggest that the toxicity of RA differs according to cell types.

In an experiment using three-dimensional skin substitutes, RA treatment, 1 mg/mL of RA (0.1% of RA), resulted in a decrease in pigmentation by 36.8 % as compared to the vehicle-treated control; however treatment of kojic acid which is commonly known to be the most effective whitening agent, resulted in a decrease in pigmentation by 31.9 % at the concentration of 2 % (w/v). Moreover, the inhibitory effects of arbutin and kojic acid on pigmentation in a clinical test were evident at 4 weeks; however the effect of RA was evident at 2 weeks in thesis. These results obviously indicate that RA has equal or even better whitening efficacy on the human skin than commercially available whitening agents.

Recently, other groups showed that autophagy inhibits melanogenesis by increasing the degradation of melanosomes in melanocytes (Kim, Jo et al. 2013, Kim, Shin et al. 2013, Murase, Hachiya et al. 2013, Kim, Chang et al. 2014). Treatment of ARP101, resveratrol, and 3-ODI increases melanin degradation via autophagy activation (Kim, Shin et al. 2013, Kim, Chang et al. 2014). In addition, depletion of ULK1, which is the upstream autophagy regulatory gene, was shown to increase melanin content in MTN1 cells, which are human melanoma cells (Kalie, Razi et al. 2013). Hence, the effect of RA on autophagy activation was further addressed. Treatment with RA strongly promoted autophagy activation in B16F1 cells. Treatment of B16F1/GFP-LC3 cells with RA upregulated

autophagy flux and increased lysosomal activity (Fig 3.3). Moreover, blocking autophagy by a chemical inhibitor reversed the α-MSH-induced reduction in melanin content as well as autophagy activation in α-MSH-treated B16F1 cells, suggesting that the anti-melanogenic effect of RA is modulated by autophagy activation. In accordance with thesis, Feng et al., recently reported that agglutinin isolated from *Arisema Heterophyllum*, which is also used as a source of RA, enhanced accumulation of LC3 II and ATG7 proteins in A459 cells (Feng, Sun et al. 2016). Taken together, these results suggest that autophagy may contribute to regulation of melanogenesis in RA-treated cells. Beside autophagy activation, it was observed that treatment of RA in α-MSH-treated cells reduced the expression of tyrosinase and TRP1, which are critical regulators of melanin production (Fig 3.1D). Regulation of melanin production at the genetic level is well described. Several signaling pathways such as the PI3K/AKT signaling and cAMP signaling, regulate transactivation of MITF in α-MSH-treated cells (Park, Kosmadaki et al. 2009). Various tyrosinase inhibitors, including arbutin and resveratrol, have been used as anti-pigmentation agents (Gunia-Krzyzak, Popiol et al. 2016, Pillaiyar, Manickam et al. 2017). However, the role of RA in melanogenesis remained to be addressed.

Table 3.1 Composition of cream formulations.

Ingredient	Control Cream (w/w, %)	RA Cream (w/w, %)
Phase A		
Deionized water	To 100	To 100
Glycerin	5.00	5.00
1,3-Butylene glycol	4.00	4.00
1,2-Hexanediol	2.00	2.00
Phase B		
Montanov 202	2.50	2.50
Simulsol 165	1.50	1.50
Dragoxat 89	5.00	5.00
Miglyol 8810	3.00	3.00
DC200	0.50	0.50
Kalcol 6850	1.50	1.50
Sepiplus 400	0.70	0.70
RA	-	0.05

Table 3.2 Candidate list of anti-melanogenic plant extracts

Latin name	Scientific (Botanical) name
Rhizoma *Arisaematis*	*Arisaema amurense* Maxim.
Cassiae Herba	*Cassia mimosoides* var. *Nomame*

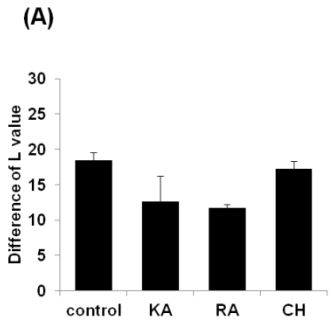

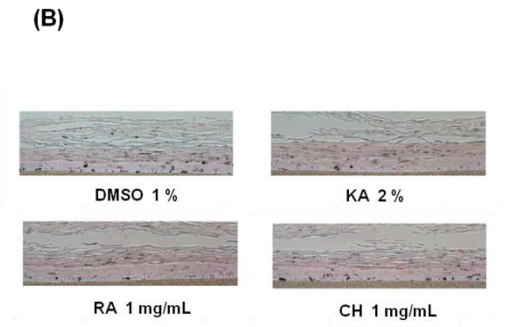

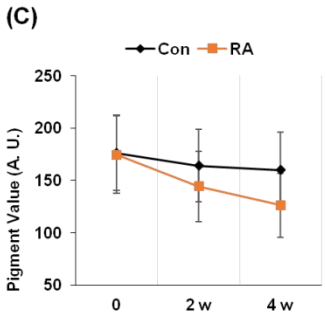

(D)

		M-value	Improvement Rate	P-value
RA cream	before	174.60	-	< 0.001
	2 W	144.17***	17.43%	
	4W	126.12***	27.77%	
Control cream	before	176.24	-	< 0.001
	2 W	163.99***	6.95%	
	4W	159.83***	9.31%	

Fig 3.1 The suppression of pigmentation in 3D skin substitutes and human skin by *R. arisaematis*. (A, B) The 3-dementional human skin substitutes (Melano-Derm tissue) were treated with Kojic acid (2%, KA) or RA (1 mg/mL) or CH (1 mg/mL) for 12 days. Pigmentation of the skin substitutes was measured the lightness (ΔL) and calculated between the control and treated groups (A). The amount of melanin was confirmed by Fontana-Masson tissue staining (B). (C, D) Human skin was treated with control cream or RA containing cream. After 2 weeks and 4 weeks, Melanin values (arbitrary unit) of skin and improvement rate was calculated compared with the initial value. Data were collected from 22 volunteer.

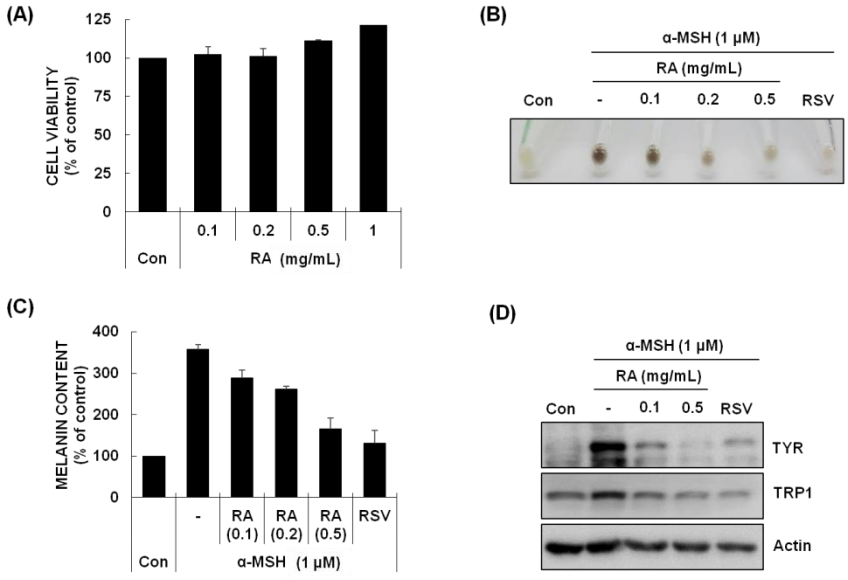

Fig. 3.2 The inhibition of α-MSH-stimulated melanogenesis in B16F1 cells by *R. Arisaematis*. (A) B16F1 cells were treated with various concentrations of *Rhizoma arisaematis* (RA, 0.1 – 1 mg/mL) for 24 hr, then cell viability was determined by CCK-8 assay. (B-D) B16F1 cells pre-treated with α-MSH (1 μM) for 24 hr were further incubated with either RA or resveratrol (RSV, 100 μM). Cell pellets were obtained (B), and melanin content was determined as described in the Materials and Methods (C). The expression of tyrosinase (TYR) and tyrosinase-related protein-1 TRP1) was analyzed by western blotting (D). Data were obtained from least three independent experiments and values are presented as means ± S.E.M. (* p<0.01)

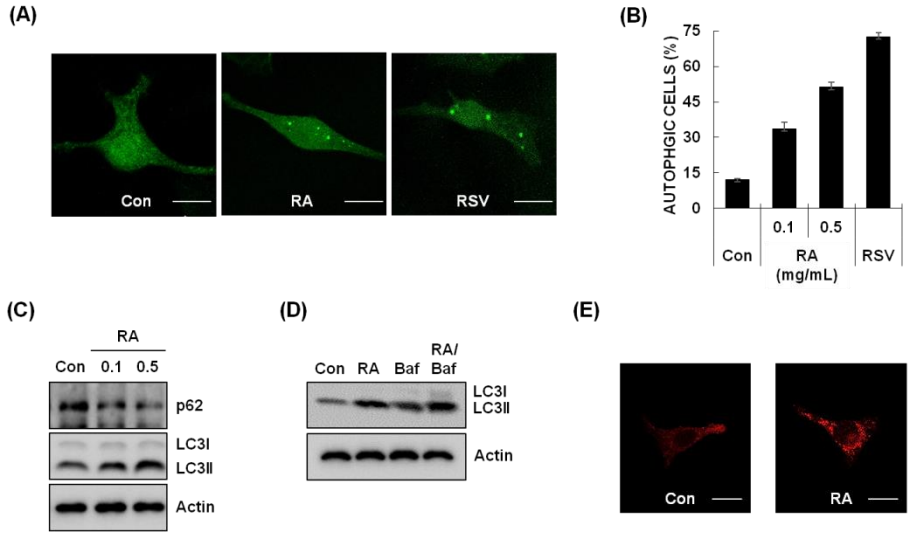

Fig 3.3 The induction of autophagy activation in B1gF1 cells by *R. Arisaematis*. (A) B16F1 cells stably expressing GPF-LC3 (B16F1/GFP-LC3) were treated with either *Rhizoma arisaematis* (RA, 0.1 mg/mL) or resveratrol (RSV, 100 μM) for 24 hr. Cells were then fixed for imaging. The scale bar indicates 10 μm. (B, C) B16F1/GFP-LC3 cells were incubated with increasing concentrations of RA (0.1, 0.5 mg/mL) or RSV (100 μM). After 24 hr, cells that had autophagic punctate structures with GFP-LC3 were counted under a fluorescence microscope (B). Cells were further assessed by western blotting using the indicated antibodies (C). (D) B16F1 cells were treated with RA in the presence or absence of an autophagy inhibitor, bafilomycin A1 (Baf-A1; 20 nM). The level of LC3 protein was then assessed by western blotting. (E) B16F1 cells treated

with RA (0.5 mg/mL) for 24 hr were stained with a lyso-tracker. Then cells were fixed to observe fluorescence by confocal microscopy. Data were obtained from at least three independent experiments and values are presented as means ± S.E.M. (* $p<0.01$).

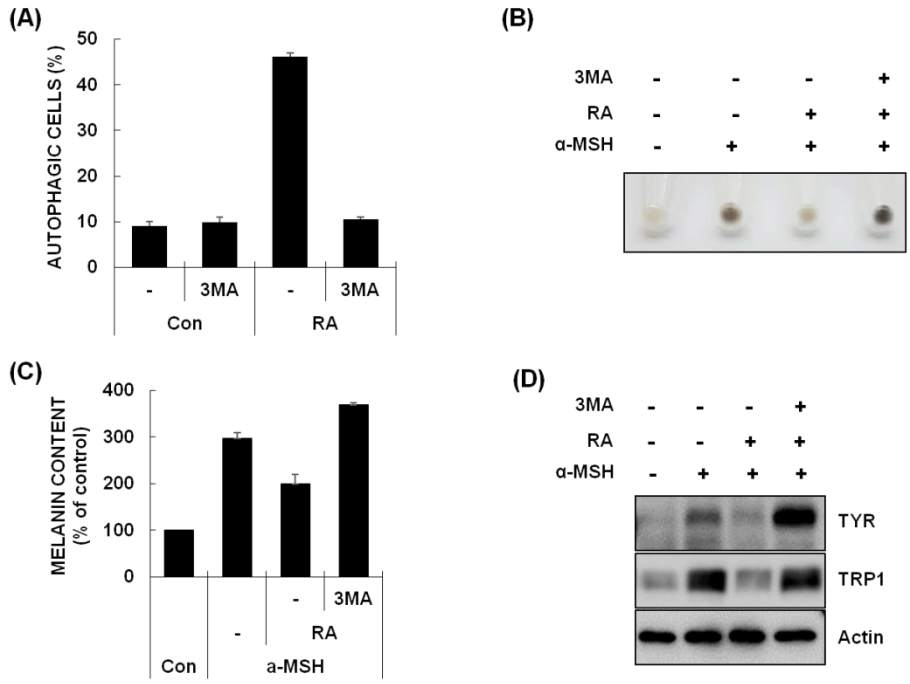

Fig 3.4 Inhibition of autophagy suppressed RA-mediated anti-melanogenic activity in B16F1 cells. (A) B16F1/GFP-LC3 cells pretreated with 3-methyladenine (3MA, 5 mM) for 12 hr were further incubated with RA (0.5 mg/mL). Cells with autophagy activation were determined by counting punctate GFP-LC3 dots under a fluorescence microscope. (B, C) B16F1 cells pretreated with α-MSH (1 μM) for 24 hr were further incubated with RA (0.5 mg/mL) in the presence or absence of 3MA (5 mM). Then cells were harvested (B) and lysed to measure melanin content (C). (D) B16F1 cells pretreated with α-MSH (1 μM) for 24 hr were additionally incubated with RA (0.5 mg/mL) in the presence or absence of 3MA (5 mM). Protein levels of tyrosinase (TRY) and

tyrosinase-related protein 1 (TRP1) were further analyzed by western blotting. Data were obtained from least three independent experiments and values are presented as means ± S.E.M. (* $p<0.01$).

Chapter 4

Conclusions and future directions

4.1. Conclusions from anti-osteoporotic natural products

There have been rapid changes in social circumstances and expectations, such as increased life expectancy and the subsequent growth of the aging population. The anti-osteoporotic drugs available in the market have limited usefulness and severe side effects. This has increased the demand for new therapeutic agents and nutritional supplements for the promotion of bone health. Therefore, it is necessary to identify new anti-osteoporotic candidates from natural sources and to develop them as drug and health supplement ingredients. In order to achieve thesis objectives, the following studies were serially conducted: 1. Construction of a natural plant extract library and the development of HTS compatible assays; 2. *In vitro* screening for anti-osteoclastic materials; 3. *In vitro* screening for osteogenic materials; 4. *In vivo* test using a preventive mouse model; 5. *In vivo* test using a therapeutic rat model; 6. Identification of the active ingredients in the selected plant extracts; and 7. Identification of a new anti-osteoporotic plant and its phytochemicals.

These efforts led to the identification of *E. papyrifera*, which showed the ability to inhibit the differentiation of osteoclasts and to boost the calcification of osteoblasts. Furthermore, *E. papyrifera* exerted potent preventive and therapeutic activities in an animal model of osteoporosis.

HPLC-HRMS profiling and *in vitro* biochemical analyses of *E. papyrifera* revealed that edgeworoside A was the active ingredient that most significantly contributed to its bioactivity. These results may serve as a basis for further detailed exploration of the potential applications of *E. papyrifera* extracts and edgeworoside A, with the ultimate goal of providing new insights into the treatment of osteoporosis.

4.2. Conclusion from whitening natural products

In this study, the anti-melanogenic potential of *R. arisaematis* was confirmed in three-dimensional human skin substitutes and in a clinical trial. The anti-melanogenic effects of *R. arisaematis* were confirmed through the regulation of autophagy. Although these findings indicate that *R. arisaematis* has anti-melanogenic activity, this study did not investigate which components of *R. arisaematis* were responsible for this activity. Therefore, further studies to discover the active compounds in *R. arisaematis* that regulate melanogenesis are required. In conclusion, the present study was the first to show that *R. arisaematis* exerts an anti-pigmentation effect through the induction of autophagy activation in melanocytes, and this supports the development of *R. arisaematis* as a novel anti-pigmentation agent.

In conclusion, two new anti-osteoporotic natural products, *E. papyrifera* and edgeworoside A, and a new natural product for whitening, *R. arisaematis*, were discovered, and these natural products could be developed to into therapeutic drugs and cosmetic ingredients.

4.3. Future directions

Ongoing and future work toward addressing the two main objectives are outlined below.

• Further research on the screening and evaluation of new anti-osteoporotic natural plants, involving active phytochemicals such as daphnoretin, rutin, and edgeworoside A, which appear to be active supplements as well as anti-osteoporotic agents, is being worked on. In addition, the study of the cellular mechanism of edgeworoside A is also ongoing as an immediate next step to my thesis project.

• Additional applications for the phytochemicals and natural products developed in this study, such as the treatment of related diseases, (e.g. metabolic and age-related diseases), will be explored.

References

Ainger, S. A., K. Jagirdar, K. J. Lee, H. P. Soyer and R. A. Sturm (2017). "Skin Pigmentation Genetics for the Clinic." Dermatology **233**(1): 1-15.

Allan, E. H., K. D. Hausler, T. Wei, J. H. Gooi, J. M. Quinn, B. Crimeen-Irwin, S. Pompolo, N. A. Sims, M. T. Gillespie, J. E. Onyia and T. J. Martin (2008). "EphrinB2 regulation by PTH and PTHrP revealed by molecular profiling in differentiating osteoblasts." J Bone Miner Res **23**(8): 1170-1181.

Alves, H., K. Dechering, C. Van Blitterswijk and J. De Boer (2011). "High-throughput assay for the identification of compounds regulating osteogenic differentiation of human mesenchymal stromal cells." PLoS One **6**(10): e26678.

Anding, A. L. and E. H. Baehrecke (2017). "Cleaning House: Selective Autophagy of Organelles." Dev Cell **41**(1): 10-22.

Arlot, M., P. J. Meunier, G. Boivin, L. Haddock, J. Tamayo, R. Correa-Rotter, S. Jasqui, D. W. Donley, G. P. Dalsky, J. S. Martin and E. F. Eriksen (2005). "Differential effects of teriparatide and alendronate on bone remodeling in postmenopausal women assessed by histomorphometric parameters." J Bone Miner Res **20**(7): 1244-1253.

Baek, J. M., J. Y. Kim, Y. H. Cheon, S. H. Park, S. J. Ahn, K. H. Yoon, J. Oh and M. S. Lee (2014). "Dual Effect of Chrysanthemum indicum Extract to Stimulate Osteoblast Differentiation and Inhibit Osteoclast Formation and Resorption In Vitro." Evid Based Complement Alternat Med **2014**: 176049.

Barmada, S. J., A. Serio, A. Arjun, B. Bilican, A. Daub, D. M. Ando, A. Tsvetkov, M. Pleiss, X. Li, D. Peisach, C. Shaw, S. Chandran and S. Finkbeiner (2014). "Autophagy induction enhances TDP43 turnover and survival in neuronal ALS models." Nat Chem Biol **10**(8): 677-685.

Baylink, D. J., R. D. Finkelman and S. Mohan (1993). "Growth factors to stimulate bone formation." J Bone Miner Res **8 Suppl 2**: S565-572.

Bellido, T., A. A. Ali, I. Gubrij, L. I. Plotkin, Q. Fu, C. A. O'Brien, S. C. Manolagas and R. L. Jilka (2005). "Chronic elevation of parathyroid hormone in mice reduces expression of sclerostin by osteocytes: a novel mechanism for hormonal control of osteoblastogenesis." Endocrinology **146**(11): 4577-4583.

Beral, V. and C. Million Women Study (2003). "Breast cancer and

hormone-replacement therapy in the Million Women Study." Lancet **362**(9382): 419-427.

Bharti, A. C., Y. Takada and B. B. Aggarwal (2004). "Curcumin (diferuloylmethane) inhibits receptor activator of NF-kappa B ligand-induced NF-kappa B activation in osteoclast precursors and suppresses osteoclastogenesis." J Immunol **172**(10): 5940-5947.

Bilezikian, J. P. (2008). "Combination anabolic and antiresorptive therapy for osteoporosis: opening the anabolic window." Curr Osteoporos Rep **6**(1): 24-30.

Black, D. M., S. L. Greenspan, K. E. Ensrud, L. Palermo, J. A. McGowan, T. F. Lang, P. Garnero, M. L. Bouxsein, J. P. Bilezikian, C. J. Rosen and T. H. S. I. Pa (2003). "The effects of parathyroid hormone and alendronate alone or in combination in postmenopausal osteoporosis." N Engl J Med **349**(13): 1207-1215.

Boivin, G., D. Farlay, M. T. Khebbab, X. Jaurand, P. D. Delmas and P. J. Meunier (2010). "In osteoporotic women treated with strontium ranelate, strontium is located in bone formed during treatment with a maintained degree of mineralization." Osteoporos Int **21**(4): 667-677.

Bone, H. G., R. W. Downs, Jr., J. R. Tucci, S. T. Harris, R. S. Weinstein, A. A. Licata, M. R. McClung, D. B. Kimmel, B. J. Gertz, E. Hale and W. J. Polvino (1997). "Dose-response relationships for alendronate treatment in osteoporotic elderly women. Alendronate Elderly Osteoporosis Study Centers." J Clin Endocrinol Metab **82**(1): 265-274.

Bonewald, L. F. and M. L. Johnson (2008). "Osteocytes, mechanosensing and Wnt signaling." Bone **42**(4): 606-615.

Bouxsein, M. L. (2003). "Bone quality: where do we go from here?" Osteoporos Int **14 Suppl 5**: S118-127.

Brey, D. M., N. A. Motlekar, S. L. Diamond, R. L. Mauck, J. P. Garino and J. A. Burdick (2011). "High-throughput screening of a small molecule library for promoters and inhibitors of mesenchymal stem cell osteogenic differentiation." Biotechnol Bioeng **108**(1): 163-174.

Briscoe, J. and P. P. Therond (2013). "The mechanisms of Hedgehog signalling and its roles in development and disease." Nat Rev Mol Cell Biol **14**(7): 416-429.

Burge, R., B. Dawson-Hughes, D. H. Solomon, J. B. Wong, A. King and A. Tosteson (2007). "Incidence and economic burden of osteoporosis-related fractures in the United States, 2005-2025." J Bone Miner Res **22**(3): 465-475.

Chambers, T. J. and K. Fuller (1985). "Bone cells predispose bone surfaces to resorption by exposure of mineral to osteoclastic contact." J Cell Sci **76**: 155-165.

Chavassieux, P. M., M. E. Arlot, C. Reda, L. Wei, A. J. Yates and P. J. Meunier (1997). "Histomorphometric assessment of the long-term effects of alendronate on bone quality and remodeling in patients with osteoporosis." J Clin Invest **100**(6): 1475-1480.

Chavassieux, P. M., M. E. Arlot, J. P. Roux, N. Portero, A. Daifotis, A. J. Yates, N. A. Hamdy, M. P. Malice, D. Freedholm and P. J. Meunier (2000). "Effects of alendronate on bone quality and remodeling in glucocorticoid-induced osteoporosis: a histomorphometric analysis of transiliac biopsies." J Bone Miner Res **15**(4): 754-762.

Chen, G., J. Xu, X. Miao, Y. Huan, X. Liu, Y. Ju and X. Han (2012). "Characterization and antitumor activities of the water-soluble polysaccharide from Rhizoma Arisaematis." Carbohydr Polym **90**(1): 67-72.

Chen, H., Q. Y. Weng and D. E. Fisher (2014). "UV signaling pathways within the skin." J Invest Dermatol **134**(8): 2080-2085.

Chesnut, C. H., 3rd, S. Majumdar, D. C. Newitt, A. Shields, J. Van Pelt, E. Laschansky, M. Azria, A. Kriegman, M. Olson, E. F. Eriksen and L. Mindeholm (2005). "Effects of salmon calcitonin on trabecular microarchitecture as determined by magnetic resonance imaging: results from the QUEST study." J Bone Miner Res **20**(9): 1548-1561.

Choi, E. M. and Y. S. Lee (2011). "Involvement of PI3K/Akt/CREB and redox changes in mitochondrial defect of osteoblastic MC3T3-E1 cells." Toxicol In Vitro **25**(5): 1085-1088.

Choi, H., J. H. Shin, E. S. Kim, S. J. Park, I. H. Bae, Y. K. Jo, I. Y. Jeong, H. J. Kim, Y. Lee, H. C. Park, H. B. Jeon, K. W. Kim, T. R. Lee and D. H. Cho (2016). "Primary Cilia Negatively Regulate Melanogenesis in Melanocytes and Pigmentation in a Human Skin Model." PLoS One **11**(12): e0168025.

Christensen, S. T., L. B. Pedersen, L. Schneider and P. Satir (2007). "Sensory cilia and integration of signal transduction in human health and disease." Traffic **8**(2): 97-109.

Cohen, A., D. W. Dempster, R. R. Recker, E. M. Stein, J. M. Lappe, H. Zhou, A. J. Wirth, G. H. van Lenthe, T. Kohler, A. Zwahlen, R. Muller, C. J. Rosen, S. Cremers, T. L. Nickolas, D. J. McMahon, H. Rogers, R. B. Staron, J. LeMaster and E. Shane (2011). "Abnormal bone microarchitecture and evidence of osteoblast dysfunction in premenopausal women with idiopathic osteoporosis." J Clin Endocrinol Metab **96**(10): 3095-3105.

Cooper, C., G. Campion and L. J. Melton, 3rd (1992). "Hip fractures in the elderly: a world-wide projection." Osteoporos Int **2**(6): 285-289.

Cornish, J., K. Callon, A. King, S. Edgar and I. R. Reid (1993). "The effect of leukemia inhibitory factor on bone in vivo." Endocrinology **132**(3): 1359-1366.

Cummings, S. R., J. San Martin, M. R. McClung, E. S. Siris, R. Eastell, I. R. Reid, P. Delmas, H. B. Zoog, M. Austin, A. Wang, S. Kutilek, S. Adami, J. Zanchetta, C. Libanati, S. Siddhanti, C. Christiansen and F. Trial (2009). "Denosumab for prevention of fractures in postmenopausal women with osteoporosis." N Engl J Med **361**(8): 756-765.

d'Ischia, M., K. Wakamatsu, F. Cicoira, E. Di Mauro, J. C. Garcia-Borron, S. Commo, I. Galvan, G. Ghanem, K. Kenzo, P. Meredith, A. Pezzella, C. Santato, T. Sarna, J. D. Simon, L. Zecca, F. A. Zucca, A. Napolitano and S. Ito (2015). "Melanins and melanogenesis: from pigment cells to human health and technological applications." Pigment Cell Melanoma Res **28**(5): 520-544.

D'Mello, S. A., G. J. Finlay, B. C. Baguley and M. E. Askarian-Amiri (2016). "Signaling Pathways in Melanogenesis." Int J Mol Sci **17**(7).

DeCaen, P. G., M. Delling, T. N. Vien and D. E. Clapham (2013). "Direct recording and molecular identification of the calcium channel of primary cilia." Nature **504**(7479): 315-318.

Delaisse, J. M., Y. Eeckhout and G. Vaes (1988). "Bone-resorbing agents affect the production and distribution of procollagenase as well as the activity of collagenase in bone tissue." Endocrinology **123**(1): 264-276.

Dempster, D. W., H. Zhou, R. R. Recker, J. P. Brown, M. A. Bolognese,

C. P. Recknor, D. L. Kendler, E. M. Lewiecki, D. A. Hanley, D. S. Rao, P. D. Miller, G. C. Woodson, 3rd, R. Lindsay, N. Binkley, X. Wan, V. A. Ruff, B. Janos and K. A. Taylor (2012). "Skeletal histomorphometry in subjects on teriparatide or zoledronic acid therapy (SHOTZ) study: a randomized controlled trial." J Clin Endocrinol Metab **97**(8): 2799-2808.

Dobnig, H., A. Sipos, Y. Jiang, A. Fahrleitner-Pammer, L. G. Ste-Marie, J. C. Gallagher, I. Pavo, J. Wang and E. F. Eriksen (2005). "Early changes in biochemical markers of bone formation correlate with improvements in bone structure during teriparatide therapy." J Clin Endocrinol Metab **90**(7): 3970-3977.

Dobnig, H., J. J. Stepan, D. B. Burr, J. Li, D. Michalska, A. Sipos, H. Petto, A. Fahrleitner-Pammer and I. Pavo (2009). "Teriparatide reduces bone microdamage accumulation in postmenopausal women previously treated with alendronate." J Bone Miner Res **24**(12): 1998-2006.

Doh, R. M., H. J. Park, Y. Rhee, H. S. Kim, J. Huh and W. Park (2015). "Teriparatide therapy for bisphosphonate-related osteonecrosis of the jaw associated with dental implants." Implant Dent **24**(2): 222-226.

Ebanks, J. P., R. R. Wickett and R. E. Boissy (2009). "Mechanisms regulating skin pigmentation: the rise and fall of complexion coloration." Int J Mol Sci **10**(9): 4066-4087.

Efeyan, A., W. C. Comb and D. M. Sabatini (2015). "Nutrient-sensing mechanisms and pathways." Nature **517**(7534): 302-310.

Eriksen, E. F., B. Langdahl, A. Vesterby, J. Rungby and M. Kassem (1999). "Hormone replacement therapy prevents osteoclastic hyperactivity: A histomorphometric study in early postmenopausal women." J Bone Miner Res **14**(7): 1217-1221.

Feng, L. X., P. Sun, T. Mi, M. Liu, W. Liu, S. Yao, Y. M. Cao, X. L. Yu, W. Y. Wu, B. H. Jiang, M. Yang, D. A. Guo and X. Liu (2016). "Agglutinin isolated from Arisema heterophyllum Blume induces apoptosis and autophagy in A549 cells through inhibiting PI3K/Akt pathway and inducing ER stress." Chin J Nat Med **14**(11): 856-864.

Finkelstein, J. S., A. Hayes, J. L. Hunzelman, J. J. Wyland, H. Lee and R. M. Neer (2003). "The effects of parathyroid hormone, alendronate, or both in men with osteoporosis." N Engl J Med **349**(13): 1216-1226.

Franzoso, G., L. Carlson, L. Xing, L. Poljak, E. W. Shores, K. D. Brown,

A. Leonardi, T. Tran, B. F. Boyce and U. Siebenlist (1997). "Requirement for NF-kappaB in osteoclast and B-cell development." Genes Dev **11**(24): 3482-3496.

Fullgrabe, J., G. Ghislat, D. H. Cho and D. C. Rubinsztein (2016). "Transcriptional regulation of mammalian autophagy at a glance." J Cell Sci **129**(16): 3059-3066.

Galluzzi, L., E. H. Baehrecke, A. Ballabio, P. Boya, J. M. Bravo-San Pedro, F. Cecconi, A. M. Choi, C. T. Chu, P. Codogno, M. I. Colombo, A. M. Cuervo, J. Debnath, V. Deretic, I. Dikic, E. L. Eskelinen, G. M. Fimia, S. Fulda, D. A. Gewirtz, D. R. Green, M. Hansen, J. W. Harper, M. Jaattela, T. Johansen, G. Juhasz, A. C. Kimmelman, C. Kraft, N. T. Ktistakis, S. Kumar, B. Levine, C. Lopez-Otin, F. Madeo, S. Martens, J. Martinez, A. Melendez, N. Mizushima, C. Munz, L. O. Murphy, J. M. Penninger, M. Piacentini, F. Reggiori, D. C. Rubinsztein, K. M. Ryan, L. Santambrogio, L. Scorrano, A. K. Simon, H. U. Simon, A. Simonsen, N. Tavernarakis, S. A. Tooze, T. Yoshimori, J. Yuan, Z. Yue, Q. Zhong and G. Kroemer (2017). "Molecular definitions of autophagy and related processes." EMBO J **36**(13): 1811-1836.

Ganesan, A. K., H. Ho, B. Bodemann, S. Petersen, J. Aruri, S. Koshy, Z. Richardson, L. Q. Le, T. Krasieva, M. G. Roth, P. Farmer and M. A. White (2008). "Genome-wide siRNA-based functional genomics of pigmentation identifies novel genes and pathways that impact melanogenesis in human cells." PLoS Genet **4**(12): e1000298.

Gao, D., Y. L. Zhang, P. Xu, Y. X. Lin, F. Q. Yang, J. H. Liu, H. W. Zhu and Z. N. Xia (2015). "In vitro evaluation of dual agonists for PPARgamma/beta from the flower of Edgeworthia gardneri (wall.) Meisn." J Ethnopharmacol **162**: 14-19.

Geng, L., C. Ma, L. Zhang, G. Yang, Y. Cui, D. Su, X. Zhao, Z. Liu, K. Bi and X. Chen (2013). "Metabonomic study of genkwa flos-induced hepatotoxicity and effect of herb-processing procedure on toxicity." Phytother Res **27**(4): 521-529.

Gerdes, J. M. and N. Katsanis (2008). "Ciliary function and Wnt signal modulation." Curr Top Dev Biol **85**: 175-195.

Gillbro, J. M. and M. J. Olsson (2011). "The melanogenesis and mechanisms of skin-lightening agents--existing and new approaches." Int J Cosmet Sci **33**(3): 210-221.

Giuliani, N., M. Pedrazzoni, G. Passeri, G. Negri, M. Impicciatore and G. Girasole (1998). "[Bisphosphonates stimulate the production of basic fibroblast growth factor and the formation of bone marrow precursors of osteoblasts. New findings about their mechanism of action]." Minerva Med **89**(7-8): 249-258.

Goetz, S. C. and K. V. Anderson (2010). "The primary cilium: a signalling centre during vertebrate development." Nat Rev Genet **11**(5): 331-344.

Greco, G., L. Panzella, A. Napolitano and M. d'Ischia (2012). "The fundamental building blocks of red human hair pheomelanin are isoquinoline-containing dimers." Pigment Cell Melanoma Res **25**(1): 110-112.

Grigoriadis, A. E., Z. Q. Wang, M. G. Cecchini, W. Hofstetter, R. Felix, H. A. Fleisch and E. F. Wagner (1994). "c-Fos: a key regulator of osteoclast-macrophage lineage determination and bone remodeling." Science **266**(5184): 443-448.

Gruber, H. E., J. Grigsby and C. H. Chesnut Ill (2000). "Osteoblast numbers after calcitonin therapy: a retrospective study of paired biopsies obtained during long-term calcitonin therapy in postmenopausal osteoporosis." Calcif Tissue Int **66**(1): 29-34.

Gruber, H. E., J. L. Ivey, D. J. Baylink, M. Matthews, W. B. Nelp, K. Sisom and C. H. Chesnut, 3rd (1984). "Long-term calcitonin therapy in postmenopausal osteoporosis." Metabolism **33**(4): 295-303.

Gunia-Krzyzak, A., J. Popiol and H. Marona (2016). "Melanogenesis Inhibitors: Strategies for Searching for and Evaluation of Active Compounds." Curr Med Chem **23**(31): 3548-3574.

Hadjidakis, D. J. and Androulakis, II (2006). "Bone remodeling." Ann N Y Acad Sci **1092**: 385-396.

Henriksen, K., M. G. Sorensen, R. H. Nielsen, J. Gram, S. Schaller, M. H. Dziegiel, V. Everts, J. Bollerslev and M. A. Karsdal (2006). "Degradation of the organic phase of bone by osteoclasts: a secondary role for lysosomal acidification." J Bone Miner Res **21**(1): 58-66.

Ho, H., R. Kapadia, S. Al-Tahan, S. Ahmad and A. K. Ganesan (2011). "WIPI1 coordinates melanogenic gene transcription and melanosome formation via TORC1 inhibition." J Biol Chem **286**(14): 12509-12523.

Holland, E. F., J. W. Chow, J. W. Studd, A. T. Leather and T. J. Chambers (1994). "Histomorphometric changes in the skeleton of postmenopausal women with low bone mineral density treated with percutaneous estradiol implants." Obstet Gynecol **83**(3): 387-391.

Hsiao, J. J. and D. E. Fisher (2014). "The roles of microphthalmia-associated transcription factor and pigmentation in melanoma." Arch Biochem Biophys **563**: 28-34.

Hu, X. J., H. Z. Jin, W. Z. Xu, M. Chen, X. H. Liu, W. Zhang, J. Su, C. Zhang and W. D. Zhang (2008). "Anti-inflammatory and analgesic activities of Edgeworthia chrysantha and its effective chemical constituents." Biol Pharm Bull **31**(9): 1761-1765.

Hu, X. J., H. Z. Jin, W. D. Zhang, W. Zhang, S. K. Yan, R. H. Liu, Y. H. Shen and W. Z. Xu (2009). "Two new coumarins from Edgeworthia chrysantha." Nat Prod Res **23**(13): 1259-1264.

Huang, C. F., R. S. Yang, S. H. Liu, P. C. Hsieh and S. Y. Lin-Shiau (2011). "Evidence for improved neuropharmacological efficacy and decreased neurotoxicity in mice with traditional processing of Rhizoma Arisaematis." Am J Chin Med **39**(5): 981-998.

Jee, W. S. and W. Yao (2001). "Overview: animal models of osteopenia and osteoporosis." J Musculoskelet Neuronal Interact **1**(3): 193-207.

Jiang, C. P., X. He, X. L. Yang, S. L. Zhang, H. Li, Z. J. Song, C. F. Zhang, Z. L. Yang, P. Li, C. Z. Wang and C. S. Yuan (2014). "Anti-rheumatoid arthritic activity of flavonoids from Daphne genkwa." Phytomedicine **21**(6): 830-837.

Jiang, Y., J. J. Zhao, B. H. Mitlak, O. Wang, H. K. Genant and E. F. Eriksen (2003). "Recombinant human parathyroid hormone (1-34) [teriparatide] improves both cortical and cancellous bone structure." J Bone Miner Res **18**(11): 1932-1941.

Jimi, E., T. Ikebe, N. Takahashi, M. Hirata, T. Suda and T. Koga (1996). "Interleukin-1 alpha activates an NF-kappaB-like factor in osteoclast-like cells." J Biol Chem **271**(9): 4605-4608.

Kai, H., T. Koine, M. Baba and T. Okuyama (2004). "[Pharmacological effects of Daphne genkwa and Chinese medical prescription, "Jyu-So-To"]." Yakugaku Zasshi **124**(6): 349-354.

Kalie, E., M. Razi and S. A. Tooze (2013). "ULK1 regulates melanin levels in MNT-1 cells independently of mTORC1." PLoS One **8**(9): e75313.

Kaur, J. and J. Debnath (2015). "Autophagy at the crossroads of catabolism and anabolism." Nat Rev Mol Cell Biol **16**(8): 461-472.

Keller, H. and M. Kneissel (2005). "SOST is a target gene for PTH in bone." Bone **37**(2): 148-158.

Khajuria, D. K., R. Razdan and D. R. Mahapatra (2011). "Drugs for the management of osteoporosis: a review." Rev Bras Reumatol **51**(4): 365-371, 379-382.

Kim, E. S., H. Chang, H. Choi, J. H. Shin, S. J. Park, Y. K. Jo, E. S. Choi, S. Y. Baek, B. G. Kim, J. W. Chang, J. C. Kim and D. H. Cho (2014). "Autophagy induced by resveratrol suppresses alpha-MSH-induced melanogenesis." Exp Dermatol **23**(3): 204-206.

Kim, E. S., Y. K. Jo, S. J. Park, H. Chang, J. H. Shin, E. S. Choi, J. B. Kim, S. H. Seok, J. S. Kim, J. S. Oh, M. H. Kim, E. H. Lee and D. H. Cho (2013). "ARP101 inhibits alpha-MSH-stimulated melanogenesis by regulation of autophagy in melanocytes." FEBS Lett **587**(24): 3955-3960.

Kim, E. S., J. H. Shin, S. H. Seok, J. B. Kim, H. Chang, S. J. Park, Y. K. Jo, E. S. Choi, J. S. Park, M. H. Yeom, C. S. Lim and D. H. Cho (2013). "Autophagy mediates anti-melanogenic activity of 3'-ODI in B16F1 melanoma cells." Biochem Biophys Res Commun **442**(3-4): 165-170.

Kim, M. B., Y. Song and J. K. Hwang (2014). "Kirenol stimulates osteoblast differentiation through activation of the BMP and Wnt/beta-catenin signaling pathways in MC3T3-E1 cells." Fitoterapia **98**: 59-65.

Klionsky, D. J., F. C. Abdalla and B. Zuckerbraun (2012). "Guidelines for the use and interpretation of assays for monitoring autophagy." Autophagy **8**(4): 445-544.

Kogianni, G., V. Mann and B. S. Noble (2008). "Apoptotic bodies convey activity capable of initiating osteoclastogenesis and localized bone destruction." J Bone Miner Res **23**(6): 915-927.

Kong, Y. Y., H. Yoshida, I. Sarosi, H. L. Tan, E. Timms, C. Capparelli, S. Morony, A. J. Oliveira-dos-Santos, G. Van, A. Itie, W. Khoo, A.

Wakeham, C. R. Dunstan, D. L. Lacey, T. W. Mak, W. J. Boyle and J. M. Penninger (1999). "OPGL is a key regulator of osteoclastogenesis, lymphocyte development and lymph-node organogenesis." Nature **397**(6717): 315-323.

Kroger, H., I. Arnala and E. M. Alhava (1992). "Effect of calcitonin on bone histomorphometry and bone metabolism in rheumatoid arthritis." Calcif Tissue Int **50**(1): 11-13.

Kyung, T. W., J. E. Lee, H. H. Shin and H. S. Choi (2008). "Rutin inhibits osteoclast formation by decreasing reactive oxygen species and TNF-alpha by inhibiting activation of NF-kappaB." Exp Mol Med **40**(1): 52-58.

Lacey, D. L., E. Timms, H. L. Tan, M. J. Kelley, C. R. Dunstan, T. Burgess, R. Elliott, A. Colombero, G. Elliott, S. Scully, H. Hsu, J. Sullivan, N. Hawkins, E. Davy, C. Capparelli, A. Eli, Y. X. Qian, S. Kaufman, I. Sarosi, V. Shalhoub, G. Senaldi, J. Guo, J. Delaney and W. J. Boyle (1998). "Osteoprotegerin ligand is a cytokine that regulates osteoclast differentiation and activation." Cell **93**(2): 165-176.

Lee, A. Y. (2015). "Recent progress in melasma pathogenesis." Pigment Cell Melanoma Res **28**(6): 648-660.

Li, L., Z. Zeng and G. Cai (2011). "Comparison of neoeriocitrin and naringin on proliferation and osteogenic differentiation in MC3T3-E1." Phytomedicine **18**(11): 985-989.

Li, S. H., L. J. Wu and H. Y. Yin (2002). "[Chemical and pharmacological advances of the study on zushima]." Zhongguo Zhong Yao Za Zhi **27**(6): 401-403.

Li, X. N., S. Q. Tong, D. P. Cheng, Q. Y. Li and J. Z. Yan (2014). "Coumarins from Edgeworthia chrysantha." Molecules **19**(2): 2042-2048.

Li, Z. Q. (1998). "Traditional Chinese medicine for primary liver cancer." World J Gastroenterol **4**(4): 360-364.

Lin, R. W., C. H. Chen, Y. H. Wang, M. L. Ho, S. H. Hung, I. S. Chen and G. J. Wang (2009). "(-)-Epigallocatechin gallate inhibition of osteoclastic differentiation via NF-kappaB." Biochem Biophys Res Commun **379**(4): 1033-1037.

Lindsay, R., F. Cosman, H. Zhou, M. P. Bostrom, V. W. Shen, J. D. Cruz, J. W. Nieves and D. W. Dempster (2006). "A novel tetracycline labeling schedule for longitudinal evaluation of the short-term effects of anabolic therapy with a single iliac crest bone biopsy: early actions of teriparatide." J Bone Miner Res **21**(3): 366-373.

Liu, R., X. Zhi and Q. Zhong (2015). "ATG14 controls SNARE-mediated autophagosome fusion with a lysosome." Autophagy **11**(5): 847-849.

Ma, Y. L., Q. Zeng, D. W. Donley, L. G. Ste-Marie, J. C. Gallagher, G. P. Dalsky, R. Marcus and E. F. Eriksen (2006). "Teriparatide increases bone formation in modeling and remodeling osteons and enhances IGF-II immunoreactivity in postmenopausal women with osteoporosis." J Bone Miner Res **21**(6): 855-864.

Marie, P. J. and F. Caulin (1986). "Mechanisms underlying the effects of phosphate and calcitonin on bone histology in postmenopausal osteoporosis." Bone **7**(1): 17-22.

Martin, T. J. and N. A. Sims (2005). "Osteoclast-derived activity in the coupling of bone formation to resorption." Trends Mol Med **11**(2): 76-81.

Masini, M., M. Bugliani, R. Lupi, S. del Guerra, U. Boggi, F. Filipponi, L. Marselli, P. Masiello and P. Marchetti (2009). "Autophagy in human type 2 diabetes pancreatic beta cells." Diabetologia **52**(6): 1083-1086.

Melton, L. J., 3rd, E. A. Chrischilles, C. Cooper, A. W. Lane and B. L. Riggs (2005). "How many women have osteoporosis? JBMR Anniversary Classic. JBMR, Volume 7, Number 9, 1992." J Bone Miner Res **20**(5): 886-892.

Mizoguchi, T., A. Muto, N. Udagawa, A. Arai, T. Yamashita, A. Hosoya, T. Ninomiya, H. Nakamura, Y. Yamamoto, S. Kinugawa, M. Nakamura, Y. Nakamichi, Y. Kobayashi, S. Nagasawa, K. Oda, H. Tanaka, M. Tagaya, J. M. Penninger, M. Ito and N. Takahashi (2009). "Identification of cell cycle-arrested quiescent osteoclast precursors in vivo." J Cell Biol **184**(4): 541-554.

Mizushima, N. (2005). "The pleiotropic role of autophagy: from protein metabolism to bactericide." Cell Death Differ **12 Suppl 2**: 1535-1541.

Mohan, S. and D. J. Baylink (1991). "Bone growth factors." Clin Orthop

Relat Res(263): 30-48.

Mukudai, Y., S. Kondo, T. Koyama, C. Li, S. Banka, A. Kogure, K. Yazawa and S. Shintani (2014). "Potential anti-osteoporotic effects of herbal extracts on osteoclasts, osteoblasts and chondrocytes in vitro." BMC Complement Altern Med **14**: 29.

Mullard, A. (2016). "Symptomatic AD treatment fails in first phase III." Nat Rev Drug Discov **15**(11): 738.

Murase, D., A. Hachiya, K. Takano, R. Hicks, M. O. Visscher, T. Kitahara, T. Hase, Y. Takema and T. Yoshimori (2013). "Autophagy has a significant role in determining skin color by regulating melanosome degradation in keratinocytes." J Invest Dermatol **133**(10): 2416-2424.

Nachury, M. V. (2014). "How do cilia organize signalling cascades?" Philos Trans R Soc Lond B Biol Sci **369**(1650).

Nakashima, T., M. Hayashi, T. Fukunaga, K. Kurata, M. Oh-Hora, J. Q. Feng, L. F. Bonewald, T. Kodama, A. Wutz, E. F. Wagner, J. M. Penninger and H. Takayanagi (2011). "Evidence for osteocyte regulation of bone homeostasis through RANKL expression." Nat Med **17**(10): 1231-1234.

Neer, R. M., C. D. Arnaud, J. R. Zanchetta, R. Prince, G. A. Gaich, J. Y. Reginster, A. B. Hodsman, E. F. Eriksen, S. Ish-Shalom, H. K. Genant, O. Wang and B. H. Mitlak (2001). "Effect of parathyroid hormone (1-34) on fractures and bone mineral density in postmenopausal women with osteoporosis." N Engl J Med **344**(19): 1434-1441.

Neuringer, L. J., B. Sears and F. B. Jungalwala (1979). "Deuterium NMR studies of cerebroside-phospholipid bilayers." Biochim Biophys Acta **558**(3): 325-329.

Nih Consensus Development Panel on Osteoporosis Prevention, D. and Therapy (2001). "Osteoporosis prevention, diagnosis, and therapy." JAMA **285**(6): 785-795.

Noble, B. S., N. Peet, H. Y. Stevens, A. Brabbs, J. R. Mosley, G. C. Reilly, J. Reeve, T. M. Skerry and L. E. Lanyon (2003). "Mechanical loading: biphasic osteocyte survival and targeting of osteoclasts for bone destruction in rat cortical bone." Am J Physiol Cell Physiol **284**(4): C934-943.

Ogata, N. and H. Kawaguchi (2007). "[Parathyroid and bone. The mechanism of anabolic function of parathyroid hormone on bone]." Clin Calcium **17**(12): 1843-1849.

Onodera, J. and Y. Ohsumi (2005). "Autophagy is required for maintenance of amino acid levels and protein synthesis under nitrogen starvation." J Biol Chem **280**(36): 31582-31586.

Oz, H. S., J. Zhong and W. J. de Villiers (2012). "Osteopontin ablation attenuates progression of colitis in TNBS model." Dig Dis Sci **57**(6): 1554-1561.

Palmieri, G. M., J. A. Pitcock, P. Brown, J. G. Karas and L. J. Roen (1989). "Effect of calcitonin and vitamin D in osteoporosis." Calcif Tissue Int **45**(3): 137-141.

Pampliega, O., I. Orhon, B. Patel, S. Sridhar, A. Diaz-Carretero, I. Beau, P. Codogno, B. H. Satir, P. Satir and A. M. Cuervo (2013). "Functional interaction between autophagy and ciliogenesis." Nature **502**(7470): 194-200.

Papandreou, I., A. L. Lim, K. Laderoute and N. C. Denko (2008). "Hypoxia signals autophagy in tumor cells via AMPK activity, independent of HIF-1, BNIP3, and BNIP3L." Cell Death Differ **15**(10): 1572-1581.

Park, H. Y., M. Kosmadaki, M. Yaar and B. A. Gilchrest (2009). "Cellular mechanisms regulating human melanogenesis." Cell Mol Life Sci **66**(9): 1493-1506.

Paschalis, E. P., E. V. Glass, D. W. Donley and E. F. Eriksen (2005). "Bone mineral and collagen quality in iliac crest biopsies of patients given teriparatide: new results from the fracture prevention trial." J Clin Endocrinol Metab **90**(8): 4644-4649.

Pederson, L., M. Ruan, J. J. Westendorf, S. Khosla and M. J. Oursler (2008). "Regulation of bone formation by osteoclasts involves Wnt/BMP signaling and the chemokine sphingosine-1-phosphate." Proc Natl Acad Sci U S A **105**(52): 20764-20769.

Peng, Y., Q. Kang, Q. Luo, W. Jiang, W. Si, B. A. Liu, H. H. Luu, J. K. Park, X. Li, J. Luo, A. G. Montag, R. C. Haydon and T. C. He (2004). "Inhibitor of DNA binding/differentiation helix-loop-helix proteins mediate bone morphogenetic protein-induced osteoblast differentiation

of mesenchymal stem cells." J Biol Chem **279**(31): 32941-32949.

Pillaiyar, T., M. Manickam and V. Namasivayam (2017). "Skin whitening agents: medicinal chemistry perspective of tyrosinase inhibitors." J Enzyme Inhib Med Chem **32**(1): 403-425.

Qiao, Y., Y. Zhao, Q. Wu, L. Sun, Q. Ruan, Y. Chen, M. Wang, J. Duan and D. Wang (2014). "Full toxicity assessment of Genkwa Flos and the underlying mechanism in nematode Caenorhabditis elegans." PLoS One **9**(3): e91825.

Recker, R. R., F. Marin, S. Ish-Shalom, R. Moricke, F. Hawkins, G. Kapetanos, M. P. de la Pena, J. Kekow, J. Farrerons, B. Sanz, H. Oertel and J. Stepan (2009). "Comparative effects of teriparatide and strontium ranelate on bone biopsies and biochemical markers of bone turnover in postmenopausal women with osteoporosis." J Bone Miner Res **24**(8): 1358-1368.

Reeve, J., J. N. Bradbeer, M. Arlot, U. M. Davies, J. R. Green, L. Hampton, C. Edouard, R. Hesp, P. Hulme, J. P. Ashby and et al. (1991). "hPTH 1-34 treatment of osteoporosis with added hormone replacement therapy: biochemical, kinetic and histological responses." Osteoporos Int **1**(3): 162-170.

Reginster, J. Y., D. Felsenberg, S. Boonen, A. Diez-Perez, R. Rizzoli, M. L. Brandi, T. D. Spector, K. Brixen, S. Goemaere, C. Cormier, A. Balogh, P. D. Delmas and P. J. Meunier (2008). "Effects of long-term strontium ranelate treatment on the risk of nonvertebral and vertebral fractures in postmenopausal osteoporosis: Results of a five-year, randomized, placebo-controlled trial." Arthritis Rheum **58**(6): 1687-1695.

Reginster, J. Y., E. Seeman, M. C. De Vernejoul, S. Adami, J. Compston, C. Phenekos, J. P. Devogelaer, M. D. Curiel, A. Sawicki, S. Goemaere, O. H. Sorensen, D. Felsenberg and P. J. Meunier (2005). "Strontium ranelate reduces the risk of nonvertebral fractures in postmenopausal women with osteoporosis: Treatment of Peripheral Osteoporosis (TROPOS) study." J Clin Endocrinol Metab **90**(5): 2816-2822.

Rich, K. A., C. Burkett and P. Webster (2003). "Cytoplasmic bacteria can be targets for autophagy." Cell Microbiol **5**(7): 455-468.

Riggs, B. L. and A. M. Parfitt (2005). "Drugs used to treat osteoporosis: the critical need for a uniform nomenclature based on their action on bone remodeling." J Bone Miner Res **20**(2): 177-184.

Riggs, B. L., H. W. Wahner, E. Seeman, K. P. Offord, W. L. Dunn, R. B. Mazess, K. A. Johnson and L. J. Melton, 3rd (1982). "Changes in bone mineral density of the proximal femur and spine with aging. Differences between the postmenopausal and senile osteoporosis syndromes." J Clin Invest **70**(4): 716-723.

Rishton, G. M. (2008). "Natural products as a robust source of new drugs and drug leads: past successes and present day issues." Am J Cardiol **101**(10A): 43D-49D.

Robling, A. G., T. Bellido and C. H. Turner (2006). "Mechanical stimulation in vivo reduces osteocyte expression of sclerostin." J Musculoskelet Neuronal Interact **6**(4): 354.

Schneider, J. L. and A. M. Cuervo (2014). "Autophagy and human disease: emerging themes." Curr Opin Genet Dev **26**: 16-23.

Schultz, I., J. Wurzel and L. Meinel (2015). "Drug delivery of Insulin-like growth factor I." Eur J Pharm Biopharm **97**(Pt B): 329-337.

Seeman, E. and P. D. Delmas (2006). "Bone quality--the material and structural basis of bone strength and fragility." N Engl J Med **354**(21): 2250-2261.

Shen, L. N., Y. T. Zhang, Q. Wang, L. Xu and N. P. Feng (2014). "Preparation and evaluation of microemulsion-based transdermal delivery of total flavone of rhizoma arisaematis." Int J Nanomedicine **9**: 3453-3464.

Sims, N. A., B. J. Jenkins, J. M. Quinn, A. Nakamura, M. Glatt, M. T. Gillespie, M. Ernst and T. J. Martin (2004). "Glycoprotein 130 regulates bone turnover and bone size by distinct downstream signaling pathways." J Clin Invest **113**(3): 379-389.

Song, L., J. Zhao, X. Zhang, H. Li and Y. Zhou (2013). "Icariin induces osteoblast proliferation, differentiation and mineralization through estrogen receptor-mediated ERK and JNK signal activation." Eur J Pharmacol **714**(1-3): 15-22.

Sophocleous, A. and A. I. Idris (2014). "Rodent models of osteoporosis." Bonekey Rep **3**: 614.

Srivastava, S., R. Bankar and P. Roy (2013). "Assessment of the role of flavonoids for inducing osteoblast differentiation in isolated mouse bone

marrow derived mesenchymal stem cells." Phytomedicine **20**(8-9): 683-690.

Steiniche, T., C. Hasling, P. Charles, E. F. Eriksen, L. Mosekilde and F. Melsen (1989). "A randomized study on the effects of estrogen/gestagen or high dose oral calcium on trabecular bone remodeling in postmenopausal osteoporosis." Bone **10**(5): 313-320.

Sun, H., L. Li, A. Zhang, N. Zhang, H. Lv, W. Sun and X. Wang (2013). "Protective effects of sweroside on human MG-63 cells and rat osteoblasts." Fitoterapia **84**: 174-179.

Tabatabaei-Malazy, O., P. Salari, P. Khashayar and B. Larijani (2017). "New horizons in treatment of osteoporosis." Daru **25**(1): 2.

Tang, Y., X. Wu, W. Lei, L. Pang, C. Wan, Z. Shi, L. Zhao, T. R. Nagy, X. Peng, J. Hu, X. Feng, W. Van Hul, M. Wan and X. Cao (2009). "TGF-beta1-induced migration of bone mesenchymal stem cells couples bone resorption with formation." Nat Med **15**(7): 757-765.

Tang, Z., M. G. Lin, T. R. Stowe, S. Chen, M. Zhu, T. Stearns, B. Franco and Q. Zhong (2013). "Autophagy promotes primary ciliogenesis by removing OFD1 from centriolar satellites." Nature **502**(7470): 254-257.

Tatsumi, S., K. Ishii, N. Amizuka, M. Li, T. Kobayashi, K. Kohno, M. Ito, S. Takeshita and K. Ikeda (2007). "Targeted ablation of osteocytes induces osteoporosis with defective mechanotransduction." Cell Metab **5**(6): 464-475.

van Bezooijen, R. L., B. A. Roelen, A. Visser, L. van der Wee-Pals, E. de Wilt, M. Karperien, H. Hamersma, S. E. Papapoulos, P. ten Dijke and C. W. Lowik (2004). "Sclerostin is an osteocyte-expressed negative regulator of bone formation, but not a classical BMP antagonist." J Exp Med **199**(6): 805-814.

Vedi, S. and J. E. Compston (1996). "The effects of long-term hormone replacement therapy on bone remodeling in postmenopausal women." Bone **19**(5): 535-539.

Verborgt, O., N. A. Tatton, R. J. Majeska and M. B. Schaffler (2002). "Spatial distribution of Bax and Bcl-2 in osteocytes after bone fatigue: complementary roles in bone remodeling regulation?" J Bone Miner Res **17**(5): 907-914.

Visagie, A., A. Kasonga, V. Deepak, S. Moosa, S. Marais, M. C. Kruger and M. Coetzee (2015). "Commercial Honeybush (Cyclopia spp.) Tea Extract Inhibits Osteoclast Formation and Bone Resorption in RAW264.7 Murine Macrophages-An in vitro Study." Int J Environ Res Public Health **12**(11): 13779-13793.

Wang, S. and Y. Cheng (2006). "Separation and determination of the effective components in the alabastrum of Edgeworthia chrysantha Lindl. by micellar electrokinetic capillary chromatography." J Pharm Biomed Anal **40**(5): 1137-1142.

Weinstein, R. S., A. M. Parfitt, R. Marcus, M. Greenwald, G. Crans and D. B. Muchmore (2003). "Effects of raloxifene, hormone replacement therapy, and placebo on bone turnover in postmenopausal women." Osteoporos Int **14**(10): 814-822.

Wright, C. D., N. J. Garrahan, M. Stanton, J. C. Gazet, R. E. Mansell and J. E. Compston (1994). "Effect of long-term tamoxifen therapy on cancellous bone remodeling and structure in women with breast cancer." J Bone Miner Res **9**(2): 153-159.

Wu, X., L. Pang, W. Lei, W. Lu, J. Li, Z. Li, F. J. Frassica, X. Chen, M. Wan and X. Cao (2010). "Inhibition of Sca-1-positive skeletal stem cell recruitment by alendronate blunts the anabolic effects of parathyroid hormone on bone remodeling." Cell Stem Cell **7**(5): 571-580.

Xu, H., D. Lawson, A. Kras and D. Ryan (2005). "The use of preventive strategies for bone loss." Am J Chin Med **33**(2): 299-306.

Xue, K., Y. Wang, Y. Hou, Y. Wang, T. Zhong, L. Li, H. Zhang and L. Wang (2014). "Molecular characterization and expression patterns of the actinin-associated LIM protein (ALP) subfamily genes in porcine skeletal muscle." Gene **539**(1): 111-116.

Yang, F. L., K. Q. Hu, X. Wang, Z. M. Liu, Q. Hu, J. F. Li and H. He (2011). "Combination of raloxifene, aspirin and estrogen as novel paradigm of hormone replacement therapy in rabbit model of menopause." Acta Pharmacol Sin **32**(8): 1031-1037.

Yogesh, H. S., V. M. Chandrashekhar, H. R. Katti, S. Ganapaty, H. L. Raghavendra, G. K. Gowda and B. Goplakhrishna (2011). "Anti-osteoporotic activity of aqueous-methanol extract of Berberis aristata in ovariectomized rats." J Ethnopharmacol **134**(2): 334-338.

Yoon, H. Y., S. I. Yun, B. Y. Kim, Q. Jin, E. R. Woo, S. Y. Jeong and Y. S. Chung (2011). "Poncirin promotes osteoblast differentiation but inhibits adipocyte differentiation in mesenchymal stem cells." Eur J Pharmacol **664**(1-3): 54-59.

Yun, J. W., S. H. Kim, Y. S. Kim, J. R. You, E. Kwon, J. J. Jang, I. A. Park, H. C. Kim, H. H. Kim, J. H. Che and B. C. Kang (2015). "Evaluation of subchronic (13week) toxicity and genotoxicity potential of vinegar-processed Genkwa Flos." Regul Toxicol Pharmacol **72**(2): 386-393.

Zhang, C. F., S. L. Zhang, X. He, X. L. Yang, H. T. Wu, B. Q. Lin, C. P. Jiang, J. Wang, C. H. Yu, Z. L. Yang, C. Z. Wang, P. Li and C. S. Yuan (2014). "Antioxidant effects of Genkwa flos flavonoids on Freunds adjuvant-induced rheumatoid arthritis in rats." J Ethnopharmacol **153**(3): 793-800.

Zhang, H. and E. H. Baehrecke (2015). "Eaten alive: novel insights into autophagy from multicellular model systems." Trends Cell Biol **25**(7): 376-387.

Zhang, Y., H. Guan, J. Li, Z. Fang, W. Chen and F. Li (2015). "Amlexanox Suppresses Osteoclastogenesis and Prevents Ovariectomy-Induced Bone Loss." Sci Rep **5**: 13575.

Zhao, C., N. Irie, Y. Takada, K. Shimoda, T. Miyamoto, T. Nishiwaki, T. Suda and K. Matsuo (2006). "Bidirectional ephrinB2-EphB4 signaling controls bone homeostasis." Cell Metab **4**(2): 111-121.

국문 초록

천연 식물자원은 지난 수 세기 동안 의약품, 건강기능식품, 기능성 화장품의 원료로 사용되어 왔다. 천연물로부터 약물과 유사한 특성을 보유한 새로운 생리활성 성분을 발견하려는 노력은 천연물 유래 라이브러리 (추출물, 분획물, 정제 화합물)와 고속검색기술(high throughput screening technology)등에 의해 급속히 발전 되어왔다. 본 연구에서는 한국에서 자생하는 4,200 종의 식물에서 추출한 추출물을 이용하여 항골다공증 및 멜라닌 축척 저해 후보물질을 발굴하였다.

먼저 골다공증 치료제 후보물질의 선별을 위하여 추출물 라이브러리로부터 파골세포와 조골세포의 바이오마커에 미치는 소재를 단계별로 선별하였다. 즉 파골세포인 RAW264.7 세포에서 RANKL 유도 NF-κB 발현을 억제하는 능력, MC3T3-E1 조골세포에서 ALP 활성 조절 능력, 조골세포에서 세포 외 칼슘의 침착을 증진하는 능력을 테스트하였다. 선별된 소재의 성분 분석과 프로파일링을 통하여 *Edgeworthia papyrifera* (삼지닥)의 뼈 강화 생리활성을 발견하였으며 삼지닥에 함유된 edgeworoside A 천연화합물을 동정하고 기능성을 규명하였다.

폐경기 골다공증 동물 모델인 난소 적출 동물모델에서 삼지닥 추출물은 골다공증 관련 조직학적 주요 인자와 생화학적 지표 및 구조적 측면 모두에서 개선하는 효능을 보였으며, 이러한 결과는 본 연구에서 발굴한 천연소재가 기능성 성분으로 사용되어 뼈의 강도를 높이고 골다공증 치료를 위한 치료제로 사용될 수 있음을 보여준다.

다음으로 멜라닌 축적 억제 후보물질 동정을 위하여 *in vitro* 에서 α-MSH 에 의해 유도된 멜라닌 생성 및 B16F1 세포에서의 티로시나제와 TRP1 발현의 정량화를 이용하는 일련의 시험을 수행하였다. 그 결과, α-MSH 처리된 B16F1 세포에서 멜라닌의 생합성과 티로시나제 및 TRP1 의 발현을 억제하는 *Rhizoma arisaematis*(천남성)이 선별되였다. 천남성의 autophagy 활성 촉진 효과와 autophagy 저해제에 의한 α-MSH 처리된 B16F1 세포에서 천남성에 의한 멜라닌 생성억제 효과가 감소됨을 확인함으로써 천남성의 멜라닌 생성억제 효과는 autophagy 활성화를 통해 매개됨을 증명하였다. 마지막으로 인공피부 대체물을 이용한 기능성 및 안전성 시험과 인체 적용시험에서 천남성은 색소침착을 현저하게 억제하였고, 인체 피부에 미백효능이 있음이 밝혀졌다. 이러한

결과는 기능성 화장품 제품 개발 및 새로운 기능성 원료 개발에 기초 자료로 이용될 수 있을 것으로 기대된다.

주요어: 골다공증, 파골세포, 조골세포, 난소적출모델, 삼지닥, Egiworiside A, 골다공증 치료제, 기능성식품, 천남성, 기능성화장품

학번: 2008-30925